2010

Microfluidic devices interfaced to matrix-assisted laser desorption/ionization mass spectrometry for proteomics

Jeonghoon Lee
Louisiana State University and Agricultural and Mechanical College, jlee62@tigers.lsu.edu

Follow this and additional works at: https://digitalcommons.lsu.edu/gradschool_dissertations

Part of the Chemistry Commons

Recommended Citation

MICROFLUIDIC DEVICES INTERFACED TO MATRIX-ASSISTED LASER
DESORPTION/IONIZATION MASS SPECTROMETRY FOR PROTEOMICS

A Dissertation

Submitted to the Graduate Faculty of the
Louisiana State University and
Agricultural and Mechanical College
in partial fulfillment of the
requirement for the degree of
Doctor of Philosophy

in

The Department of Chemistry

by
Jeonghoon Lee
B.S., Kyungpook National University, Korea, 1994
M.S., Kyungpook National University, Korea, 1996
May 2010

DEDICATION

To my family and church members

ACKNOWLEDGMENTS

TABLE OF CONTENTS

LIST OF TABLES

LIST OF FIGURES

ABSTRACT

Microfluidic interfaces were developed for off-line matrix-assisted laser desorption/ionization mass spectrometry (MALDI). Microfluidic interfaces allow samples to be manipulated on-chip and deposited onto a MALDI target plate for analysis. For this research, microfluidic culturing devices and automated digestion and deposition microfluidic chip platforms were developed for the identification of proteins. The microfluidic chip components were fabricated on a poly(methyl methacrylate), PMMA, wafer using the hot embossing method and a molding tool with structures prepared via micromilling. One of the most important components of the chip system was a trypsin microreactor. An open channel microreactor was constructed in a 100 µm wide and 100 µm deep channel with a 4 cm effective channel length. This device integrated frequently repeated steps for MALDI-based proteomics such as digestion, mixing with a matrix solution, and depositing onto a MALDI target. The microreactor provided efficient digestion of proteins at a flow rate of 1 µL/min with a residence time of approximately 24 s in the reaction channel. An electrokinetically driven microreactor was also developed using a micropost structured chip for digestion. The micropost chip had a higher digestion efficiency due to the higher surface area-to-volume ratio in the channel. Also, the electrokinetic flow eliminated the need for an external pumping system and gave a flat flow profile in the microchannel. The post microreactor consisted of a 4 cm × 200 µm × 50 µm microfluidic channel with trypsin immobilized on an array of 50 µm in diameter micropost support structures with a 50 µm edge-to-edge inter-post spacing. This micropost reactor was also used for fingerprint analysis of whole bacterial cells. The entire tryptic digestion and deposition procedure for intact bacteria took about 1 min. A contact deposition solid-phase bioreactor coupled with MALDI-TOF MS allowed for low-volume fraction deposition with a smaller spot

xiii

size and a higher local concentration of the analyte. A bacterial cell-culturing chip was constructed for growing cells on-chip followed by off-line MALDI analysis. Coupling MALDI-TOF MS whole cell analysis with microfluidic culturing resulted in more consistent spectra as well as reduction of the total processing time. The microfluidic cell culturing was performed in a PMMA chip with a polydimethylsiloxane (PDMS) cover to allow gas permeation into the culture channel, which contained a 2.1 μL volume active culture chamber. After incubation of *E. coli* in a microfluidic culture device at 37 ℃ for 24 h, the cultured cells were analyzed with MALDI MS. Also, a microfluidic cell culture device containing continuous perfusion of culture medium was developed using a polycarbonate membrane. This microfluidic culturing format was improved with a fluidic manifold and thermostatted microheaters. Fingerprint mass spectra distinguishing *E. coli* strains tested were obtained after a 6 h incubation time, which was shorter compared to the 24 h incubation time using conventional culturing techniques. In addition, an enhanced identification procedure for bacteria was achieved by integrating on-chip digestion of cultured bacteria.

The work reported in this chapter has been published in the *Journal of Mass Spectrometry*[1] and *Analytica Chimica Acta.*[2]

1.1 Basic Principles of Proteomics

Since the sequencing of the human genome, proteomics has become an important research topic in chemistry, biology, medicine and even engineering.[3-6] Protein analysis has generated great interest as a means for the elucidation of cell function at the molecular level as well as for investigating the relationship between disease states and the protein complement for clinical diagnostics.[7]

There are two general strategies for whole proteome analysis: bottom-up and top-down. With the bottom-up approach,[8] proteins are subjected to proteolytic digestion with an enzyme such as trypsin, and the resulting peptides are analyzed by peptide mass fingerprinting[9] or by tandem mass spectrometry for peptide sequence tags.[10] Typically, one or two-dimensional gel electrophoresis is used for separation of complex protein mixtures followed by proteolytic digestion of isolated spots. An alternate "shotgun" sequencing approach to bottom-up sequencing uses multi-dimensional separations, such as ion exchange chromatography (IEC) and high performance liquid chromatography (HPLC), of the proteolytic fragments generated from intact proteins.[11] Mass spectrometric peptide mapping and database searching is then performed. With the top-down approach, proteins are ionized intact and subsequently fragmented in the mass spectrometer. In this way, both the protein mass and the mass of the peptide fragments are measured.[8, 12] The top-down method uses a high resolution ion trapping instrument, such as a Fourier transform ion cyclotron resonance (FTICR)[13] or an Orbitrap[14] mass spectrometer.

Progress in the area of proteomics relies heavily on new analytical tools for the sensitive,

---

selective, and high-throughput studies of target analytes.[15] Mass spectrometry (MS) has evolved into a primary analytical tool for proteomics research, especially when coupled with separation techniques, due to the high information content that can be derived from these coupled techniques.[10] Advances in MS have been facilitated by the two ionization techniques; electrospray ionization (ESI) and matrix-assisted laser desorption/ionization (MALDI). Over the course of the past two decades, these ionization methods have become indispensible for the analysis of biological molecules, especially proteins and peptides. ESI MS produces highly charged ions directly from a liquid and is therefore useful for coupling to liquid separations.[16-18] MALDI is fast and efficient and has a high tolerance to non-volatile buffers and impurities.[19, 20] The samples for MALDI are typically applied to solid supports and used off-line with liquid or gel separations.[21-23]

Separation of the components of the proteome is challenging due to the complexity of the proteome. For example, it has been estimated that between 100,000 to 250,000 proteins can be encoded by the 20,000 to 25,000 human genes through post-translational modifications and differential splicing, which can produce 5 to 10 different proteins from each gene.[24, 25] A further complication is the dynamic range of protein expression at the cellular level, which can range from 10^6 to 10^9 copies per cell.[26] Many proteins that are disease biomarkers are low abundant and are difficult to isolate from complex mixtures containing highly abundant species with current separation methods.[27, 28] As an example, 2-D gel electrophoresis can separate up to 11,000 proteins from a whole cell lysate, but is restricted to the most highly abundant proteins in the sample.[29] High peak capacity separations of proteins with better resolution and faster run times are required for improved proteomic analysis. This can be accomplished in a bottom-up fashion, in which the proteins are proteolytically digested into peptide fragments and separated before MS analysis. Alternately, a top-down approach can be employed in which proteins are separated

2

first and then ionized with fragmentation occurring in the mass spectrometer.[11, 12]

Another critical step in proteomic sample pre-treatment is the efficient proteolytic digestion of proteins required for reliable identification. Because proteomic samples are typically available in small quantities, efficient digestion protocols are needed to achieve reliable results. Protocols for proteins and cell lysates have been developed for higher digestion efficiency using denaturation steps prior to digestion.[30] In addition, digestion efficiency can be improved through protein enrichment from crude mixtures of cell lysates.[5] Target proteins can be effectively isolated from cytosolic proteins by using affinity beds,[31-33] which selectively capture membrane proteins, or through the use of derivatized gold nanoparticles.[34]

1.2 Microfluidics for Mass Spectrometry

In the past decade, integrated microfluidic systems have been widely used to address the analytical problems faced by scientists in basic research, life sciences, pharmaceutics, and clinical research.[35] Microfluidics provides a number of unique advantages compared to the conventional bench-top systems used for processing biological samples, including reduced sample and reagent consumption, improved analysis speed, process step integration for fully automated systems and multiplexed analyses to increase sample processing throughput.[36] For these reasons, microfluidic devices are expected to play an important role in the development of high-throughput and integrated proteomic analysis systems, especially when these systems are interfaced to MS.[37]

Various schemes for coupling microfluidics to MS have been developed. Adapting microfluidic chips for on-line ESI is straightforward because the flow rate is compatible with nano-flow electrospray.[38] Various on-line separation methods are compatible with ESI, [39] and several approaches have been described for coupling chip-based separations and microreactors to ESI using electrokinetic or pressure-driven flow.[38, 40-45] MALDI is not directly suitable to an

online approach, although several novel interfaces have been described.[22, 46] Off-line coupling of

MALDI to microfluidic-based liquid separations can be accomplished by depositing the analyte

directly onto a MALDI target plate. The off-line approach decouples the separation or reaction

from the mass spectrometer both in time and space and allows for optimization and, if necessary,

reanalysis. With a microfluidic chip, deposition is not always necessary and direct analysis on

the chip without the mass spectrometer is possible.[47-51]

1.2.1   Electrospray Interfaces

One of the main advantages of ESI for proteomic analysis is that it can be used with a

flowing liquid, thus facilitating on-line coupling of chromatographic separations to the mass

spectrometer. Thus, ESI is an obvious approach for on-line interfacing of microfluidic chips to

mass spectrometry. In particular, the nL to μL per minute flow rate used in microfluidics is a

good match to that used in nanoflow ESI sources.

Several approaches to coupling microfluidic devices containing electrospray emitters

with ESI-MS have been developed. Figure 1-1 is a schematic diagram of various approaches for

the chip ESI interfaces. The simplest approach is to spray directly from the chip (Figure 1-1a).

Here, a glass chip can be scored and broken across a channel for direct spraying from the

opening with either pressure or electrokinetic liquid transport used to generate liquid flow.[52, 53]

More sophisticated spray devices can be fabricated by attaching a capillary to the chip channel or

(Figure 1-1b) by fabricating a spray tip in the device itself (Figure 1-1c). [54, 55] Multichannel

microchips can be interfaced to ESI-MS for parallel analysis to increase system throughput.[52]

Direct from Chip

The first interface of a microfluidic chip with mass spectrometry was reported in 1997

with a chip containing nine microfluidic channels.[52, 53] The spray was formed from the blunt

edge of a glass chip, which consisted of 60 μm wide and 25 μm deep channels connected to a

4

syringe pump generating a pressure driven flow of 100 to 200 nL/min. In the same year, a glass

chip was reported with open exits at the end of the channel.[53] The electrospray was generated

from the flat edge of the glass channel through an electrokinetically-driven flow.
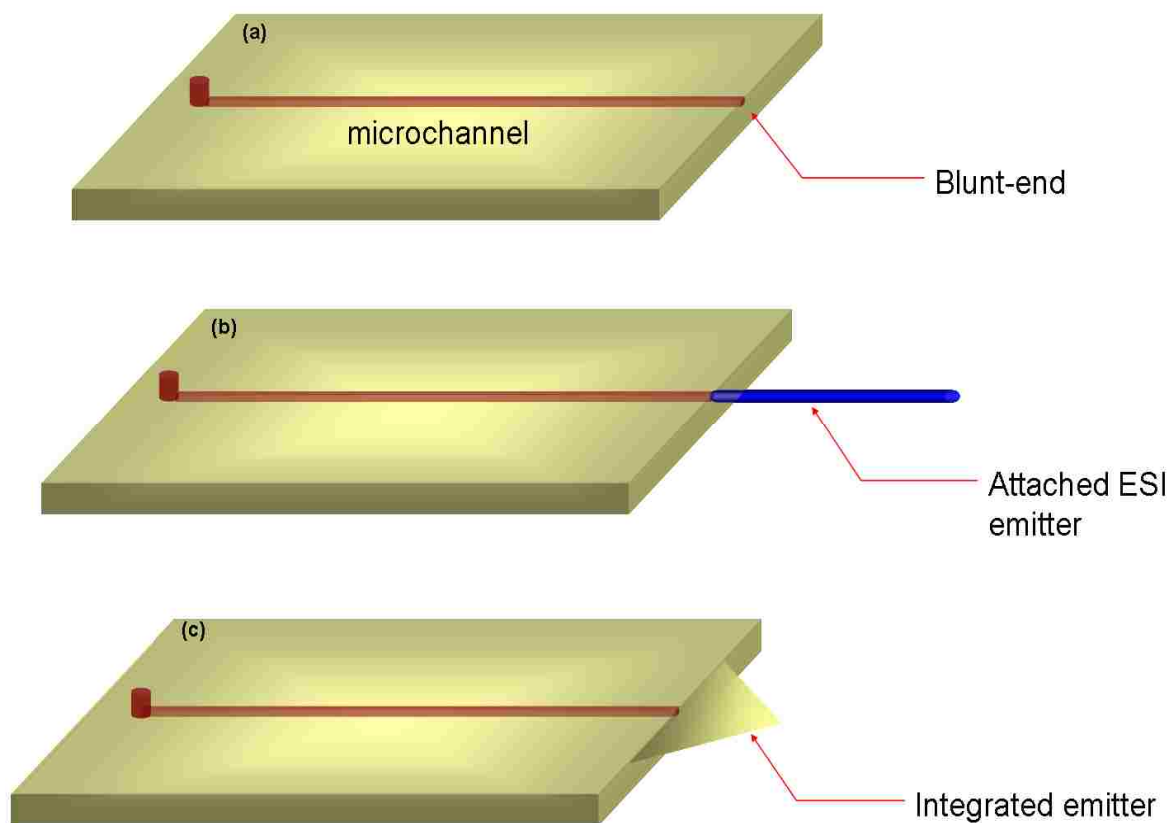
Figure 1-1. Schematic of various microfluidic chip interfaces for ESI for MS using (a) a blunt-end chip, (b) a chip with an attached ESI emitter, and (c) a chip with an integrated emitter.

The performance of a direct-from-chip spray is limited by effluent spreading at the

interface due to the hydrophilic properties of glass. This ultimately causes difficulty in

controlling the spray direction.[38] Moreover, polar liquids wet a large area at the edge of the

hydrophilic glass chip, which limits the resolution of separations due to the relatively large dead

volume of the electrospray.[56] To prevent spreading of the liquid, the channel exit can be treated

to render it more hydrophobic; for example, silanized or polytetrafluoroethylene surfaces have been formed at the edge of the chip to reduce surface wetting artifacts.[57]

Attached Capillary

An alternate approach to spraying directly from the chip is to attach an electrospray capillary to the chip channel.[58, 59] The first approach used a fused silica capillary inserted into a microchip serving as the mass spectrometer interface.[60] A 12 cm long fused silica capillary was glued to the edge of the microfluidic chip and transport of the analyte was accomplished with an electroosmotic pump. Although this work demonstrated the use of capillary emitters for electropspray from a chip, the device was limited to sample infusion and suffered from difficulties in alignment.

A drilling procedure was developed for low dead volume connections between a glass microfluidic chip and an electrospray emitter.[61] The chip had 200 µm holes for emitter attachment produced by 200 µm tungsten carbide bits producing a 700 pL dead volume. The dead volume created by using a conical-shaped carbide bit was effectively removed with a flat-tipped drill bit. Sub-attomole detection limits for peptides was reported by using microfluidic devices with a nanospray tip inserted into a hole perpendicular to the cover of the chip.[54] The tip was 50 µm i.d. and pulled to 5 µm i.d. at the tip. Time-of-flight (TOF) MS was used for detection at its maximum acquisition rate of 100 spectra/s. Approximately 0.5 amol of gramicidin S was detected using a 10 ms acquisition time period with an observed S/N ratio of 4.

A chip-based integrated liquid junction configuration with a removable electrospray tip has also been developed.[62, 63] The liquid junction was maintained with a make-up buffer between the cathode end of a capillary electrophoresis channel and the inlet of the ESI.[64] Approximately 10 pmol of cytochrome *c* was detected using this liquid junction. The junction provided an

effective technique for transferring trace-level samples from a CE separation and improved the spray stability for ESI.[65]

Although capillary spray emitters are more stable, dead volumes in the coupling between the chip and capillary can compromise separation performance and thus liquid separation resolution. Also, attachment of the emitters is labor-intensive and potentially a high-cost process for commercial devices. In addition, the glue used to attach the emitter can be dissolved by certain organic solvents and thus, produce interference peaks or render the device inoperable.

<u>Microfabricated Sprayer</u>

Electrospray emitter tips from microfluidic chips can be constructed in the microfluidic chip itself.[66] Microfabrication procedures allow for microfluidic channels and emitters to be constructed during chip fabrication and therefore many chip components can be made simultaneously. Integrated emitters have been constructed on polymer substrates such as polyethylene terephthalate (PET), polycarbonate (PC), poly(methyl methacrylate) (PMMA), and polydimethylsiloxane (PDMS),[67-70] as well as on silicon and glass devices.[43, 71] A micromilling machine was used to fabricate an electrospray emitter from PMMA.[67] This method eliminated the dead volume between the channel and tip and resulted in a stable spray. Parylene surface micromachining has also been developed for fabricating integrated ESI emitters.[72-75] In this process, a microchip was fabricated by alternately depositing layers of parylene and photoresist on a silicon wafer. After dissolving the photoresist, the desired parylene structures were formed.

A multi-nozzle chip was developed with an array of hundreds of microfabricated high aspect ratio spray tips formed from silicon using deep reactive ion etching (DRIE).[71] The multi-electrospray nozzle chip is now available commercially (Nanomate, Advion, Ithaca, NY).[76] However, no on-chip microfluidic components have been developed.

Another commercial device (Agilent, Santa Clara, CA) has been developed that uses a multi-layer polyimide chip with an integrated spray tip formed by laser ablation.[66, 77] The chip consists of enrichment and separation channels and an integrated electrospray tip.[78] The microfluidic chip is inserted between a stator and a rotary switching valve. The off-chip valving reduces the chip complexity, but increases the off-chip size and complexity. During operation, the sample is introduced into the enrichment column, which traps the peptides. By switching the valve, trapped peptides are eluted and injected onto the separation column. The performance of this microfluidic device coupled to MS is comparable to conventional HPLC-ESI methods.[79]

1.2.2 MALDI Interfaces

MALDI is typically carried out on crystallized sample spots containing matrix and analyte, most often under vacuum. Off-line coupling can be accomplished by dropping, spraying, or spotting the sample onto a sample target and adding matrix for analysis.[80-84] On-line coupling of microfluidic devices to MALDI is challenging, but can be achieved using spray,[85-87] continuous flow,[88, 89] or mechanical interfaces.[90, 91] Of these, only continuous flow and mechanical interfaces have been coupled to microfluidic chips.

<u>On-line MALDI</u>

On-line interfaces for MALDI MS can be grouped into those using (1) aerosol particles, (2) capillaries, or (3) mechanical means to deliver the matrix and analyte into the mass spectrometer.[22] Aerosol MALDI methods use a spray of particles to deliver the sample to a time-of-flight mass spectrometer. [85] The particles are dried in a heated tube and irradiated by a pulsed UV laser to form ions. A flow rate of 0.5 mL/min is typical and, for this reason, the approach is not suited for microfluidic chip interfacing, which requires the use of much smaller volume flow rates. The capillary-based continuous flow (CF) MALDI interface uses a narrow bore capillary to deliver analyte into a liquid matrix to the point of laser desorption and ionization.[92] Typical flow

rates are a few μL/min. A continuous pressure driven self-activating flow on-chip microfluidic device connected to a MALDI-TOF mass spectrometer has been reported for on-line sample transfer of material and monitoring of reaction products.[88] This approach has been adapted for microfluidic chip analysis using the vacuum of the mass spectrometer to pull the reactants through the chip and to move them into position for analysis.[89] The microfluidic chip was prepared from a borosilicate glass wafer consisting of inlet reservoirs, an exit reservoir, and a reaction microchannel with a 1.2 μL active volume. The integration was achieved by placing the micro-device on a modified target plate and loading the reagents before inserting it into the mass spectrometer. Chemical syntheses as well as biochemical reactions were carried out entirely inside the vacuum chamber and analyzed by MALDI-TOF MS.

Two mechanical interfaces for on-line MALDI have been developed; both of them are compatible with more widely used solid matrices. With one of these approaches, liquid samples are transported into the mass spectrometer through a capillary at a flow rate of hundreds of nL/min and deposited onto a rotating quartz wheel.[93] Solvent evaporation results in a thin sample trace on the wheel, which is rotated into position for laser desorption. The most significant drawback to this continuous vacuum deposition method is the requirement for manual cleaning of the wheel. A second mechanical approach is a modification of the rotating ball inlet. [94, 95] For the rotating ball MALDI analysis, a solution containing matrix and analyte are delivered to the surface of a stainless steel ball that rotates several times each minute. As the ball rotates, the solution is exposed to vacuum where the volatile solvent evaporates leaving the matrix and analyte on the rotating ball. When the ball has rotated one-half turn, it is in position for laser desorption and thus, MALDI analysis using a time-of-flight mass spectrometer.

Several studies have been performed for incorporating chip-based capillary electrophoresis (CE) with MS.[96-101] Direct coupling of microchip CE separations with the

rotating ball inlet has been described.[90, 91] PMMA microfluidic chips were hot embossed and mechanically cut to generate a sharp V-shaped tip at the channel exit of the microchip. The tip was held in contact with a rotating ball at atmospheric pressure. The interface was demonstrated with an on-chip CE separation of tryptic peptides and peptide standards. The separation was performed in an 8 cm long channel that was 50 μm wide and 100 μm deep. The chip effluent was deposited onto the rotating ball and the matrix solution was applied to the ball surface as well using an external capillary. This system demonstrated the feasibility of on-chip CE separations followed by on-line MS detection of the tryptic peptides of cytochrome *c* as well as a series of standard peptides. The main advantage of this on-line microchip interface was the capability of continuous deposition on the surface of a rotating ball at atmospheric pressure and introduction into the vacuum chamber without the need for breaking vacuum.

Off-line with Deposition

In off-line MALDI, samples are deposited directly on a target for later analysis in the mass spectrometer. The most direct method for sample deposition is spotting, for example with a robotic target spotter. Here the matrix is mixed with the analyte before deposition or spotted onto a matrix-coated target. In this manner, fractions from a microcolumn HPLC separation can be collected onto a MALDI target. In one example, [102] the microcolumn was packed with 5 μm C_{18} modified silica particles. The matrix solution was coaxially mixed with fractions using a capillary mounted at the exit of the separation column. The fraction volumes from the system were approximately 145 nL with a 1 mm spot size. Using this system, peptides contained in single neurons from a snail were fractioned and identified by MALDI-MS.

The primary difficulty with target spotting is the relatively large volume contained in a droplet from a small diameter capillary. For example, a 50 μm capillary produces droplets that are approximately 300 nL, which can be a significant volume compared to peak volumes

emanating from microfluidic separation components. It can also be difficult to control the spotting volume with high precision. To overcome these problems, piezoelectric dispensing of samples onto the MALDI target can be used.[103] A piezoelectric droplet dispenser has been developed for interfacing a microfluidic chip to a high-density array of nanovials etched into a silicon MALDI target.[82] The nanovials were 300 µm square and 20 µm deep and served to collect and concentrate the sample by multiple droplet depositions on the same spot. The device generated droplets ranging from 65 pL to 300 nL at a droplet frequency of 50-100 Hz. The system was demonstrated with peptides generated from a chip tryptic-based microreactor.

An alternate sampling approach is electrospray deposition onto a MALDI target. Several studies have demonstrated the viability of electrospray deposition of eluent from CE, HPLC, and size-exclusion chromatography (SEC) onto the MALDI plate.[104] The eluent is delivered to the electrospray capillary operated at 2 to 4 kV and the spray is directed onto a MALDI target several cm away. Rapid solvent evaporation from the small droplets leads to homogeneous spots on the target. A hydrophobic membrane electrospray deposition device has been developed for interfacing polycarbonate microfluidic chips to MALDI.[83] The system consisted of a 50 µm thick polytetrafluoroethylene (PTFE) membrane thermally annealed to the outlet of a PC microfluidic chip. The PTFE provided a hydrophobic spray surface and a T-junction was used for the electrical contact for the electrospray and the analyte solution was flowed through the chip with a syringe. Multiple electrospray tips deposited parallel sample spots spaced 150 µm apart on the MALDI target.

Off-line MALDI Directly from the Microfluidic Chip

There have been several innovative off-line approaches that use the chip itself as the MALDI target. For example, the rapid open access channel electrophoresis (ROACHE) technique employs an electrophoretic separation in an open channel.[96] The separation is run for a

period of time without eluting the sample. The solvent is then evaporated from the channel before transfer of the entire chip into the MALDI source under vacuum.

In a similar approach, a UV-embossed polymeric chip was developed for protein separation by capillary isoelectric focusing (CIEF) and MALDI analysis.[105] The CIEF technique separates proteins based on their amphoteric properties in a pH gradient under an electric field. It offers the advantages of high resolution (up to 0.05 pI), low sample consumption, and little effect on sample concentration. Five different microfluidic chips were fabricated from UV-curable resins that were exposed to UV light on a soft PDMS mold. After the CIEF separation, a matrix was sprayed onto the separated proteins using electrospray, which produced small and uniform crystals without sample diffusion. The chip was then inserted into the mass spectrometer for MALDI analysis. Among the tested materials, a polyester-based resin produced the highest mass signal and best signal-to-noise ratio. One of the problems with coupling CIEF to MALDI is evaporation of the solvent due to Joule heating that is generated by the strong electric field. To overcome this problem, a removable cover plate was developed.[51] While the separation is performed the microchannel is covered; after the separation is complete, the cover plate is removed for MALDI analysis.

Another approach using a removable cover plate is a CIEF chip sealed with a removable resin tape.[49] In this approach, CIEF is performed in a serpentine channel to achieve high resolution. Four meandering microchannels were fabricated on a glass plate using photolithography and dry etching. The dimensions of each channel were 400 μm wide, 10 μm deep, and 60 mm long. Sample proteins were separated in the resin tape covered channel. Once the separation was complete, the samples were immediately frozen to prevent diffusion. The resin tape was then removed and the samples were freeze-dried for 15 min. After the dried channels were treated with a matrix solution, the chip was placed in a MALDI-TOF MS. The

mass spectra were obtained at 500 μm increments along the channel and then a two-dimensional (2-D) map was constructed by plotting p*I* versus *m/z*. The removable resin tape allowed easy access for matrix addition to the separated samples yet prevented the sample solution from drying out during the separation. In addition, the freeze-drying method limited redistribution of the sample solution in the channel during evaporation, which compared favorably to a heat-drying process.

Infrared MALDI from a capillary gel microfluidic chip has been developed using a pulsed infrared source with the gel acting as an intrinsic matrix.[47, 48] The chip was fabricated from PMMA with a removable PDMS cover slip. The microchip had a standard tee channel, which was 300 μm wide and 150 μm deep. A cross-linked gel was formed in the channels by polymerization. After gel electrophoresis, the cover was removed and either the chip or the cover plate was mounted on a modified MALDI target holder for analysis. The channel was irradiated with 2.95 μm radiation from a pulsed optical parametric oscillator (OPO), which was coincident with IR absorption wavelength of the gel and water within the gel. An advantage of the IR laser when combined with gel separations for on-chip detection is the greater depth of penetration compared to a UV laser, thereby overcoming the limited accessibility to biomolecules inside the gel structure.

A combination surface plasmon resonance (SPR) and MALDI chip has been developed for direct MS detection of isolated proteins. The combination of SPR and MS was first described in 1996,[106, 107] and since then several approaches using SPR sensor chips have been described.[108-112] SPR is an excellent method for label-free protein quantification and investigations of protein interactions with surface-immobilized ligands or antibodies. The addition of MS allows for the determination of protein structure. Recently, a novel SPR-MS array platform for high-throughput analysis of proteins was described.[113] In this work, self-assembled monolayers were formed

using 11-mecaptoundecanoic acid on a gold-coated glass chip and then the carbonyl groups were activated with 1,1"-carbonyldimidazole. The arrays consisted of five different antibodies immobilized on 10×10 wells with 450 μm spacing. After individual target proteins were deposited on the array, SPR images were obtained across the surface of the chip to monitor binding of target proteins to their corresponding antibodies. Immuno-captured proteins were then directly analyzed with MALDI MS. Specific proteins were detected from individual spots on this SPR chip with negligible cross-reactivity.

1.3 Materials for Microfabrication

Over the past decade, fabrication technologies for microfluidics have evolved with a variety of new materials employed for building devices.[114-117] Glass and fused silica are particularly beneficial for proteomics analyses due to their well-defined surface properties, established microfabrication techniques, good electroosmotic characteristics, and suitability for optical detection. In addition, various surface coating techniques and modification methodologies previously developed for capillary electrophoresis (CE) can be easily transferred to the microchip format. For these reasons, glass-based substrates for microfluidics have been used for many electrophoretic separation applications.[114, 118, 119] Alternately, conductive materials such as glassy carbon can be used as a substrate for the microfluidic device in cases where the optical properties of the material are less important, for example when used as an interface to MS.[120] Although these materials allow for high spatial definition and reproducible fabrication results, the main drawback to fabricating microchips in glass or fused silica is the unit cost for large production runs and their fragility, which can make them difficult to produce at low-cost. Furthermore, processing steps such as wet etching using corrosive agents such as hydrofluoric acid (HF) require special safety precautions and produce low aspect ratio structures (aspect ratio is defined as the ratio of the structure height to lateral width).[121]

14

Recently, polymer-based microfluidic devices have been developed as alternatives to glass-based substrates.[122, 123] The main advantages of polymers compared to glass or quartz is the ease in fabricating large quantities of devices at low-cost using micro-replication technologies. In addition, high aspect ratio mixed-scale structures with multiple levels can be constructed and a wide range of materials with different physical properties and surface-modification protocols can be employed.[124] The most widely used polymers for microfluidic devices are polydimethylsiloxane (PDMS),[125, 126] poly(ethylene terephthalate) (PET),[127, 128] poly(methyl methacrylate) (PMMA),[129, 130] and polycarbonate (PC).[131] These polymers are easily machined with the substrate thermally bonded to the cover plate due to their lower glass transition temperature compared to glass or quartz. For example, glass requires a temperature of 600 ºC or more for thermal fusion bonding, whereas polymer substrates require much lower temperatures: ~75 ºC for PET, ~106 ºC for PMMA, and ~148 ºC for PC.[124] PDMS microfluidic devices have not been widely used for proteomic analysis due to their poor surface properties that lead to the adsorbtion of proteins; however, surfactants such as sodium dodecyl sulfate can prevent sticking.[132]

Surface modification methods have been developed for polymer substrates with immobilization chemistries that are simple and robust compared to the siloxane chemistry typically used for glass. For example, to suppress the electroosmotic flow (EOF) in CE separations with polymer substrates, different reagents such as diaminoalkanes, surfactants, and poly(ethylene glycol) can be used as dynamic or covalently-tethered surface coating materials.[133-136] Covalent antibody and enzyme surface immobilization techniques have also been demonstrated for polymer-based microfluidics for isolation of target proteins, digestion, and immunoassay applications.[137] The high production rates achievable using polymer-based chips result in low-cost devices that can be disposable and thereby eliminate contamination between

samples, which is an important consideration for clinical applications where sample carryover artifacts cannot be tolerated.[138]

One of the main challenges associated with polymer microfluidic devices is their relatively low thermal conductivity compared to glass. This can result in significant Joule heating due to current flow through an electrokinetically driven buffer solution such as those employed in electrophoretic separations.[139] Also, when nonconductive polymers are used for MALDI sample arrays, precise measurements for proteins and peptides are challenging due to charge accumulation on the surface during laser irradiation, resulting in ion mass shifts.[140] Furthermore, adequate heat dissipation is critical for temperature-sensitive chemical reactions and thermally labile analytes. Polymer chips are also sensitive to organic solvents and may not be sufficiently transparent at wavelengths required for monitoring optical responses from the chip. Autofluorescence can be a problem as well. In most cases, the optical properties of glass or quartz are superior to those of most polymers.

1.4 Microfluidic MS Devices for Proteomics

Although proteomic analysis methods have advanced significantly in recent years, many analysis steps such as digestion, separation, and other necessary sample preparation steps remain time consuming and labor-intensive.[141] Achieving high sensitivity analysis with low sample consumption and high protein sequence coverage are the principal analytical challenges of many proteomic projects.[142] Microfluidic systems have been proposed as a means of automating sequential sample pre-treatment steps and also as a means to increase sample throughput in parallel proteomic analysis.[82, 143] These devices have the advantages of improved portability due to miniaturization, reduced sample and reagent consumption, and accelerated speed of reaction and analysis for high-throughput and highly parallel analysis.[37] In addition, multiple processing steps can be seamlessly integrated to a single chip or multiple chips to allow fully automated

sample processing that can address the labor-intensive issues associated with proteomic analyses. Different types of fluidic architectures can be invoked with chips to realize unique processing strategies compared to the conventional bench-top approaches that can offer significantly reduced processing times as well.

1.4.1 Sample Purification

A sample is typically purified to remove salts and buffers and concentrate the sample prior to analysis by MS and some of these procedures have been adapted to chip formats. An on-line desalting method for ESI MS has been developed.[144] In this device, a hydrophobic poly(vinylidene difluoride), PVDF, membrane was integrated into an inlet channel of a polyimide chip. This membrane was used for capturing target analytes and, after removing salts by washing with water, a methanol/water solution was pumped into the chip to elute the retained analytes. The cleanup of drugs, peptides, and proteins was demonstrated and it was found that the background was comparable to salt-free solutions.

A novel compact disk (CD) microfluidic chip for parallel processing of protein digests for MALDI has been described.[145] The microfluidic CD chip is available commercially from Gyros AB, Uppsala, Sweden.[145, 146] Spinning the chip leads to a centrifugal force that was used to move liquids through multiple microstructures. For example, samples can be concentrated and desalted in 96 micro-columns packed with 15 μm C_{18} beads with salts and impurities directed to a waste outlet by the centrifugal force. Samples are eluted from the column using a matrix solution controlled by the disk rotation speed. After the microfluidic analysis, the chip is mounted in the mass spectrometer for MALDI. In addition, the CD chip technology has been used for the detection of phosphopeptides at the femtomole level.[147] In this application, an immobilized metal affinity chromatography (IMAC) resin was packed into each microcolumn for phosphopeptide enrichment before MS analysis. Polymeric integrated selective enrichment

17

target (ISET) has been developed for purification and concentration of proteomic sample before MALDI MS analysis.[148] This polymeric ISET device was fabricated in polyetheretherketone (PEEK) by injection molding. The device was composed of an array of perforated nanovials filled with beads for solid-phase extraction. Compared to a commercial affinity-based bed, such as ZipTip sample preparation for human seminal plasma, the ISET device offered higher capture capacity for biomolecules.

A method for manipulating small volumes of sample and matrix for MALDI has been demonstrated using the electrowetting-on-dielectric (EWOD) principle.[149, 150] An EWOD microfluidic chip consisted of a bottom plate with electrodes, a top plate, and spacers. The bottom plate was made from quartz wafers coated with polysilicon from which electrodes were formed by photolithography and reactive ion etching. The top plate was made from indium-tin oxide (ITO) coated glass plates. For the EWOD technique, the local wettability of a surface is manipulated by the application of voltages between electrodes placed beneath hydrophobic dielectric layers. This allows small liquid droplets to be moved on the surface through the use of applied voltages. Here, droplets containing the peptide and protein analytes were moved to specific positions on the chip. Water soluble impurities in a sample were removed by passing droplets of water over the spots. After impurity removal, a droplet of MALDI matrix was moved to the sample spot. When deposition was complete and the plate dried, MALDI spectra were collected directly from the device, which was attached to a stainless steel MALDI target. A modified EWOD microfluidic device has been developed for the investigation of pre-steady-state chemical kinetics.[151] This microfluidic device consisting of individually addressable Cr/Au electrodes was capable of controlling precise time intervals for droplets to initiate a reaction and to quench the reaction.

1.4.2   Separation

Microfluidic chip separations for proteomics uses either CE or liquid chromatography

(LC) with packed beads or porous monolith stationary phases.[43, 152, 153] CE is suited to the

microfluidic chip formats due to fast separation times and the ability to drive the flow with an

electric field rather than a mechanical pump. With LC, the microfluidic channels typically must

contain packed beds or monoliths to reduce the diffusion distance for efficient separations.

Capillary Electrophoresis

There have been a number of approaches to coupling chip-based CE separations to

MS.[154-156] These have used different variants of CE, such as capillary gel electrophoresis

(CGE),[157, 158] capillary zone electrophoresis (CZE),[159] micellar electrokinetic chromatography

(MEKC),[160] and isoelectric focusing (IEF).[161] An electrophoresis separation of biological

mixtures in open channels has been coupled off-line with MALDI-MS.[96] The chip was made of

glass with 250 μm wide and 250 μm deep channels. After the CE separation of oligosaccharides

and peptides, the chip was placed on a moving stage installed inside the source chamber for

MALDI analysis directly from the chip.

A microfluidic chip was developed for CE separations coupled to ESI MS.[43] The device

was made from a borosilicate glass substrate with a 75 µm wide and 10 µm deep separation

channel. The electrospray was generated at the corner of the chip. The channel surfaces were

coated with polyamine to minimize surface interactions and enhance electroosmotic flow.

Peptides and proteins were tested for on-chip CE separation coupled to MS. The separation

efficiency of this chip was about 200,000 theoretical plates for the 20.5 cm long channel with a

calculated peak capacity of 43. The separation was accomplished in less than a minute to several

minutes depending on the channel length.

19

Several technical challenges remain for on-chip CE separations.[162] For example, separation efficiency can be reduced due to the interaction of analytes with chip surfaces. Additionally, the injection volume is limited for CE microchip separations, necessitating a sample enrichment unit such as solid-phase extraction prior to injection for some proteomic applications directed toward analyzing low abundant proteins.[163] Further, there remains the problem of the compatibility of the reagents used for the on-chip separations with the on-line electrospray. A liquid junction or sheath flow may be required to couple on-chip CE with ESI-MS because separation buffers and other reagents used for the separation are not compatible with ESI.[58]

Liquid Chromatography

LC capillary columns have inner diameters in the range of 75 to 500 µm that are similar to the sizes of microfluidic channels and, therefore, separation protocols can be readily adapted to a chip format.[164] Chip separation channels are typically under 300 µm internal diameter and are non-cylindrical, for example square, rectangular, or semicircular, and are fabricated in silicon, glass, quartz, or polymer.[42] The stationary phase can be formed using packed beads or on monolithic support formed by *in situ* polymerization.

Packed bead chromatography inside a microchannel is similar to conventional HPLC. Thus, many established concepts can be directly applied to microfluidic systems for proteomic analysis. However, packing a microchannel with beads is a technically difficult process due to the resistance to fluid flow, which can result in uneven packing and voids within a column.[165] The high pressure in the channels can cause leaks or bubbles and it can be difficult to introduce frits or other structures to trap the beads and prevent their movement through the channels.

To create a packed stationary phase for microfluidic chips, the channel can be filled with beads having diameters between 3 and 5 µm and pore sizes selected according to the analyte and

20

required separation efficiency. For example, 3.5 μm C_{18} beads with 30 nm pore size were used to pack a chip separation channel, which had 75 μm width, 50 μm depth, and 45 mm length.[66] This chip was demonstrated for the separation of tryptic peptides of BSA with on-line ESI-MS analysis. The retention times for tryptic peptide peaks from an extracted ion chromatogram were reproducible over 3 runs with less than 0.1 min standard deviation. Recently, the relation between the packing density and separation efficiency of packed-bed microchips was investigated.[152] A custom-built stainless steel holder and ultrasonication were used for high packing density. The separation channel had a 75 μm × 50 μm trapezoidal cross section and the packing material used was 5 μm C_{18} with an 80 Å pore size. These optimized packing procedures resulted in separation efficiencies for organic compounds comparable to those of commercial nano-HPLC.

<u>Monolithic Supports</u>

Monolithic supports for HPLC stationary phases were first introduced twenty years ago and have emerged as an alternative to packed columns due to the simplicity of *in situ* polymerization.[166-168] These columns are completely filled with porous material and thus have no interparticle voids, which allows all of the mobile phase to flow through the pores of the stationary phase. Aside from these merits, monolithic columns have several advantages over packed columns for microfluidic chip applications, including simple modification of porosity, surface area, and functionality and the ability to form the column in place without the need for retaining frits.[169] Disadvantages are the limited chromatographic media[66, 169] and difficulties in producing homogeneous supports due to large differences in polarity of monomers.[50, 170]

Polymer and silica-based monolithic columns have been developed for microfluidic separations in proteomics;[171] the former have shown excellent properties for large molecule separations, whereas the latter are desirable for the separation of small molecules. A cyclic olefin

copolymer (COC) microfluidic device coupled off-line to MALDI-MS has been reported. [172] The chip was prepared with an array of methacrylate monolithic columns that were formed by UV-initiated polymerization. For peptide mass mapping of digested BSA, a 59% sequence coverage was obtained using the on-chip separation device with MALDI-MS analysis compared to 23% sequence coverage without separation. The chip was tested for separation efficiency and reproducibility of peptide mixtures in each column. A sensitivity test showed that a target peptide at 10 fmol/μL could be identified in the presence of 10 pmol/μL digested BSA.

High-performance thin-layer chromatography has been coupled to MS,[173, 174] and there have been several approaches that use direct laser desorption analysis of materials directly from TLC plates.[175-177] A novel approach for direct coupling of thin-layer chromatography to infrared MALDI was developed for the analysis of gangliosides from cultured cells.[176] The liquid matrix, glycerol, was used for MALDI sample preparation. Two different protocols for matrix addition to the silica gel were evaluated, spotting and spraying. An orthogonal time-of-flight mass spectrometer was used to obtain high mass accuracy, which otherwise would have been reduced by the irregular surface of the TLC plate. The lateral resolution for spots on the target was 200 μm.

A porous polymer monolith layer attached to a glass plate has been used for TLC separations of peptides and proteins as well as small molecules with subsequent direct detection by MALDI.[50] The polymer monolith layers were prepared using photoinitiated polymerization of butyl methacrylate and ethylene dimethacrylate monomers on activated glass plates. The thickness of the monolith layers was controlled using a Teflon gasket that was placed on a glass plate or MALDI target. While photopolymerized monolith layers can be used to separate small from large molecules, a greater peak capacity and fewer polymer layers is necessary for the

separation of complex samples. Also, longitudinal diffusion and surface irregularities of the polymer layer can reduce the sensitivity and ionization efficiency in the MALDI analysis.

1.4.3   Enzymatic Digestion

Efficient digestion is an essential tool for protein identification with bottom-up proteomic strategies.[178, 179] Three different approaches can be used for proteolytic digestion: in-gel,[180] in-solution,[30] or solid phase.[181] In-gel digestion is accomplished by cutting spots from two-dimensional gel electrophoretic bands that contain the proteins of interest that are then subjected to *in situ* digestion.[182] Drawbacks to this method are limited accessibility to the proteins inside the gel[183] and gel destaining procedures that can cause poor digestion yields due to residual destaining solvents.[184] Further, the process cannot easily be moved to microfluidic chip formats to realize process automation. A second approach is to digest proteins in-solution. This approach requires long incubation times due to the need for low proteolytic enzyme concentrations to minimize autodigestion artifacts and the need to run with relatively high temperatures to achieve high digestion efficiencies.[185] Excessively high temperatures, enzyme concentrations, or reaction times can lead to autolysis of trypsin, non-specific cleavage, and deamidation.[185-187]

Solid-phase digestion uses proteolytic enzymes chemically immobilized or adsorbed on the surface of a solid support.[137, 188] This digestion protocol has the advantages of fast response, low sample consumption, and high throughput,[189] and it is easily adaptable to microfluidic chip formats. A solid-phase microreactor minimizes sample loss during treatment and reduces autolysis products of proteolytic enzymes;[190] the short diffusion distance for properly designed reactors, and a high enzyme-to-substrate concentration ratio results in higher digestion efficiencies compared to in-solution digestion.[40]

The digestion efficiency of solid-phase microreactors depends on the geometry of the reactor, the digestion temperature, the composition of digestion solvents, and the transport

velocity of the target protein through the reactor.[40, 191-193] Also, the digestion efficiency can be enhanced by physical means such as microwave energy[194] or ultrasound.[195, 196] Organic solvents can improve digestion efficiency by denaturing the proteins; however, this can be a disadvantage for solid-phase digestion due to damage of the immobilized enzyme by the solvent.[197] Thermal and electrical denaturation are relatively free of contamination because additional reagents are not added.[198, 199] However, these methods require additional control systems for temperature and voltage, which increases the overall chip complexity.

The geometry of the microreactor can be in an open channel or a three-dimensional (3-D) structure. An open channel format is the simplest configuration, but digestion efficiency is limited by the relatively long diffusional distances, which can limit the digestion rate. Also, diffusion rates of proteins depend on their concentrations as well.[200] Lower diffusion rates are expected at higher concentrations of proteins in an open channel, thereby achieving low digestion efficiency due to limited encounter numbers between proteolytic enzymes and proteins. A 3-D solid phase reactor format can be configured from a monolithic porous network,[44, 201] or a packed channel.[202] The high surface-to-volume ratio compared to open channel increases the digestion efficiency due to the lower diffusion path length, which allows for more encounters between the substrate and immobilized enzyme.[203] A microfluidic chip packed with trypsin-derivatized beads in a fluidic channel has been reported.[202] The bead-packed chip provided faster protein digestion and fewer trypsin autolysis products compared to a homogeneous digestion.

Solid-phase microreactors can be formed *in situ* by immobilization of enzymes through covalent attachment to supports or encapsulation within gel matrices.[44, 181, 201, 204] This avoids the difficulties arising from packing beads into the microchannels. Monolithic supports for immobilizing proteolytic enzymes can be generated through a polymerization reaction of a monomer solution into a microfluidic channel.[205] For example, a porous organic polymer

monolithic microreactor was developed in which trypsin was immobilized within the monolith using azlactone functional groups for covalent attachment of the enzyme.[201, 204] The sequence coverage of tryptic peptides from myoglobin was determined by off-line MALDI and found to be 67% for a 12 s residence time. A silica sol-gel monolith containing zeolite nanoparticles has been reported.[181] This device had a high surface area for the immobilized enzyme, allowing for a high load level within the microreactor. A 0.5 μL volume containing 0.2 μg/μL of the proteins cytochrome c and BSA were digested within 5 s in the microreactor as indicated by off-line MALDI-TOF MS. The bioreactor could be used repeatedly and the enzyme remained active for more than a month when it was stored at temperatures below 4 ºC. A pepsin microreactor was developed using a sol-gel monolithic column photo-polymerized within a fused silica capillary.[44] The column was used for on-line ESI CE/MS. Although monolithic microreactors are fast and efficient, it can require more than 24 h for their preparation and can be difficult to make them reproducibly.

A 3-D microreactor can be created using microstructures within the channel, which bypasses problems associated both with bead packing and with monolith formation in the channel.[206, 207] The channel structure is fixed, for example by the mold master when used to replicate a polymeric device, which provides a reproducible microreactor. Furthermore, the support structures are placed in a desired location within the device and can provide unrestricted substrate access to the immobilized enzyme.

1.4.4   Cell Culture

New capabilities for quick and reliable identification of microorganisms are required for the detection of environmental pathogens and for clinical applications such as cancer screening, the detection of blood-borne pathogens, respiratory tract infections, and quality analysis of donated blood.[208-211] Cell culturing is an essential technique in the biological sciences as well as

in many important clinical applications.[212] Conventional cell cultivation methods have been developed over many decades.[213-215] In general, cell culturing is performed in an incubator using either agarose gel or liquid broth culture media. Detection and identification can be accomplished using dye-conjugated antibodies.[216] Conventional cell culture processes require large fluid volumes, bench-scale equipment, large quantities of supplies, and are labor-intensive. Also, it can be difficult to control the cell culture environment, which can result in considerable variation during the growth of the microorganisms.[217] For high-throughput screening and bioprocess development, small volume micro-scale bioreactors are advantageous for rapid and accurate identification of both natural and bioengineered microorganisms.[218, 219]

Microfluidic devices have been used for cell culturing due to their numerous advantages over traditional cell culture methods.[220] Microfluidic devices can be batch-fabricated with provisions for automated cell loading, fluid exchange, and cell quantification without contamination.[221, 222] The micro-scale components allow the use of small solvent volumes with minimal evaporation due to their closed architecture. Compared to typical 2-D and 3-D culture reactors, which require milliliter quantities of broth nutrients, the volume for microfluidic culture devices is smaller by more than three orders of magnitude. In addition, microfluidic devices allow more precise control of growing conditions such as temperature, pH, and nutrients, thereby providing more accurate identification of species.[223, 224] Heat and mass transfer are fast on a microfluidic chip so that the conditions for cell growth can be changed quickly.[225, 226] The microenvironment can be precisely controlled, and cells can be isolated from each other to create conditions of uniform growth.[227, 228] Cells can also be subjected to mechanical strain and shear in the physiological range in order to affect their physical and biochemical properties.[229]

Various materials are used to construct microfluidic devices for cell culture: glass, silica, and polymers. Glass-based substrates have been used for microfluidic devices due to their well-

26

defined surface properties, established microfabrication methods, and suitability for optical detection.[1] However, the substrates require a temperature of more than 600 ℃ for thermal bonding to make a channel. Also, the substrates are difficult and expensive to mass produce a microfluidic device. Different polymers have been used for microfluidic cell culturing. Poly(dimethylsiloxane) (PDMS) is an elastomeric polymer that can be used for cell-based applications due to its nontoxic and gas permeable properties.[230, 231] The channels of PDMS devices can be sealed without heat adhesive or heat. PMMA is a thermoplastic polymer that can be mass-produced by injection molding or hot-embossing.[124] It has optical properties that are advantageous for UV and fluorescence detection. PDMS has been used to make microfluidic devices for the culture of bacterial and yeast cells under precisely controlled conditions for cell growth.[232] Human colon cells were cultured in an integrated PMMA chip and compared with those cultured in culture flasks.[225] *Escherichia coli* (*E. coli*) cells were cultured in a microbioreactor composed of PDMS and PMMA that integrated real-time measurements of optical density, pH, and dissolved oxygen.[233] A high aspect ratio PDMS microfluidic device with an array of microchambers was recently developed for culturing human carcinoma cells.[234]

1.5 Research Objectives

The objective of this research was to develop microfluidic devices for the fast and effective analysis of proteins with specific focus on coupling microfluidic devices to off-line MALDI-MS detection. In order to achieve this goal, the specific aims of the project were (1) to develop microfluidic bioreactors coupled with MALDI MS analysis for protein digestions, (2) to evaluate different strategies of sample depositions for MALDI MS analysis, and (3) to develop microfluidic cell culturing devices for MALDI MS detections of whole cells. The first set of experiments, described in Chapter 3, was designed to develop an open channel bioreactor operated by a pressure-driven flow for protein sample preparations. A micropost structured

bioreactor was fabricated to obtain higher digestion efficiencies and the experiments, demonstrating its performance for sample preparation is discussed in Chapter 4. The second set of experiments, described in Chapter 5, used a continuous deposition to deposit low-volume samples with a small spot size on a MALDI target and to compare with a spotting deposition. For the third set of experiments, novel microfluidic culturing devices for MALDI MS detection, were evaluated for fingerprint analysis of bacteria and there are described in Chapters 6 and 7.

Part of the work reported in this chapter has been published in *Analytica Chimica Acta*.[2]

2.1 Overview of Mass Spectrometry

Mass spectrometry (MS) is one of the most common analytical techniques used to determine the masses of molecules by measuring the mass-to-charge ratios (*m/z*) of their ions. A mass spectrometer is composed of four basic parts as shown in Figure 2-1: A sample inlet, an ion source, a mass analyzer, and an ion detector. Samples can be introduced into the ionization region of the instrument using direct insertion, such as a sample probe or a sample target plate for laser desorption ionization. Samples in the gas phase or in solution can be directly infused into the ionization region using a capillary. In the ion source, the samples are converted into gas-phase ions.
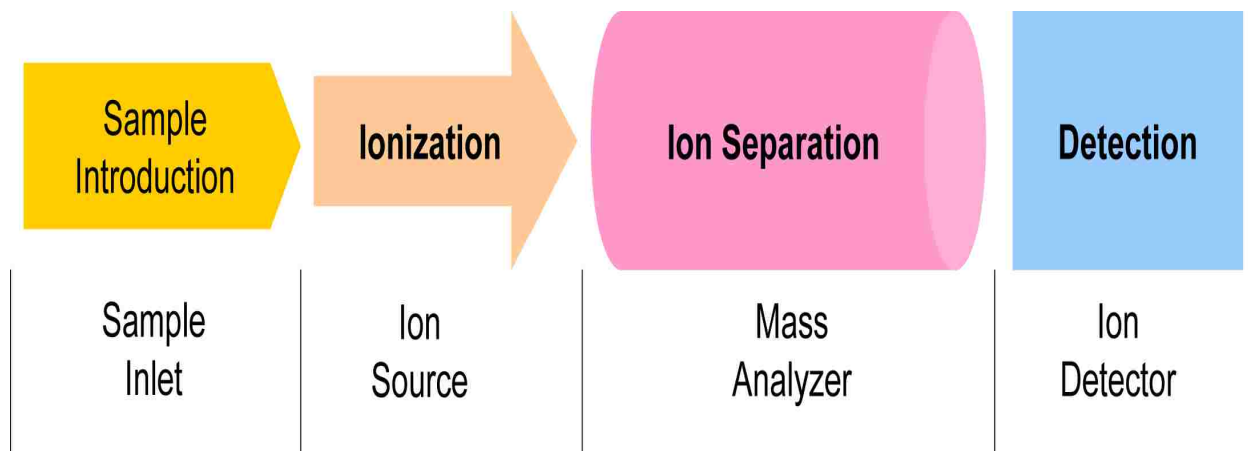
Figure 2-1. Components of a Mass Spectrometer.

The most widely used types of ionization for the analysis of large molecules are matrix-assisted laser desorption/ionization (MALDI) and electrospray ionization (ESI).[235, 236] These ionization techniques are called "soft ionization" that produce ions representing the intact

molecules with little or no fragmentation due to low internal energy. The techniques are designed to produce ions of biomolecules such as peptides, proteins, oligonucleotides, and lipids without fragmenting them. Ions generated in the ion source are transferred into a mass analyzer where thery are separated according to their *m/z* ratios. A detector measures the ion current for the separated ions. In this work, a MALDI-TOF mass spectrometer was used for the detection of proteins and peptides.

2.1.1   Matrix-Assisted Laser Desorption/Ionization

Matrix-assisted laser desorption/ionization (MALDI) is a "soft" ionization technique that has been widely used in biological mass spectrometry. It can provide molecular weight and structural information for intact biomolecules.[237] In MALDI, the molecules to be analyzed are deposited onto a metal target plate with an excess of an UV-absorbing organic compound called a matrix, dried and co-crystallized on the surface of the target.[238] The target is inserted into the mass spectrometer and ionization is performed with the radiation of a pulsed laser of 0.5 to 25 ns duration and 20 to 200 J/m^2 fluence onto the target.[239] Various lasers have been used to irradiate the co-crystallized samples such as N_2 laser (337 nm), Nd:YAG laser (355, 266 nm), KrF excimer laser (248 nm), and ArF excimer laser (193 nm).[240-242]

The matrix plays an important role in this ionization technique by absorbing the laser energy and causing desorption of the matrix, which entrains the analyte in the gas-phase plume. The desorbed analyte is then ionized by proton-transfer reactions.[241] In addition, the matrix must be soluble in solvents compatible with analytes and must be vacuum stable. The choice of matrix plays a role in the MALDI analysis of biomoelcules. Several common UV matrices and their applications are shown in Table 2-1.[243]

Table 2-1. Some commonly used UV matrices.

Matrix	Structure	$(M+H)^+$ (mono)	Laser	Sample Types
α-cyano-4-hydroxycinnamic acid **CHCA**		190.0504	337 355	Polar biomolecules, 500<MW<10,000
2,5-dihydroxybenzoic acid (Gentisic acid) **DHB**		155.0344	337 355	Polar biomolecules, 500<MW<5,000
trans-3,5-dimethoxy-4-hydroxycinnamic acid (Sinapinic acid, Sinapic acid) **SA**		225.0763	266 337 355	Polar biomolecules, MW>10,000
3-hydroxypicolinic acid **HPA**		140.0348	337 355	oligonucleotides

2.1.2 Time-of-Flight Mass Spectrometry

Time-of-flight (TOF) is a common mass analyzer. The primary advantage of TOF over the other mass analyzers is the acquisition speed.[244] An entire mass spectrum can be obtained simultaneously only limited by the time it takes ions to travel the flight tube, typically within hundreds of microseconds. A TOF is a vacuum chamber with a pressure of 10^{-6} torr or lower to avoid target ion collisions with background gas molecules. TOF mass spectrometer uses the differences in the flight time of ions through a field free region to separate ions of different m/z. Once ions are generated in the source, they are accelerated into the flight tube. All ions have the same kinetic energy if differences in initial position and velocities are neglected. In the field-free drift region, the lighter ions travel faster and arrive at the detector first due to their higher velocity (v). The arrival time of ions at the detector depends on their mass (m) according to;

$$E_{KE} = \frac{1}{2}mv^2 \tag{2-1}$$

where E_{KE} is the kinetic energy of the ions, v is the velocity, and m is the ion mass.[245] The kinetic energy of the ions is determined by the acceleration voltage;

$$E_{KE} = zeV \tag{2-2}$$

where z is the charge number of the ion, e is the charge of an electron, and V is the acceleration voltage. Equation 2-1 can be solved for velocity in the field free region giving;

$$v = \left(\frac{2eV}{m}\right)^{\frac{1}{2}} \tag{2-3}$$

Equation 2-3 can be rearranged to solve for the flight time (t) assuming a singly charged ion ($z = 1$);

$$t = \frac{L}{v} = L\left(\frac{m}{2eV}\right)^{\frac{1}{2}} \tag{2-4}$$

where L is the length of the flight tube. By grouping constants, $k = L/(2V)^{1/2}$, giving;

$$t = k\left(\frac{m}{e}\right)^{\frac{1}{2}} \tag{2-5}$$

where k is a constant representing factors related to the instrument settings. As shown in this equation, the time of flight of the ion varies with the square root of its mass-to-charge (m/z) ratio. If the flight time is measured, then the time can be used to calculate the m/z ratio of the ion. If the TOF is calibrated using the flight times of two known masses, the times can be directly converted into m/z values for the mass spectra.

Mass resolution (R) in mass spectrometry can be defined as;

$$R = \frac{m}{\Delta m} = \frac{t}{2\Delta t} \tag{2-5}$$

where m is mass of the ion and t is the flight time, and Δm and Δt are mass and time at the full-width at half-maximum (FWHM) of the peak, respectively.

Mass accuracy is a measurement of mass difference between the calculated mass and the observed mass. Mass accuracy can be calculated by:

$$Mass\ accuracy = \frac{(M_T - M_O)}{M_T} \tag{2-6}$$

where M_T is the calculated mass and M_O is the observed mass. Typically, mass accuracy can be described as a percent (%) or part per million (ppm).
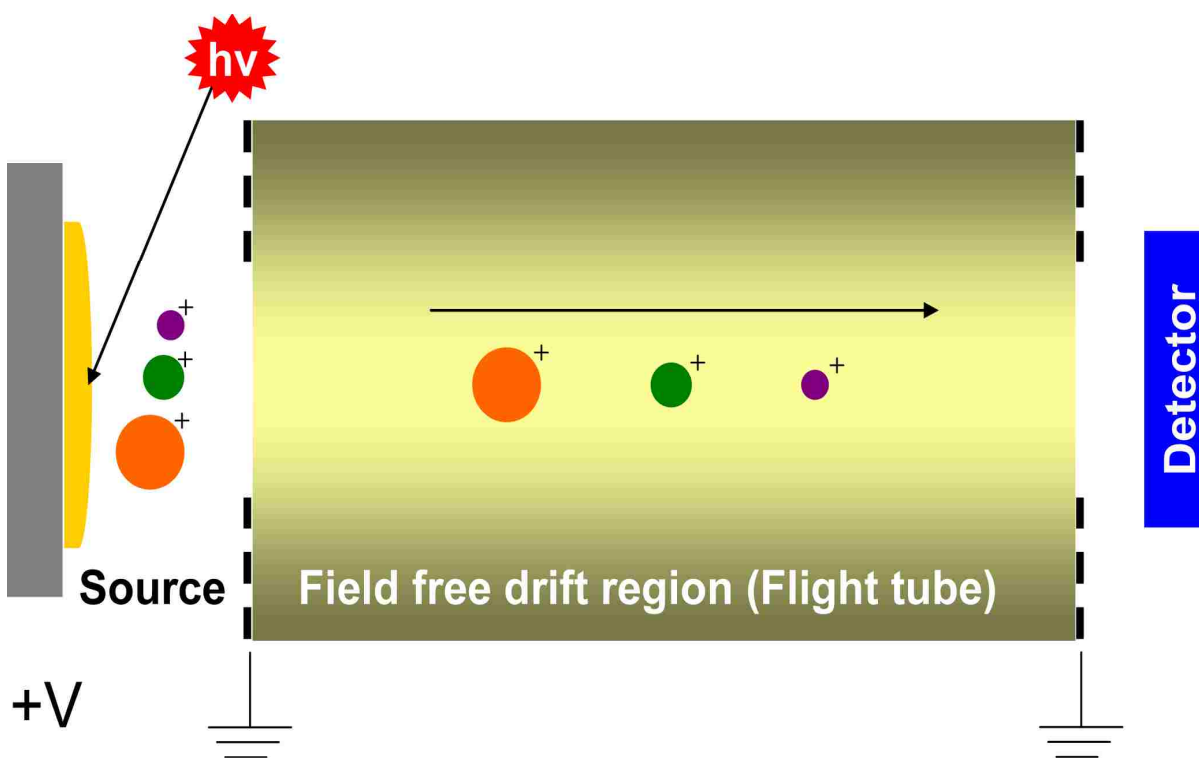
Figure 2-2. Schematic of a linear TOF mass spectrometer.

The linear configuration of TOF mass spectrometers is a simple and robust technique, which provides moderate mass resolution.[243] In a linear TOF MS, there is no theoretical limit to the m/z range. However, the mass range of a linear TOF MS is limited by its detector, which has

low detection efficiency for large molecules due to their slow movement resulting in difficulty of inducing secondary ion emission at the detector. The schematic of a linear TOF mass spectrometer is shown in Figure 2-2. As shown in this figure, the accelerated ions reach the detector at the end of the flight tube, which is typically 1-2 m in length.[19] The acquisition cycle for a TOF mass spectrometer is pulsed. A typical linear TOF mass spectrometer has a resolution of up to 8,000, mass accuracy of 100 ppm, and a mass range of up to 350 kDa.[246]

One of the major limitations for the linear TOF mass spectrometer is low mass resolution. When ions are formed in the ion source, they have spatial distribution and different kinetic energies in the acceleration field. Even the same m/z ions enter the field drift region, different flight times are recorded due to different initial velocities and positions. These initial spatial and velocity dispersions result in lower resolution.[19] To correct the resolution problems especially due to kinetic energy distribution in a TOF mass spectrometer, delayed ion extraction and an ion reflectron can be used.[247] In delayed ion extraction, ions are extracted from the ion source after a period of a few hundred nanoseconds following laser irradiation on the sample. The ions with lower velocity are accelerated more and the ions with higher velocity are accelerated less, ultimately reducing the temporal spread of ions.

The other technique to improve resolution is an ion mirror or reflectron. The reflectron focus ions with the same m/z and different kinetic energies within the flight tube by compensating for the differences in flight times. The reflectron is an electrostatic mirror, which is composed of a series of ring electrodes to which a repelling potential is applied. Figure 2-3 shows a single stage reflectron. In this figure, identical ions have different kinetic energies during ion formation in the desorption process. Ions with higher kinetic energy penetrate deeper into the reflectron field. Ions with lower kinetic energy take a shorter path in the reflectron field. After the direction of ion motion is reversed, the detector is placed at focus (L1 + L2). The

longer path length is an additional factor that can enhance mass resolution.[248] A typical reflectron TOF mass spectrometer has a resolution of up to 40,000, mass accuracy of 2 ppm, and a mass range of up to 60 kDa.[246]
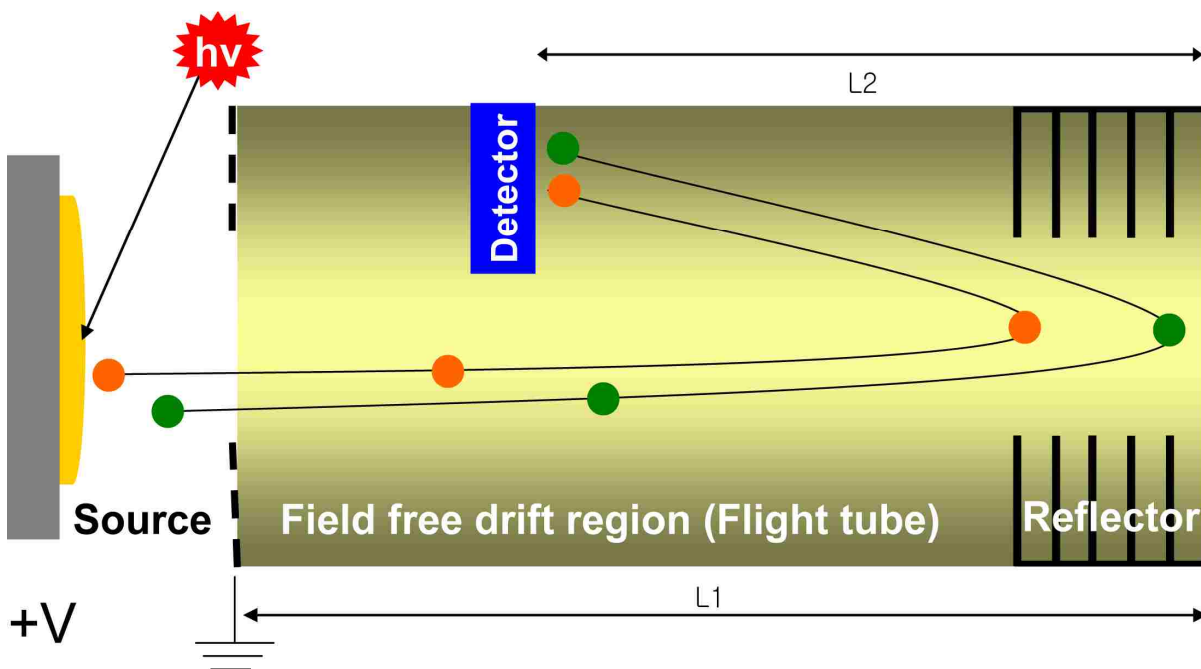
Figure 2-3. Schematic of a reflectron time-of-flight mass spectrometer.

2.1.3 Detector

A microchannel plate (MCP) is a common detector for TOF mass spectromety. [249-251] This detector is a multichannel version of an electron multiplier, which amplifies an electron signal through the inner surface of a channel to which a high voltage is applied.[252] MCP is a specially fabricated plate of 1-2 mm thickness and has several million independent channels which are approximately 10 micrometers in diameter. Each channel works as an independent electron multiplier. A general mechanism of the MCP is shown in Figure 2-4. An incident ion enters a channel and causes ejection of secondary electrons from the surface of the channel. These secondary electrons are accelerated by an electric field from a voltage applied across the MCP. After several multiplications of electrons along the surface along the length of the

channels, the electrons emerge from the rear of the plate of the MCP. These are subsequently converted into a signal by anodes mounted after the MCP. The gain of each individual channel is approximately 10^4 after the cascade process.[253]
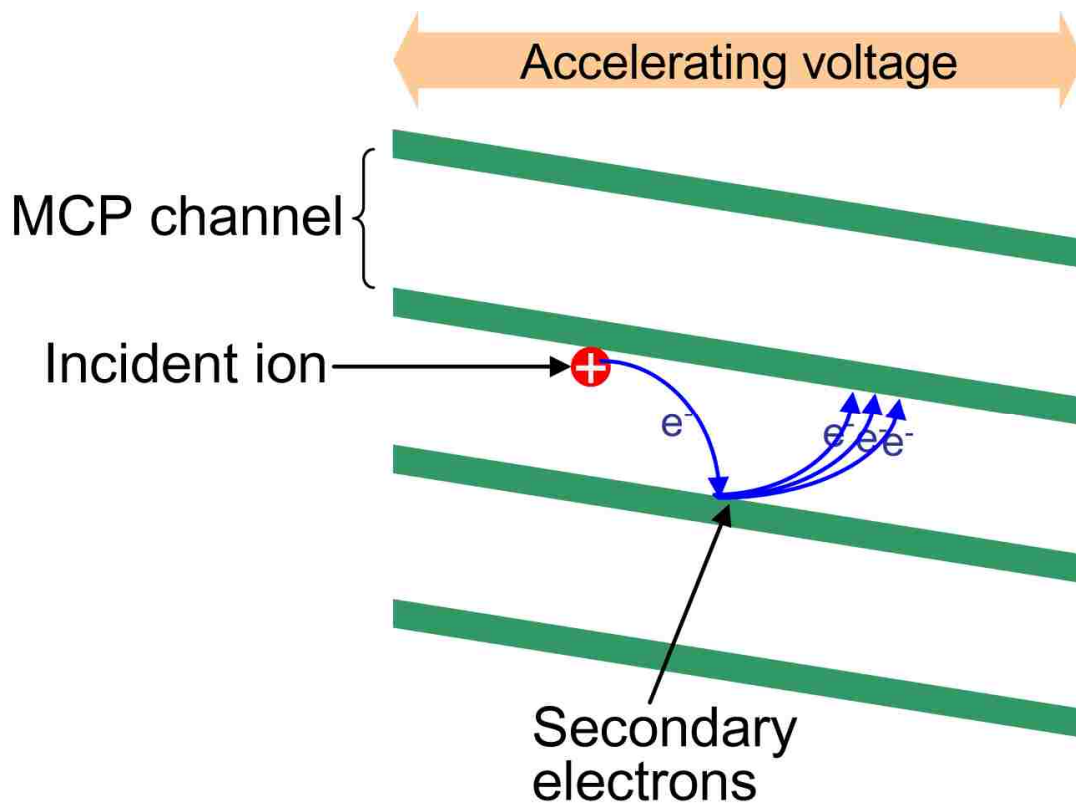
Figure 2-4. Illustration of the mechanism of electron multiplication inside a channel of MCP.

2.2 MALDI-TOF Mass Spectrometer

For the experiments reported in this dissertation, mass spectra were recorded using a MALDI TOF mass spectrometer (OmniFLEX, Bruker Daltonik, Bremen, Germany) shown in Figure 2-5. This MALDI-TOF mass spectrometer was used to analyze intact proteins and digested peptides from typsin-immobilized bioreactors (Chapters 3, 4, and 5), and to detect biomolecules from whole *E. coli* cells from microfluidic culturing chips (Chapters 6 and 7). A dual MCP detector was used for linear mode and reflectron mode detection. A pulsed nitrogen laser ($\lambda = 337$ nm; pulse width = 3 ns; pulse energy = 150 µJ maximum) at a repetition rate of 2

Hz was used for desorption/ionization of analytes. The total acceleration voltage was 19 kV with delayed ion extraction. Positive ions were detected and 50 single-shot spectra were averaged from each sample spot.
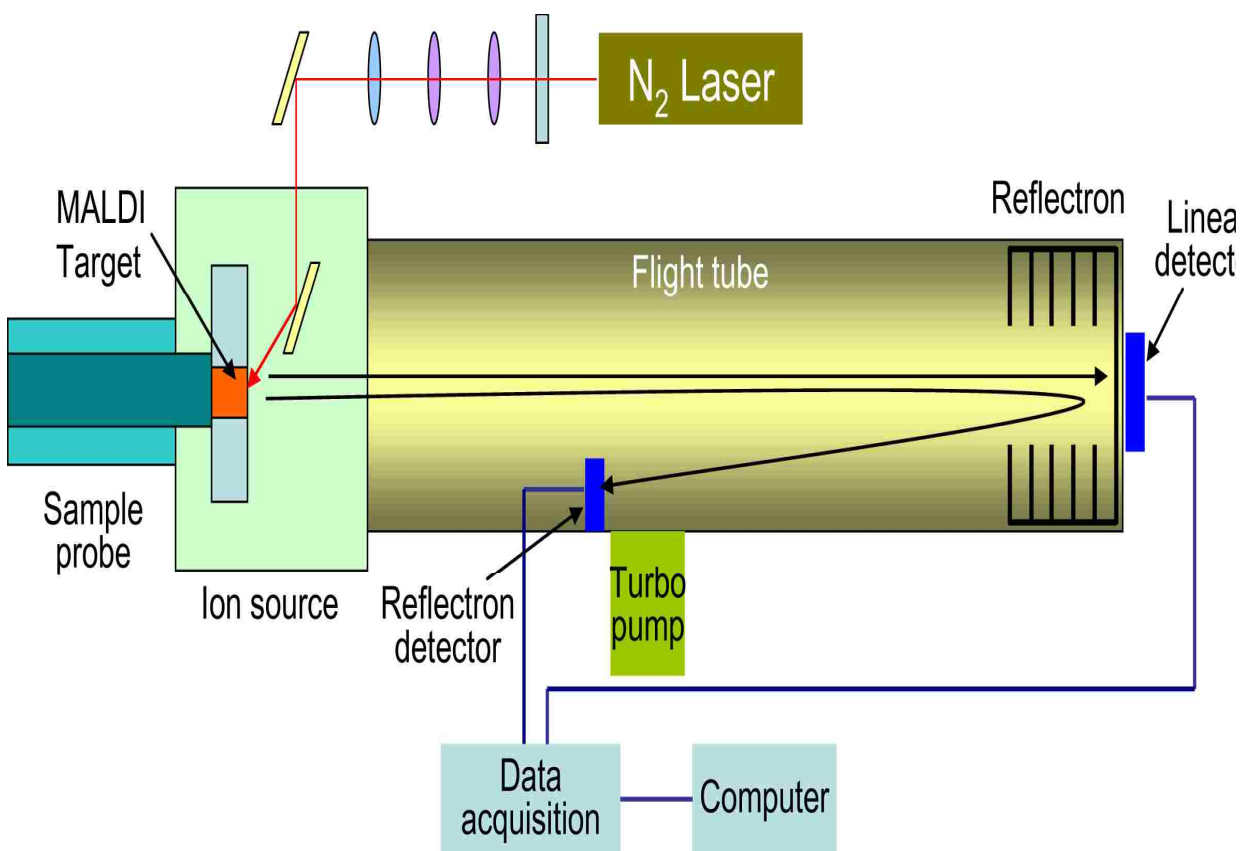
Figure 2-5. Diagram of OmniFLEX MALDI time-of-flight mass spectrometer.

2.3 Microfabrication Methods

The choice of microfabrication method depends on the device material. Glass and silicon substrates are hard and brittle, but can be etched with HF following a photolithographic step. Polymer substrates are more versatile and can be shaped into the required structures using a variety of techniques such as etching, micromachining, imprinting, injection molding or hot embossing.

2.3.1   Photolithography

   Photolithography is one of the most frequently used procedures for creating

microfabricated devices in glass, silicon, and quartz.[254-257] It is typically used for microfabricated

devices with channel widths larger than 1 μm and aspect ratios less than 10.[37, 254] In the

lithographic process, protective photoresist layers and masks are used to create the desired

pattern. Figure 2-6 illustrates the typical procedures for creating a microfluidic device using

photolithography. The substrate material is coated with a thin protective layer of metal, such as

gold or chromium, followed by a layer of photoresist that is added by spin coating.
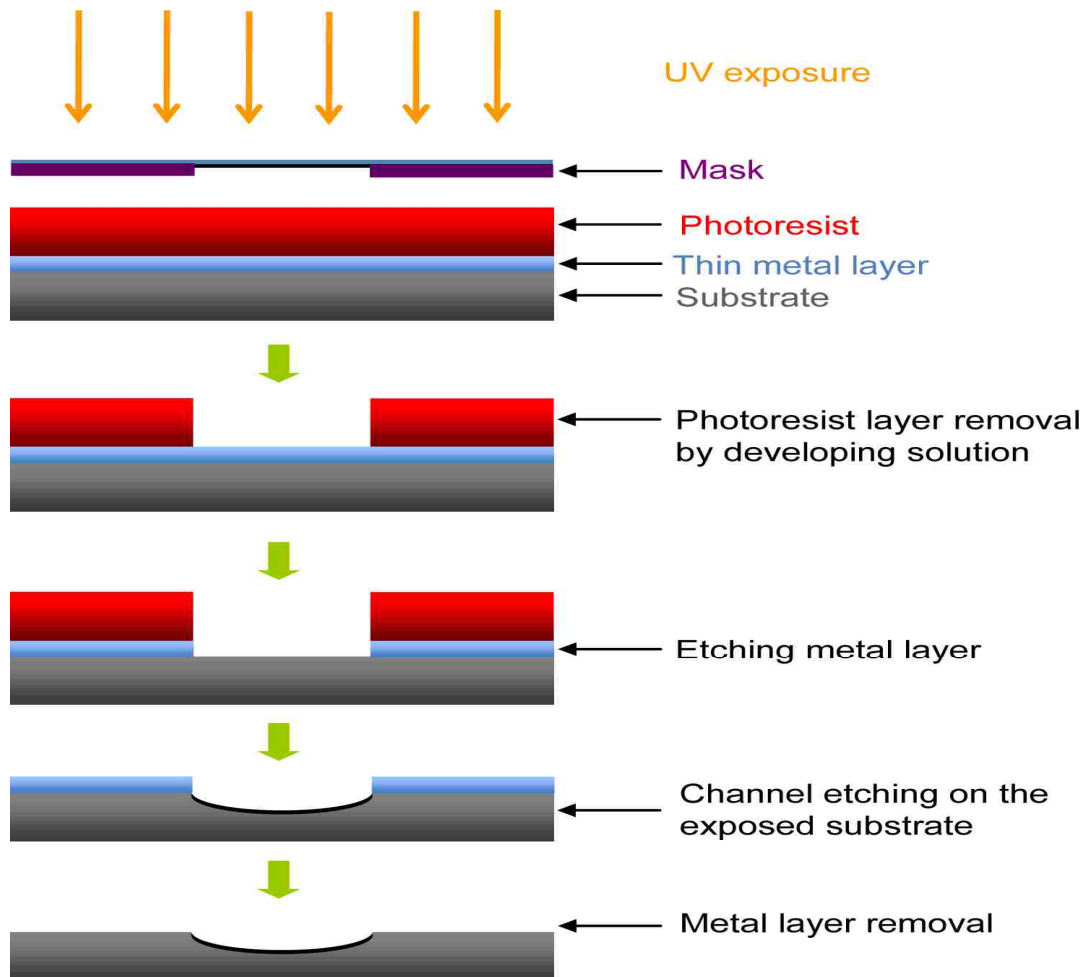
Figure 2-6. Fabrication procedures of photolithographic microfabrication using a positive
photoresist.

The photoresist is a photoactive polymer that is selectively exposed to UV light that, in a positive photoresist, breaks chemical bonds or, in a negative photoresist, crosslinks and thereby strengthens the polymer chains. Submicron features can be created using X-ray radiation.[255] The surface is exposed through a photomask, which blocks the light from selected areas to create a pattern of the desired structure in the photoresist. The exposed regions (positive resist) or unexposed regions (negative resist) of the patterned photoresist are removed by developing solvents to expose the metal protecting layer, which can be subsequently removed using the appropriate developing reagents.

Once the lithography process is complete, the desired substrate features are created by etching, which can be done either wet or dry.[258, 259] In wet etching, the substrate is exposed to liquid reagents, such as HF for glass etching; in dry etching, the substrate is exposed to a plasma.[260] After etching, the protective layer is removed and the chip is cleaned, followed by sealing of the channels by thermal fusion bonding a cover plate to the patterned substrate.

2.3.2   Micromachining

High-precision micromilling is widely used for microfabrication of substrate materials such as polymers and metals. This technique can be used to directly machine microstructures into substrate materials down to a few µm in size using end-mill tools rotated at speeds from 40,000 to 200,000 rpm.[261] The end-mill tools are as small as 25 µm in diameter and are selected based on the specific design requirements of the microstructures. The micromilling machine can also be used to mill a metal master to create replicate microchips by embossing or injection molding (see below). Micromilling is compatible with many different materials and can be used to create high aspect ratio structures without a clean room environment.[262] The minimum size of the milled features is approximately 5 µm.[263, 264]

Laser etching can also be used for the direct fabrication of microstructures in polymer substrates.[265] UV laser beams, which must be absorbed by the substrate for efficient ablation, are directed to the polymer surface through a mask designed by specific microstructures. Alternately, a tightly focused beam can be used to create the microstructures by moving the writing beam or work piece.[266, 267] Typically, KrF (248 nm) or ArF (193 nm) excimer lasers with fluences of 0.5 to 30 J/cm^2 are used for ablation.[268] The depth of the channels and other features is determined by the pulse energy and the number of pulses irradiating a single area on the substrate. Although the theoretical imaging resolution for an excimer laser is 0.2 ~ 0.4 µm, the practical resolution is 1-5 µm due to the limits associated with the optics.[267-269]

2.3.3 Imprinting and Embossing

Microstructures can be formed in polymers from a mold master using imprinting, injection molding or hot embossing.[261, 270] The mold master, which carries the inverse of the final structures to be replicated, can be fabricated using photolithography or micromilling. A typical polymer has a low glass temperature (T_g), in the range of 120 to 180 ℃, which makes it compatible with many of the commonly used molding techniques. With imprinting, small-diameter wires are arranged in the desired geometry and held flat against the polymer in a press.[270] The press assembly is heated in an oven to a temperature slightly below T_g then removed and cooled. Microchannels are formed when the wires are removed from the polymer substrate. Although wire imprinting is fast and simple, it is difficult to form complex channel geometries reproducibly.

Another technique used for the fabrication of microstructures in polymer substrates is hot embossing. Here, a mold master is heated and pressed into the substrate to form the microchannels and other structures using a specified force and temperature. As noted above, the metal master can be formed by micromachining or photolithography.[271] The latter process is

known as LiGA, after the German acronym for "lithographie, galvanoformung, und abformung" (lithography, electroplating, and molding). The LiGA mold master is created by electroplating nickel or a nickel-cobalt alloy over a conductive layer containing an appropriately developed photoresist that has been patterned via photolithography.[207] Hot embossing is fast, requiring about 5 min per device. Because it uses a one-piece master, replication errors are less than with imprinting and more complex geometries can be created that contain sloped, curved, multi-level and high aspect ratio structures.

The process of injection molding is different from the imprinting and hot embossing processes described above in that polymer resins (pellets) are used in contrast to polymer sheets used for imprinting and embossing. Also, a mold master is heated to T_g for imprinting and embossing, whereas a molding tool is heated to a temperature to form a free flowing melt in the case of injection molding. However, in all three cases, a molding tool is employed, which defines the shape, size and position of the desired structures. For injection molding, a polymer resin is added to a hopper, which feeds an injection barrel that consists of a large screw that moves the polymer into the molding chamber. The polymer resin melts as it is dragged by the screw through the barrel. The melted polymer is injected into the molding chamber through a nozzle and allowed to fill the injection chamber, which also contains the molding tool. Following molding of the polymer resin, the chamber is cooled and the molded piece ejected from the machine. The advantage of injection molding is that once the machine and molding conditions are set, a number of pieces can be produced at rates exceeding that associated with imprinting or hot embossing.

In the work described in this dissertation, a mold master was prepared using micro-milling[267] and was subsequently used to replicate polymer microparts via hot embossing. The desired microfluidic network was designed using computer-aided design software. The brass

plate was cut into a 12 cm diameter circle and the mold master was machined in the specified pattern with a micro-milling machine (MNP 2522, KERN Micro-und Feinwerktechnik GmbH & Co. KG, Germany). A laser measuring system (Laser Control NT, Blum-Novotest GmbH, Germany) was used to determine the tool length and radius, and an optical microscope (Zoom 6000, Navitar, Rochester, NY) was employed to monitor the micro-milling process, which was accomplished at 40,000 rpm and a feed rate of 10-20 mm/min using a 50 µm carbide bit (McMaster-Carr or Quality Tools, Hammond, LA). After milling, the master was polished using a 3 µm grain size polishing paper (Fibrmet Discs-PSA, Buehler, Lake Fluff, IL) followed by a polypropylene cloth (Engis, Wheeling, IL) with a 1 µm diamond suspension (Metadi Diamond Suspension, Buehler) to remove burrs at the surface of the microstructures.

The mold master was used to replicate PMMA chips using hot embossing on PMMA disks that were 5 mm thick and 120 mm diameter.[2, 272, 273] To emboss, the mold master and PMMA disks were mounted in a hot embossing machine (Model TS-21-H-C (4A)-5, PHI Precision Press, City of Industry, CA) and then both the master and the PMMA disk were heated separately in a vacuum chamber to a temperature of 155 ºC, which is above the glass transition temperature of PMMA ($T_g = 107$ ºC).[124] After the mold master was embossed at a pressure of 950 PSI for 150 s, it was rapidly cooled to just below 155 ºC prior to demolding.

2.4 Preparation of the Sold-Phase Bioreactor

The schematic procedure for preparing bioreactors with immobilized trypsin is shown in Figure 2-7. The PMMA chip surfaces were first activated for covalent attachment of the proteolytic enzyme by exposing the microfabricated PMMA substrate and cover slip to a 254 nm UV lamp at 15 mW cm^{-2} for 20 min.[206] This was followed by inserting stainless steel and silica tubes into guide channels on the PMMA substrate and thermally annealing the UV exposed

0.125 mm PMMA cover slip to the substrate at 98 °C for 20 min.[267] The assembled chip was then rinsed with deionized water and air-dried. Then, the UV-modified channels were chemically treated with a mixture of 5 mM EDC and 5 mM sulfo-NHS solution for 15 min. Finally, trypsin was immobilized onto the surface of the UV-exposed microchannels by inserting a 20 µM trypsin solution prepared in a 100 mM phosphate buffer (pH 7.0) into the PMMA bioreactor channel for 2 h. The chip was ready for immediate use or could be refrigerated for future use.
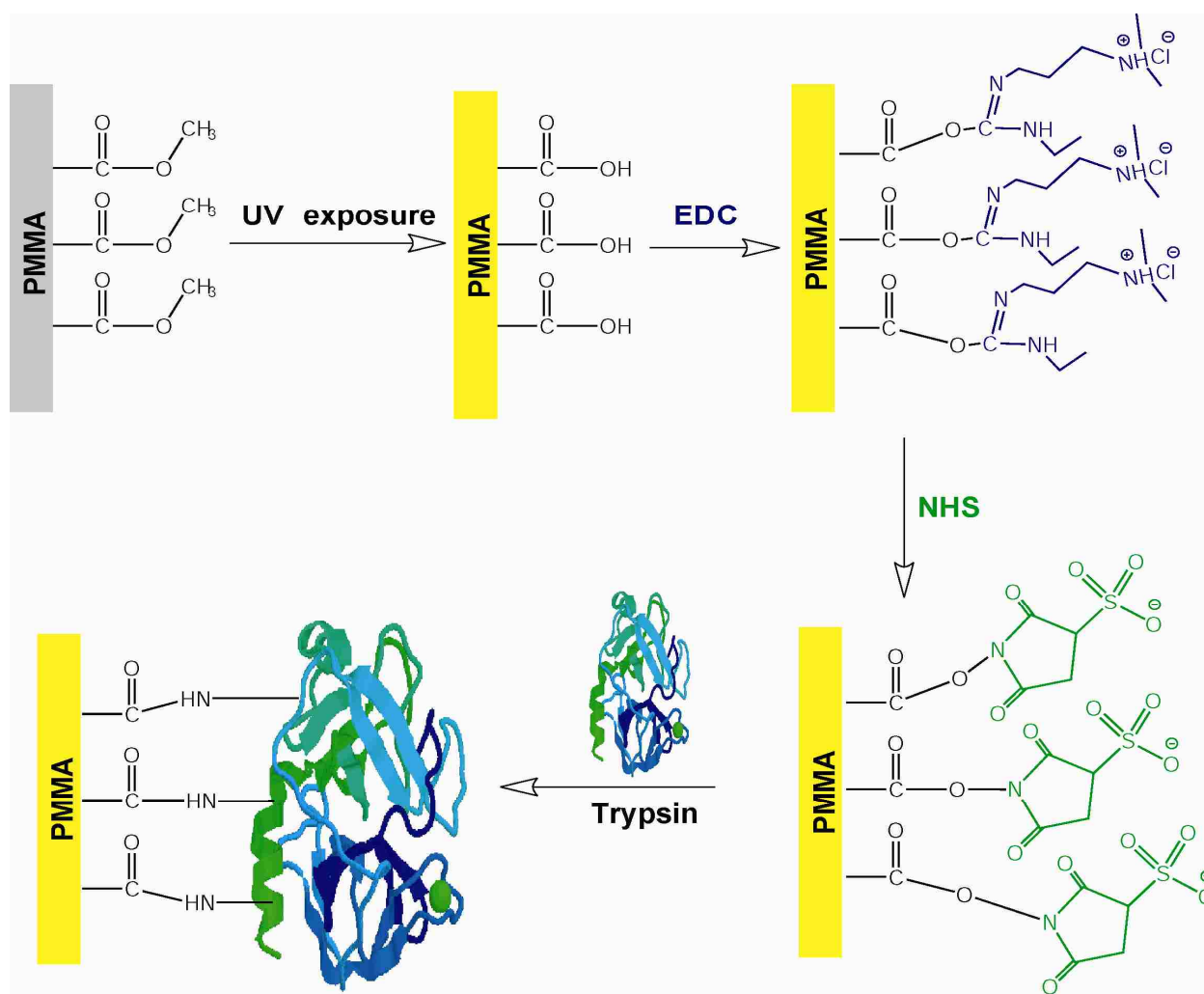
Figure 2-7. Schematic of trypsin immobilization procedure on the surface of PMMA.

2.5 Spotting Deposition

PMMA chips were designed to fit into a stationary mount of a robotic fraction collector system (Probot, Dionex, Sunnyvale, CA); the MALDI plate translated in the xy plane for spot deposition. A schematic of the assembled chip is shown in Figure 2-8. The interface capillary was 1 or 5 cm in length and had an ID of 100 µm and an OD of 363 µm. The capillary was inserted into a guide channel that was embossed into the chip and placed directly at the output end of the microreactor and finally, glued in place. The chip had a coaxial matrix and analyte mixing system with the analyte exiting the chip through a silica capillary tube, which was surrounded by a 1 or 5 cm long stainless steel tube that was 500 µm ID and 1.5 mm OD.
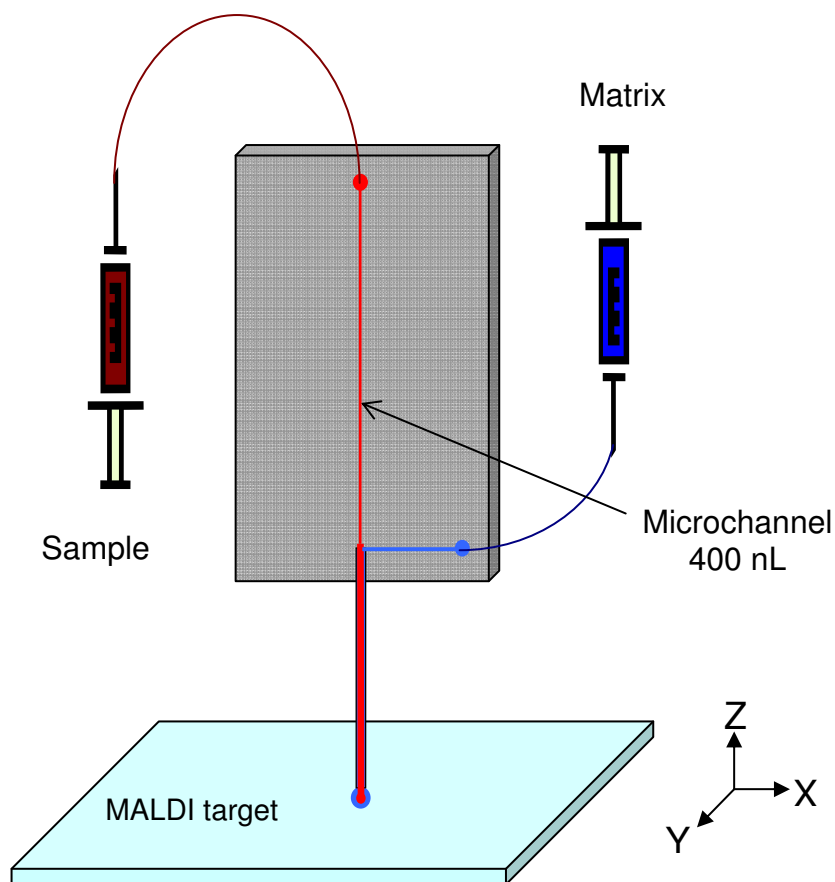
Figure 2-8. Schematic of assembled chip for spotting deposition.

Figure 2-9 shows a schematic of the fluid connection between the micropost bioreactor and the capillary tube serving as the off-line MALDI interface. The analyte flowed through the interface capillary and the matrix through an outer tube hydrostatically. These effluents were mixed at the point of target deposition on the MALDI plate. The MALDI matrix solution consisted of 5 mg/mL CHCA dissolved in 60% acetonitrile with the addition of 0.1% TFA containing an internal standard of bradykinin (5 µM). Effluent from the microchip was deposited onto the MALDI target plate with a micro-fraction collector (Figure 2-10) and then analyzed off-line by MALDI-TOF MS.
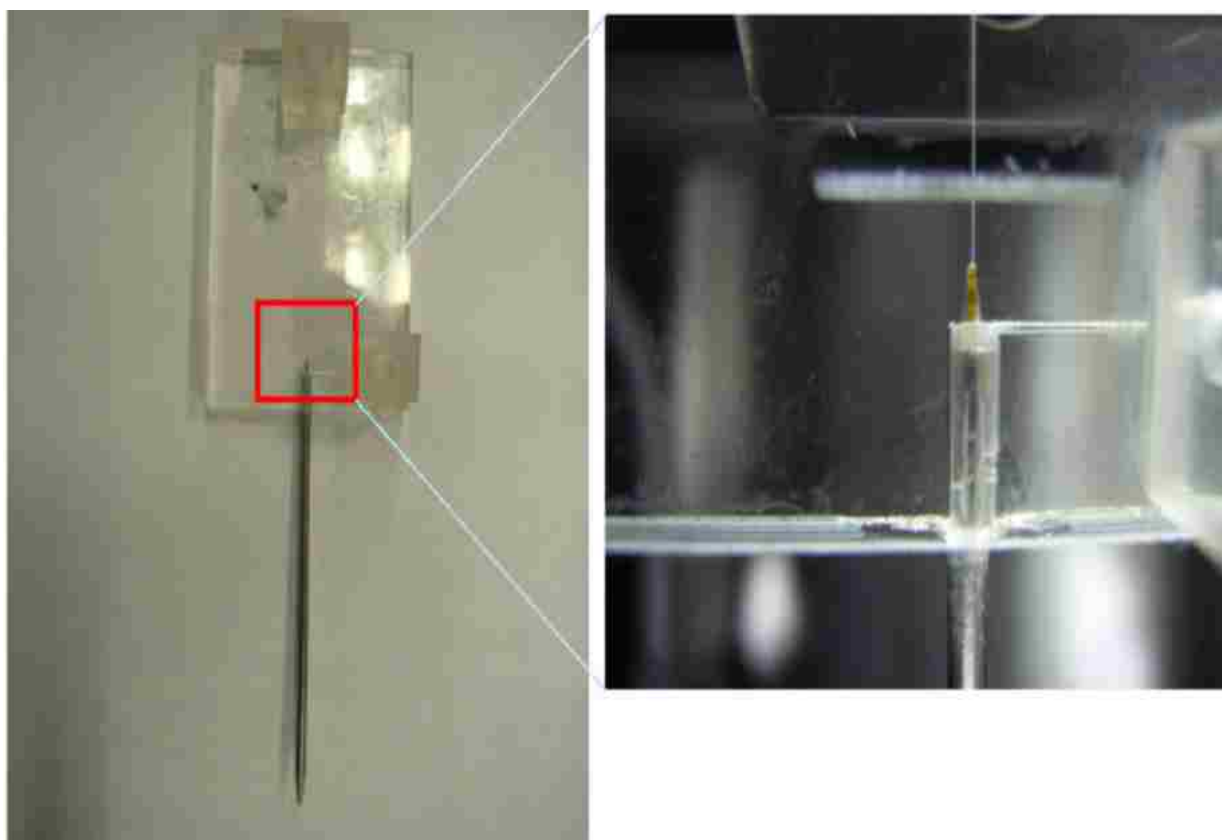
Figure 2-9. Schematic of the fluid connection between the micropost bioreactor and the capillary tube assembled chip.
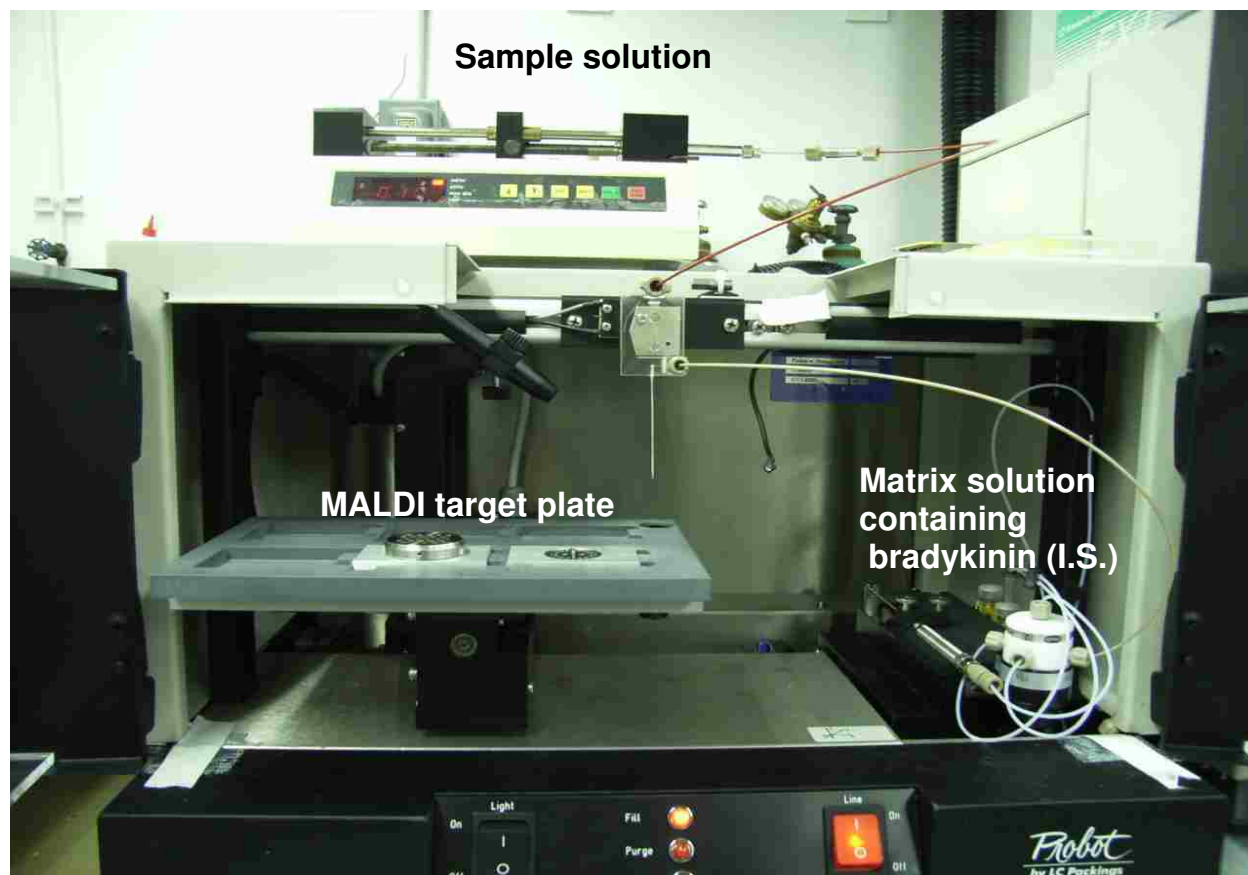
Figure 2-10. Assembled chip with robotic fraction collector system.

To control sample deposition, two pumping systems were used, pressure-driven flow and electrokinetically-driven flow. In pressure driven flow, the fluid was moved through the microchannels by a positive displacement pump, such as a syringe pump. The fluid could also be pumped electrokinetically by applying a potential across the channels.

2.5.1 Pressure-Driven Flow

A microfluidic device operated by pressure-driven flow (hydrodynamic flow) ensures completely laminar flow without turbulence resulting from low Reynolds numbers (*Re*). Typically, turbulent flow occurs above *Re* = 2000. In a microchannel, *Re* is less than 20 when flow rates are below 100 μL/min.[274] The fluid velocity at the wall is zero in the low *Re* regime, producing a parabolic velocity profile within the microchannel. Compared to electrokinetically-

driven flow, pressure-driven flow offers several advantages such as easy implementation and insensitivity to surface characteristics, ionic strength of fluids, and pH. However, band-broadening due to dispersion and diffusion reduces separation efficiency.

In this work (Chapter 3), a syringe pump (Model 11, Harvard Apparatus, MA) was used to supply the microchip with a protein solution. Solutions of cytochrome c, myoglobin, BSA, and phosphorylase b in 50 mM ammonium bicarbonate buffer solution were driven through the trypsin immobilized PMMA microchannel by a syringe pump at various volume flow rates. MALDI matrix was added to the microchip reservoir via a syringe pump at a flow rate of 5 µL/min.

2.5.2   Electrokinetically-Driven Flow

In many practical microfluidic applications, including injection and collection of analytes, electrokinetically-driven flow has been used to generate fluid motion. A high potential, typically 400 V- 1000 V, is applied across the sample through electrodes to produce an electroosmotic pump. An electrokinetic flow system can eliminate mechanical pumping systems, control back and forward flow, provide a flat flow profile in the microchannel, and easily couple electrophoresis with a mass spectrometer.[275]

Although electric fields are efficient tools for separation of molecules, especially proteins and peptides, there are limitations in using this as a general tool of fluidic transport. One of the problems for electrokinetically-driven flow is that alternating plugs of buffer with different conductivity are needed to compensate for the ionic strength of a solution. The separation of different ionic components occurs due to the demixing of solutions when heterogeneous solutions are pumped. Also, joule heating is a problem when high voltage is used for infusing solution.

In this work (Chapter 4), the sample was transported through the capillary via electroosmotic pumping, which was generated by electrokinetic flow through the bioreactor.[276] The electro-osmotic flow (EOF) in assembled devices was measured using the current-monitoring method described in previous studies.[277, 278] An in-house built high-voltage controller operated by LabView software was used to supply the microchip with the driving electric field. Sample transfer was started by applying the high voltage to the sample inlet (point A, +1.5 kV, see Figure 2-11) and a ground potential at point B (see Figure 2-11b).
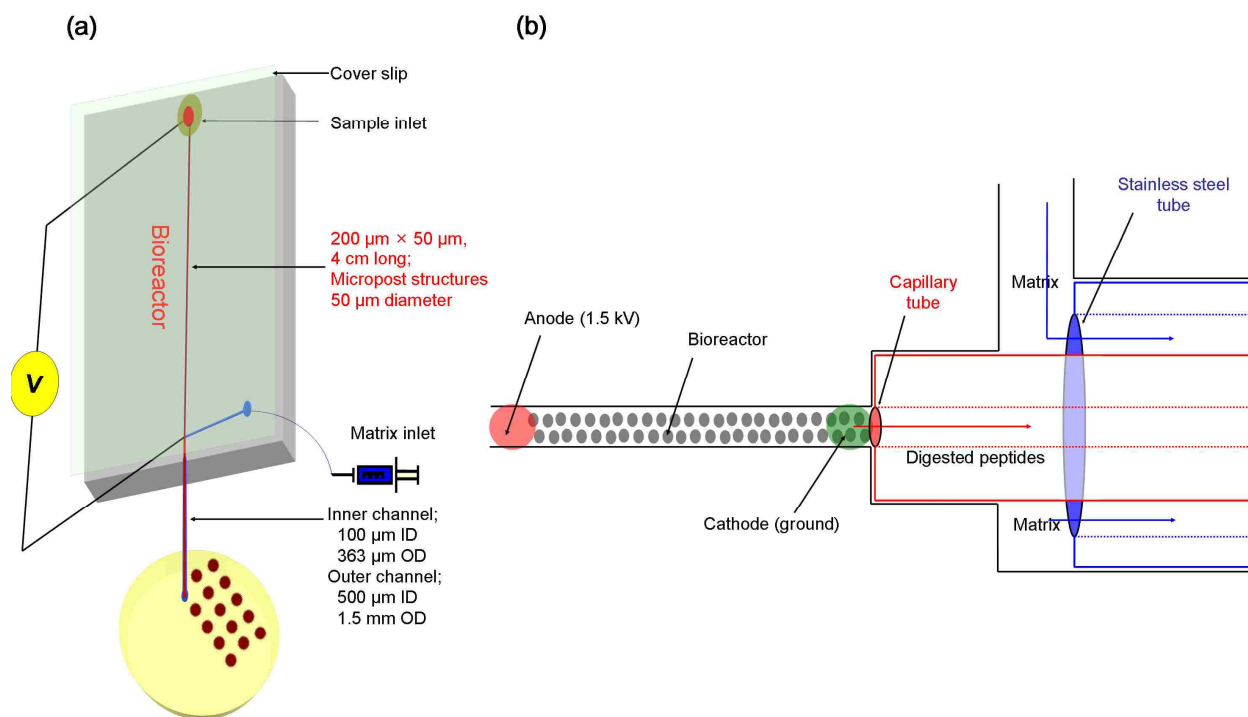
Figure 2-11. (a) Assembled tryptic digestion microfluidic chip; chip components including PMMA substrate and cover slip, inlet and outlet connectors, capillary and stainless steel tubes. The sample solution was electrokinetically infused through the bioreactor and the matrix solution was loaded hydrodynamically with a syringe pump. Coaxial tubes mixed the bioreactor output with a matrix solution for deposition on a MALDI target. (b) Schematic top view of the fluid connection between the micropost bioreactor and the capillary tube interface to the deposition system. Two Pt electrodes were inserted into the sample inlet and the end of the bioreactor to electrokinetically drive the sample through the bioreactor.

2.6 Continuous Deposition

A schematic of the continuous deposition system disscused in Chapter 5 is shown in Figure 2-12. The PMMA chip was designed to fit into the stationary mount of a xyz stage (Newport, Irvine, CA) for continuous deposition. A guide channel was embossed at the output end of the bioreactor channel to accept a PEEK capillary (360 µm o.d. × 50 µm i.d.), which was used for transporting samples onto a MALDI target.

Cover slip

Sample inlet

Bioreactor

200 µm × 50 µm,
4 cm long;
Micropost structures
50 µm diameter

Polymer capillary;
50 um ID & 360 um OD

Nitrocellulose membrane
precoated with CHCA
matrix
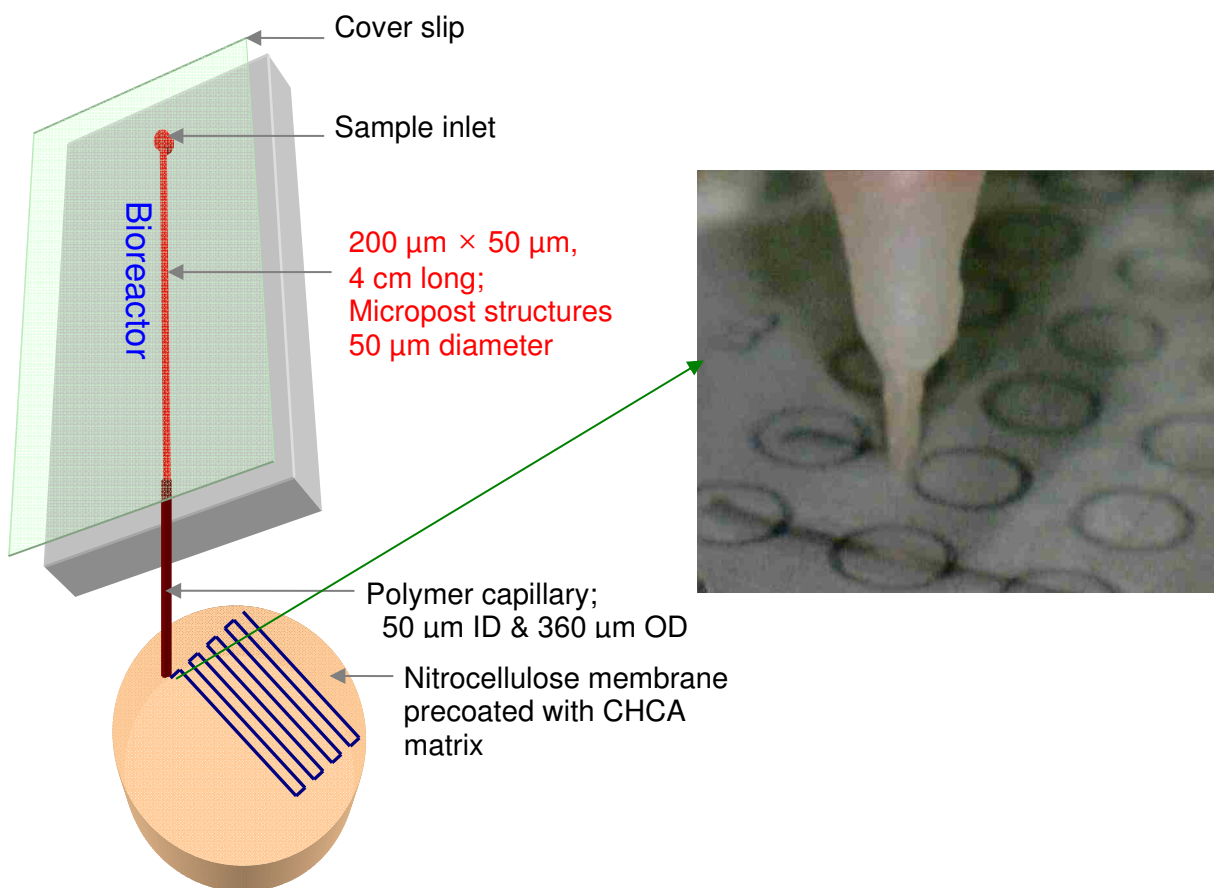
Figure 2-12. A schematic of continuous deposition mode using a PMMA microfluidic chip containing an immobilized trypsin bioreactor: The channel measured 40 mm × 200 µm × 50 µm and had an array of 50 µm diameter with a 50 µm inter-post spacing.

A 10 mg/mL CHCA MALDI matrix solution was prepared in water/acetonitrile (30/70, v/v) and mixed with an equal volume of 5 mg/mL nitrocellulose in acetone/2-propanol (80/20, v/v). A 0.5 mL aliquot of this solution was placed on the MALDI target plate. The plate was then spin-coated at 4000 rpm for 20 s to coat the surface.

The matrix-coated MALDI plate was placed on an xyz stage (M-433, Newport, Irvine) operated using actuators (LTA-HS, Newport, Irvine) and a motion controller (ESP300, Newport, Irvine) interfaced to a computer running LabView 8.0 software. During deposition, the outlet polymer capillary was brought into contact with the MALDI target for depositing tryptic digested peptides from the bioreactor.

2.7 Microfluidic Cell Culturing

PMMA chips were microfabricated using hot embossing as the polymer replication technique with die mold prepared by high-precision micromilling for cell culturing devices (Chapters 6 and 7).[267] A more complete description of the fabrication technology utilized in this study has been described previously.[81] The embossed microfluidic devices had two culture chambers that were 3 mm in diameter and 300 µm in depth. One of chambers was used for a blank, which contained nutrient medium without sample. The other was used for bacteria culturing. The total reactor volume of the culture chamber was 2.1 µL. Figure 2-13 shows a schematic of a culturing chamber and two microchannels. The sample inlet and medium solution inlet were 100 µm deep × 100 µm wide and 300 µm deep × 100 µm, respectively. Guide channels at the outlet end of the PMMA chip were embossed to fit into the 100 µm ID × 363 µm OD silica capillary for collection of cultured cells onto a MALDI target plate. A PDMS cover slip was prepared with a 10:1 ratio (v/v) of silicon and the curing agent (Sylgard 184, Dow corning Corp., Midland, MI), and then baked at 70 ℃ for 2 h for curing.

Medium inlet channel
Depth, 300 μm
Width, 200 μm

Cell culture chamber
Diameter, 3 mm
Depth, 300 μm

Sample inlet channel
Depth, 100 μm
Width, 100 μm

Sample outlet channel
Depth, 100 μm
Width, 100 μm

Medium outlet channel
Depth, 100 μm
Width, 100 μm
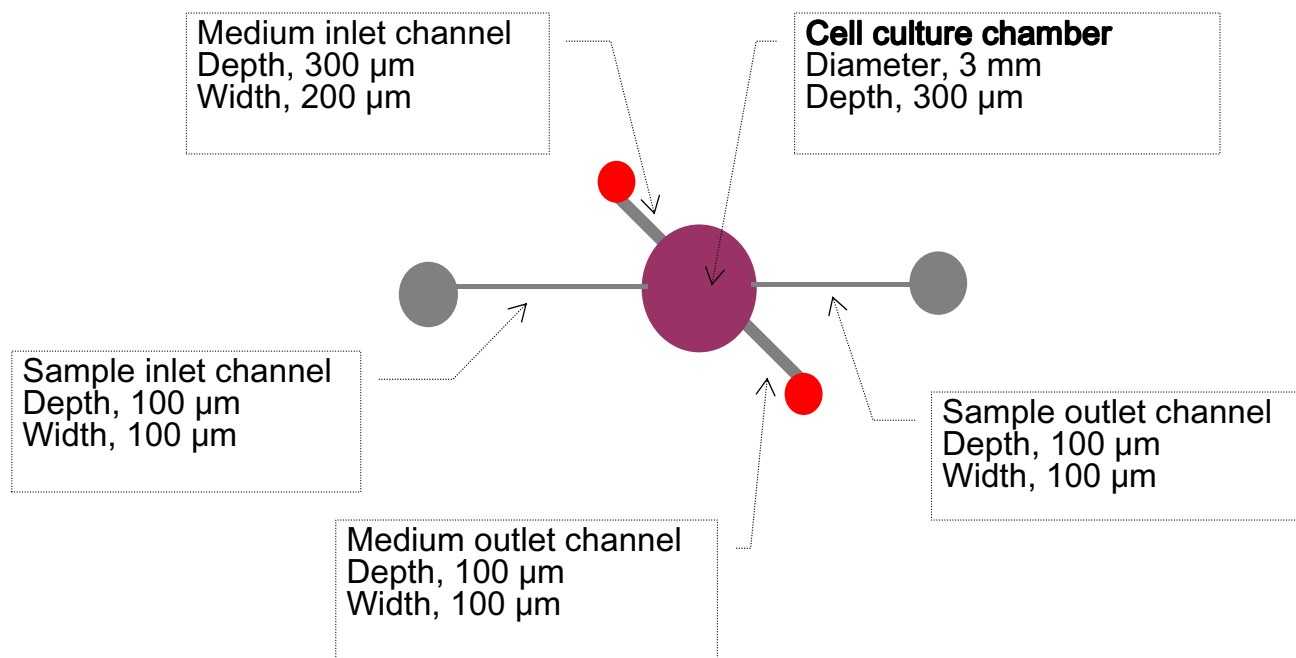
Figure 2-13. Diagram of a microfluidic cell culturing device consisting of a culture chamber, a sample channel, and a medium channel.

2.7.1   Static Culturing

A schematic of the PMMA microfluidic cell culturing device (see Chapter 6) coupled with MALDI-TOF MS is shown in Figure 2-14. Two different covers, PMMA and PDMS, were tested to investigate different cell cultivation based on culturing substrates. All culture components including tubing and connectors were sterilized with a 254 nm UV light at 15 mW cm^{-2} for 10 s (150 Jm^{-2}) prior to use.[279] This was followed by inserting 3 cm long silica capillaries into the guide channels on the PMMA substrate and thermally annealing the 0.125 mm PMMA cover slip to the substrate at 106 °C for 20 min. A thin film of epoxy resin was then applied to the capillary-device interfaces to prevent leaks. Also the PMMA culturing chip was sealed with a 1 mm PDMS cover slip without an adhesive.
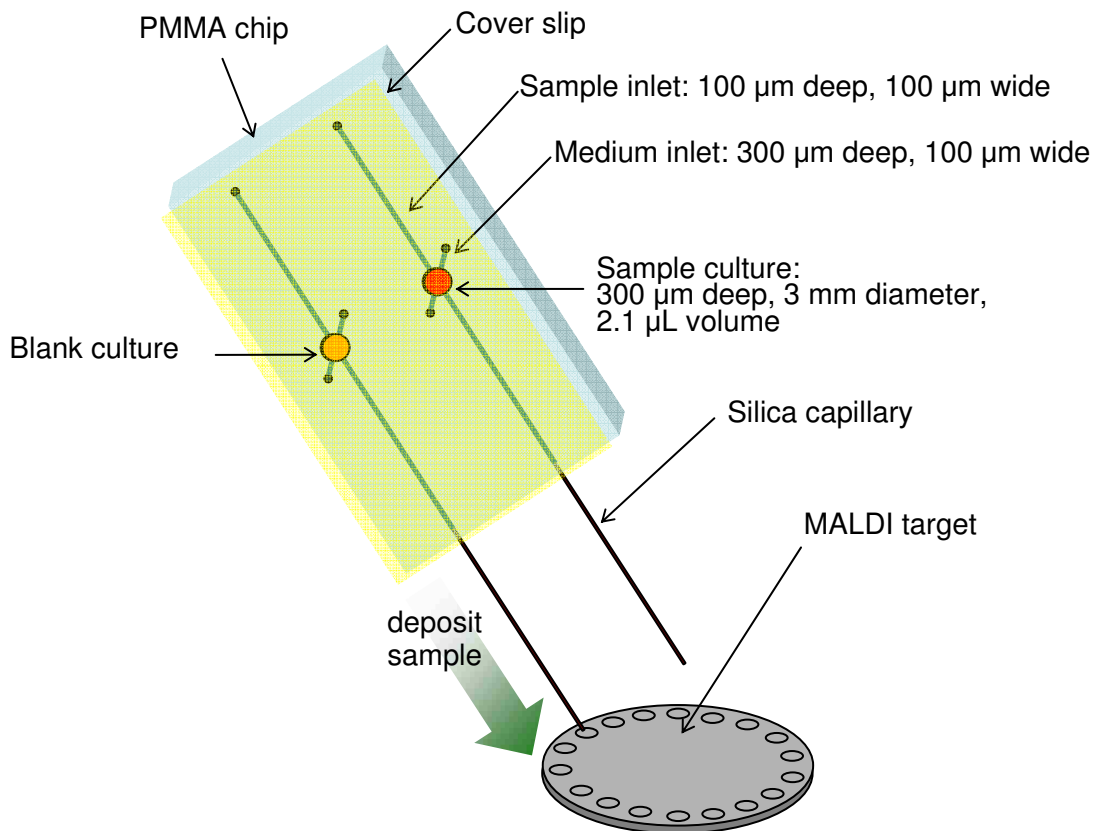
Figure 2-14. Schematic of a PMMA microfluidic cell culturing device consisting of two culture chambers for a control and a sample, respectively.

2.7.2   Dynamic Culturing

A photo of the microfluidic cell culturing device with continuous perfusion of medium interfaced to MALDI-TOF MS is shown in Figure 2-15 (Chapter 7). The cell culture device was composed of a culture bed, fluid microchannels, and a sample reservoir and a waste reservoir, which were connected to external pumps. The microfluidic cell culture device was capable of culturing with continuous perfusion of a medium to keep a favorable environment suitable for cell growth by removing metabolites from the culture chamber. A polycarbonate (PC) membrane

with 0.2 μm pore size was embedded into the outlet of the culture chamber for changing the

medium without loss of cells.
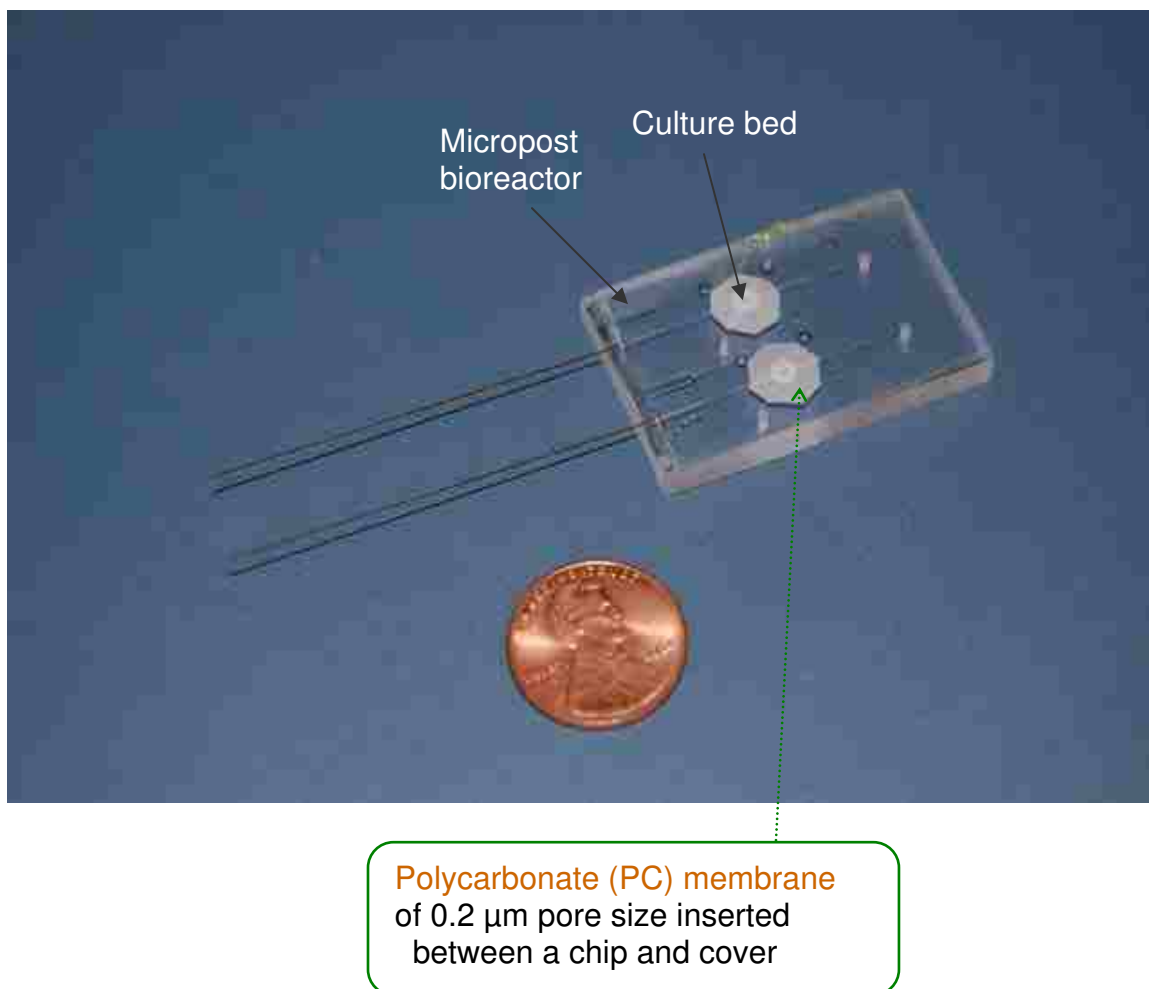
Figure 2-15. A photo of the microfluidic cell culturing device with continuous perfusion of medium using a polycarbonate membrane.

For dynamic culturing, a micropost bioreactor was fabricated after the outlet of the

culture chamber. The bioreactor consisted of a 76 mm long, 125 μm wide, and 100 μm deep

microchannel with an array of 50 μm diameter micropost structures with a 50 μm inter-post

spacing. The total volume of the micropost channel containing surface-immobilized trypsin was

750 nL with a 37.4 mm^2 surface area. There were approximately 850 posts in the bioreactor. To

eliminate temperature interferences between the culture chamber and bioreactor, the microfluidic

chip was cut horizontally to make a heat barrier of 4 mm thick and 2 mm height. The PMMA chip was designed to fit into the capillary tubes of 100 µm ID × 363 µm OD silica capillary for deposition of cultured cells and digested peptides on a MALDI target plate.

2.8 Temperature-Controlled System

A culturing chamber with continuous perfusion of fresh medium was improved by incorporating a micro thermostatic heater to keep the temperature constant. Figure 2-16 shows a photograph of the thermostatted microfluidic cell culturing device. This device was composed of a micro-heater, a Peltier cooler, and thermocouple temperature sensors. The micro-heater was used to maintain a constant temperature suitable for cell culturing. To control the temperature distribution inside the cell culturing chamber, an aluminum heating block with a Kapton insulated heater (KHLV-102, Omega, Stamford, CT) was prepared. The heater was connected to a temperature controller (CN77R344.A2, Omega, Stamford, CT) through a solid state relay (G3NA-210B-DC5-24, Omron, Schaumburg, IL). A set temperature of 37 ℃ was maintained by continuously measuring the temperature with a thermocouple (Omega, Stamford, CT) that was inserted into the front side of the culture bed. A Peltier cooler (TEC1-3108, Fujitaka, Japan) was used to maintain a temperature suitable for the immobilized trypsin in the solid-phase bioreactor. The Peltier cooler was powered by a DC voltage source, which caused one side of the device to cool, while the other side warmed. A thermocouple was inserted beneath the chip attached to the cold side of the Peltier cooler. The measured temperature was approximately 10 ℃ at 1.0 V of applied voltage and 1.5 A of current. A fan (JF0510, Jamicono, Taiwan) and a heat sink were attached on the hot side of the Peltier cooler to dissipate heat from the device.
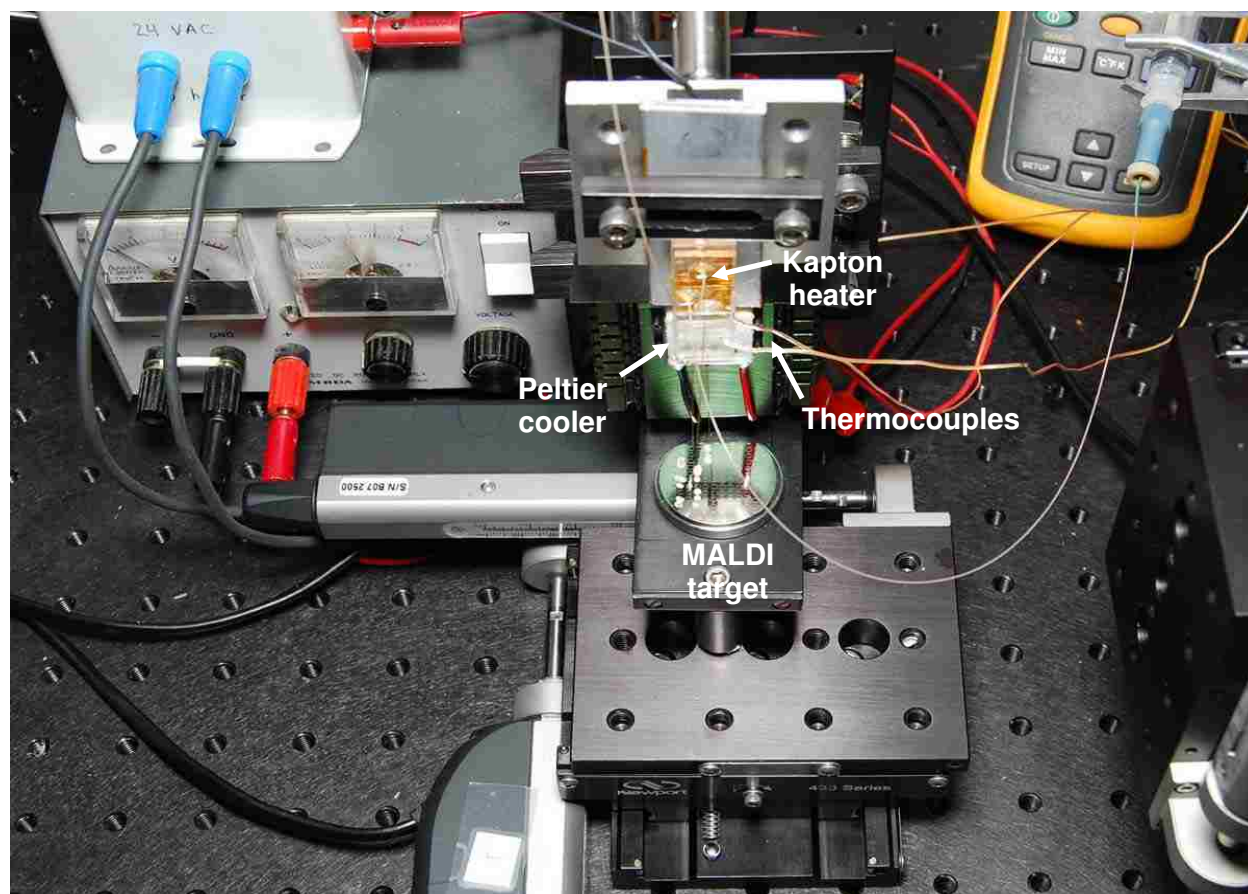
Figure 2-16. A photo of the temperature controllable system for the microfluidic cell culturing device.

2.9 Search Engines

2.9.1 MASCOT

Peptide mass fingerprinting (PMF) and identification of proteins was accomplished with the MSDB database using the MASCOT search program (Matrix Science, London, United Kingdom). MSDB is a comprehensive and non-identical protein sequence database maintained by the Proteomics Department at the Hammersmith Campus of Imperial College London. For PMF, the peptide fragment m/z values generated from the digest can be used to search the MSDB database in which *in silico* digestion was done on all proteins contained within the database. These calculated peptide masses are then matched against experimental mass values

obtained from the mass spectra through the MASCOT search engine. A mass deviation of < 0.25 Da and one missed cleavage were allowed in the database searches.

2.9.2   RMID*b*

Intact cell identification was conducted by protein molecular weight and organism searching using the Rapid Microorganism Identification Database (RMIDb, www.rmidb.org), which is designed to identify bacteria by protein mass analysis. A mass deviation of < 3Da was allowed in the database searches.

2.10   Reagents and Chemicals

Microfluidic chips were fabricated from PMMA, which was secured from MSC Industrial Supply Co. (Melville, NY) and a 0.25″ Alloy 353 engraver's brass plate was obtained from McMaster-Carr (Elmhurst, Illinois). Ammonium bicarbonate buffer (50 mM, pH 8.5) was purchased from Sigma (St. Louis, MO). *N*-(3-dimethylaminopropyl)-*N*'-ethylcarbodiimide hydrochloride (EDC) and hydroxysulfosuccinimide (Sulfo-NHS), which were used to modify the surface of the PMMA microchannels, were obtained from Sigma and Pierce (Rockford, IL, USA), respectively. Protein standards equine cytochrome *c* (C-2506), equine myoglobin (M-1882), bovine serum albumin (BSA, A-0281), β-casein(C-6905), and phosphorylase *b* from rabbit muscle (P-6635) were used as obtained from Sigma. Bradykinin (B-3259), which was used as an internal standard, trypsin (T-6567), isopropyl alcohol (IPA) and α-cyano-4-hydroxycinnamic acid (CHCA) were also obtained from Sigma. Sodium phosphate buffer (100 mM, pH 7.0) and trifluoroacetic acid (TFA) were purchased from Fluka (Buchs, Switzerland). Silica tubes (60 × 0.28 mm OD, 0.1 mm ID) and stainless steel tubes (60 × 1.5 mm OD, 0.5 mm ID) were secured from Upchurch Scientific (Oak harbor, WA, USA).

Three different *E. coli* strains were obtained from the American Type Culture Collection (Manassas, VA); ATCC 9637, ATCC 11303, and ATCC 11775. Also, lyophilized *E. coli* (ATCC

9637) was purchased from Sigma and was used for the measurement of optical density without further purification. Nutrient broth was purchased from Becton Dickson (Broth 23400, Sparks, MA).

CHAPTER 3. DEVELOPMENT OF AN AUTOMATED DIGESTION AND DROPLET DEPOSITON MICROFLUIDIC CHIPS FOR MALDI-TOF MS*

The work reported in this chapter has been published in the *Journal of the American Society for Mass Spectrometry*.[81]

3.1 Overview

The purpose of the research described in this chapter was to develop an automated proteolytic digestion bioreactor and droplet deposition system for off-line interfacing to MALDI-TOF MS. This chapter describes MALDI sample preparation using a novel trypsin-immobilized microfluidic chip consisting of an open channel reactor and a coaxial collection tip. In addition, the off-line MALDI interface included matrix addition and deposition on a MALDI target using a robotic fraction collector modified to accept the effluent from the bioreactor. Various proteins were digested with the solid-phase bioreactor and detected with off-line MALDI MS.

3.2 Introduction

Significant progress has been made toward the development of microchip-based technologies for proteomics through the integration of analytical processes into platforms that can provide rapid identification of proteins and the subsequent characterization of various post-translational modifications.[46, 121, 142, 162] The small sample and reagent requirements, rapid analysis times, high throughput processing capabilities, and low operating costs are among the driving forces for the development of these systems.[82, 178, 280, 281] Different microfluidic devices have been applied to specific aspects of protein processing, in particular, protein purification and separation, protein digestion, and protein identification by mass spectrometry.[143]

With recent advances in analytical methods for proteomics, attention has been directed toward development of efficient pretreatment protocols for protein identification.[188] Strategies for identifying proteins focus on accurate, sensitive, simple, and high throughput analyses

achieved by either reducing processing time or with multi-channel devices.[80, 282] Trypsin

digestion for protein sample preparation is the most frequently used step in proteomic analysis

due to the robust nature of this enzyme and the extensive data bases and software tools for

trypsin digests of proteins.[189, 202] However, the long sample incubation times required for trypsin

digestion in solution and the extensive sample treatment steps result in long protein processing

times. To overcome those obstacles, rapid in-solution digestion protocols have been developed

using organic solvents to denature proteins or by applying higher incubation temperatures to

accelerate reaction times.[283-286] However, efficient protein identification from in-solution

digestion of dilute protein samples can be difficult due to low proteolytic digestion rates and

background from autodigested trypsin that is typically observed in mass spectra when a high

concentration of trypsin is used.

    As an alternative to in-solution digestion, bioreactors can be used to digest small

quantities of separated proteins. Typically, the reaction time required for homogeneous solution

tryptic digestions is tens of hours to achieve a sufficient population of peptide fragments for

effective PMF because the enzyme-to-substrate ratio must be kept low to avoid interferences

from autodigested trypsin.[202] In order to overcome this problem, enzyme-immobilization on solid

supports for solid-phase bioreactors has been introduced.[44, 201, 202, 204] Many of these solid-phase

bioreactors use immobilization of proteolytic enzymes through covalent attachment to supports

or encapsulation within gel matrices. Compared to homogeneous reactors, solid-phase enzymatic

bioreactors offer several advantages such as faster and simpler sample preparation steps, fewer

enzyme autolysis products, good reproducibility, larger enzyme-to-substrate molar ratios, high

digestion efficiency, and the possibility of repeated use. Wang *et al.*[202] developed a microfluidic

chip that was packed with trypsin-loaded beads in a fluidic channel. It was found that the bead-

packed chip gave faster protein digestion and fewer trypsin autolysis products compared to a homogeneous reaction.

Functionalized 3-D support networks can also be made *in situ,*[44, 181, 201, 204] which overcomes the difficulty of packing beads into the microchannels. Typically, these *in situ* methods use a polymerization reaction of a monomer solution inside a channel to modify the support. Then, trypsin solution is infused into the bioreactor for about 24 h for complete immobilization. Even though a fast reaction time, ranging from 5 s to 1 h, was achieved, it required 12 to 24 h for enzyme immobilization. In addition to complex and time-consuming preparation, none of the above bioreactors have been adapted to MALDI target deposition.

In this study, we report on a simple microfluidic device that incorporated both trypsin digestion and MALDI matrix addition for spotting tryptic digests for MALDI-TOF MS analysis. We prepared a novel trypsin immobilized PMMA solid-phase microfluidic chip consisting of an open channel reactor and a coaxial collection tip. Also, we developed an off-line MALDI interface to combine matrix addition and deposition on a MALDI target using a robotic plate spotter modified to accept the effluent from the microfluidic chip. This system was applied to the digestion of proteins and deposition onto a MALDI target plate. The enzymatic bioreactor was used for the rapid digestion of several proteins followed by off-line MALDI TOF MS detection of the generated peptides. The fabricated bioreactor included coaxial channels for mixing digested peptides with the matrix solution.

3.3 Experimental

The microfluidic chips were fabricated in poly(methyl methacrylate), PMMA, using a micromilling machine and incorporated a bioreactor, which was 100 µm wide, 100 µm deep and had a 4 cm effective channel length (400 nL volume). The PMMA chip was designed to fit into the stationary mount of a robotic fraction collector system (Probot, Dionex, Sunnyvale, CA); the

MALDI plate translated in the x/y plane for spot deposition. Two PMMA blocks were tapped to accept 1/16" tube fittings, which were epoxy glued to the microchip. A schematic and photograph of the assembled chip is shown in Figure 2-8 and Figure 2-9.

The PMMA bioreactor contained surface immobilized trypsin, which was covalently attached to the UV-modified PMMA surface using coupling reagents, *N*-(3-dimethylaminopropyl)-*N'*-ethylcarbodiimide hydrochloride (EDC) and hydroxysulfosuccinimide (sulfo-NHS). The chip had a coaxial matrix/analyte mixing system where the analyte flowed through an inner tube and the matrix flowed through an outer tube and was mixed at the point of target deposition for off-line MALDI detection. The chip was operated by pressure-driven flow using a syringe pump (Model 11, Harvard Apparatus, MA) which was used to supply the microchip with a protein solution. Solutions of proteins in 50 mM ammonium bicarbonate buffer solution were driven through the trypsin immobilized PMMA microchannel by a syringe pump at various volume flow rates. MALDI matrix was added to the microchip reservoir via a syringe pump at a flow rate of 5 µL/min. The MALDI matrix solution consisted of 5 mg/mL CHCA dissolved in 60% acetonitrile with the addition of 0.1% TFA containing an internal standard of bradykinin (5 µM). The digested peptides were mixed with a MALDI matrix on-chip and deposited as discrete spots on MALDI targets. After the deposited samples were analyzed, mass spectral peaks were searched using the MASCOT search program.

Protein standards equine cytochrome *c* (C-2506), equine myoglobin (M-1882), bovine serum albumin (BSA, A-0281), and phosphorylase *b* from rabbit muscle (P-6635) were dissolved in 50 mM ammonium bicarbonate buffer (pH 8.2). To evaluate the chip performance, a stock solution of 50 µM cytochrome *c* was prepared. The stock solution was diluted to 10, 5, 2, 1, and 0.5 µM with 50 mM ammonium bicarbonate.

3.4 Results

3.4.1   Off-Line Microfluidic Chip Interface to MALDI-TOF MS

Cytochrome *c* was used as a model protein for evaluating the performance of the

automated tryptic digestion and droplet deposition system. A 10 µM cytochrome *c* solution in 50

mM ammonium bicarbonate buffer was pumped through the solid-phase bioreactor at a flow rate

of 1 µL/min using a syringe pump. The bioreactor was an open channel design and was 4 cm

long (100 µm width and 100 µm depth of channel) with a total reactor volume of 400 nL

containing surface-immobilized trypsin. The effluent from the bioreactor was combined with a

matrix solution on-chip delivered by a separate syringe pump and spotted onto a MALDI plate

using a robotic fraction collector system. The deposition time of each fraction was 20 s and each

drop had a total volume of 2.0 µL, which consisted of analyte with matrix solution mixed in a

ratio of 1:5 (v/v). Therefore, each drop consisted of approximately one bioreactor volume. The

spot sizes deposited were 1.5 mm in diameter with a standard deviation of ± 0.2 mm. The hold-

up volume of this system was estimated to be ~0.3 µL, which was primarily from the silica

capillary tip used for deposition. The first fraction deposited onto the MALDI plate contained

only matrix as confirmed by mass spectrometry; digested peptides could be obtained after the

second fraction deposition at the flow rate used (1 µL/min).

3.4.2   MALDI Analysis of Solid-Phase Bioreactor Digested Cytochrome *c*

Each fraction obtained by the digestion and droplet system was analyzed by MALDI-

TOF MS; a representative mass spectrum of a fraction deposited at a 60 s system run time is

shown in Figure 3-1. The 10 µM solution of cytochrome *c* was pumped through the bioreactor at

a flow rate of 1 µL/min, which afforded a residence time within the reactor of 24 s. As seen in

this figure, 11 fragments containing 70 out of the 104 possible amino acids of cytochrome *c* were

obtained, producing a sequence coverage of 67%. Peptide fragments were assigned on the basis

of the MSDB database using the MASCOT search engine. The asterisks indicated identified

peptides; the other peaks were not identified.
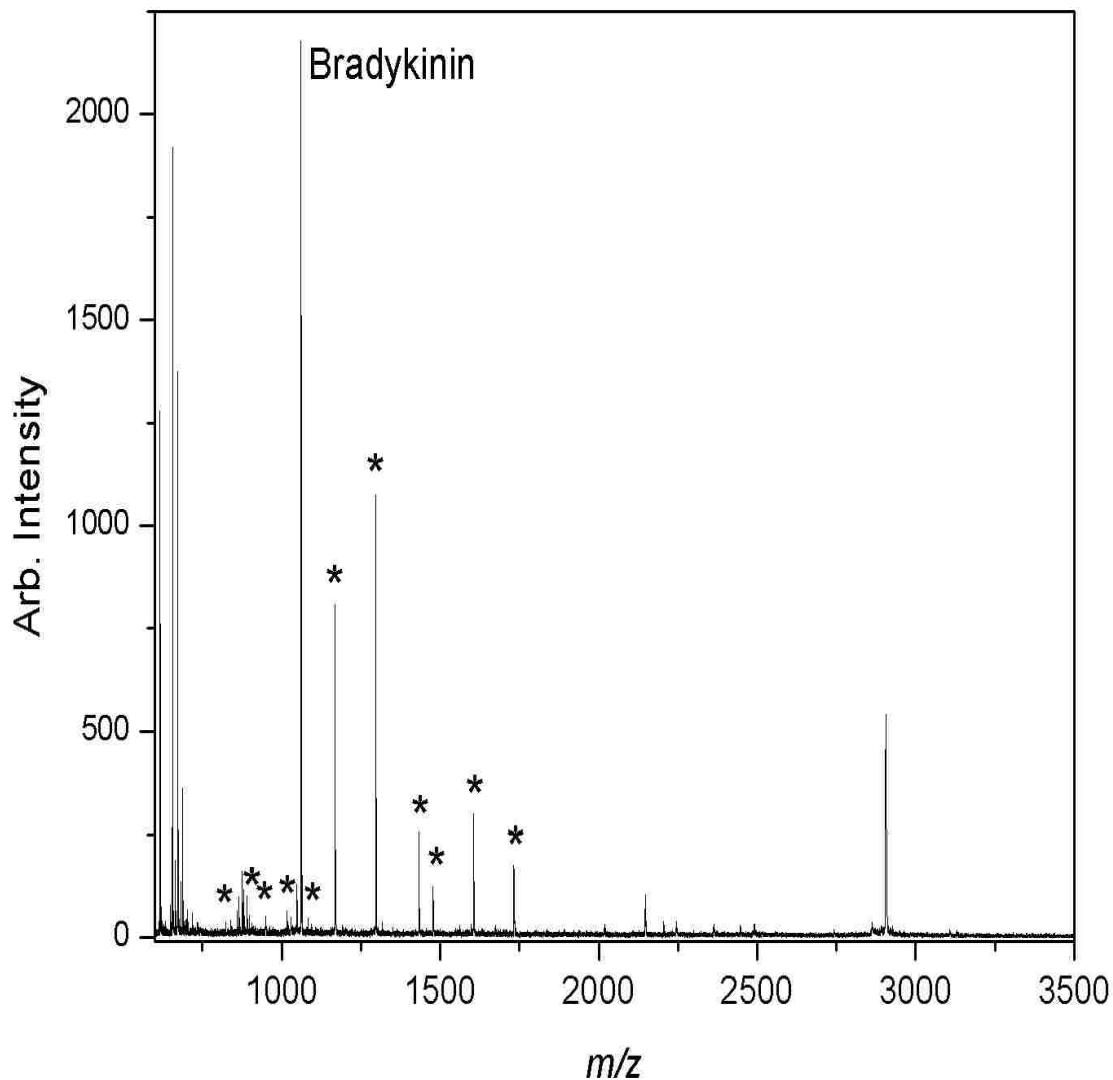
Figure 3-1. MALDI-TOF mass spectrum of tryptic digest of cytochrome *c* at 60 s: 10 µM in 50 mM ammonium bicarbonate buffer; flow rate, 1 µL/min; deposition time, 20 s (3.3 pmol); asterisks indicate matched peaks. Bradykinin is an internal standard.

This sequence coverage identification process was evaluated by the probability-based

Mowse score,[287, 288] which is defined as; -10Log (*P*), where *P* is the probability that the match is

a random event (P <0.05). This score represents the accuracy of a peptide mass fingerprint hit. The magnitude of the score is determined by the size of the database used, number of peptides and the size of the protein. In our search using digested mass lists of cytochrome c, Mowse scores greater than 78 are considered significant identifiers of the target protein. The mass spectrum in Figure 3-1 corresponds to a Mowse score of 137 and a sequence coverage of 67%. Thus the identified peptides matched the cytochrome c sequence with a high degree of certainty using our open channel bioreactor when operated at a volume flow rate of 1 μL/min. Although the digestion efficiency of this bioreactor was high, not all of the peptides were identified, which may be due to incomplete digestion for protease-inaccessible proteins, solubility of digested peptides, and lack of a denaturation step in the bioreactor protocol.[289] Sequence coverage ranging from 18 to 95 % have been reported for in-solution digestion of cytochrome c, which requires 15 minutes to 24 hours reaction time.[189, 192, 285]

The extent of protein reaction in the microfluidic chip was evaluated by comparing the mass spectrum of the unreacted protein to that of the digested protein from the chip. Figure 3-2 shows the mass spectra of 6.6 pmol cytochrome c flowed through the chip and deposited on the MALDI target. The mass spectra are from a fraction obtained 60 s after injection using MALDI-TOF in linear mode. The chip used for Figure 3-2a was not derivatized with trypsin and the intact protein is observed. Figure 3-2b was obtained from a chip with a trypsin derivatized surface and tryptic fragments are observed. The different ionization efficiency for peptides and proteins and the possibility of competitive ionization make a quantitative determination of the efficiency of the digestion difficult; however the significant decrease in the protein signal suggests that the extent of reaction is quite high.
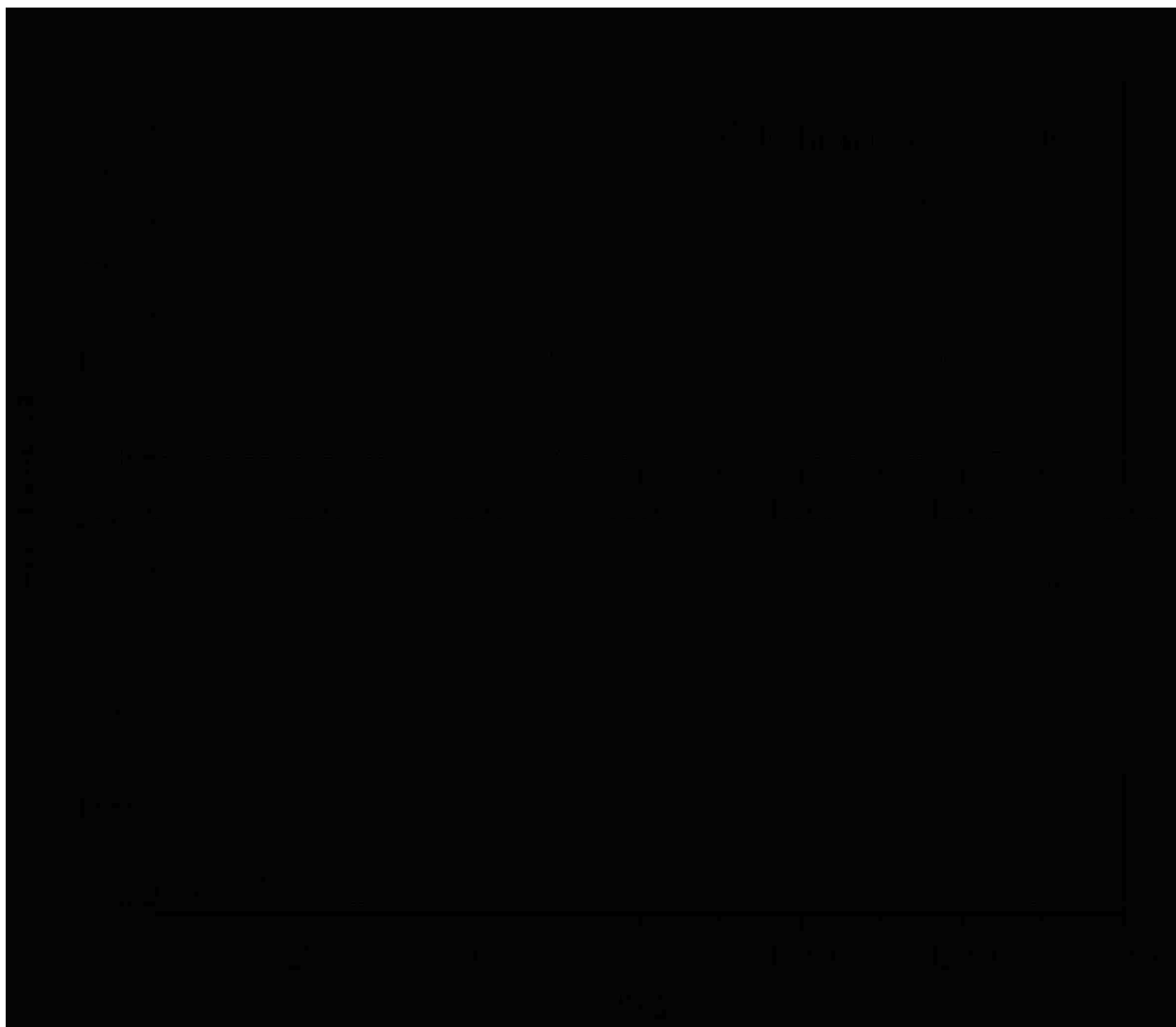
Figure 3-2. MALDI-TOF mass spectra obtained from a) intact cytochrome *c* and b) its tryptic digest at 60 s: 20 µM in 50 mM ammonium bicarbonate buffer; flow rate, 1 µL/min; deposition time, 20 s (6.6 pmol).

We next evaluated the effects of sample flow rate, which changes the residence time, on the extent of protein digestion in the solid-phase bioreactor by monitoring the sequence coverage. The flow rate of cytochrome *c* solution was set to 0.5, 1, 2, and 5 µL/min, corresponding to residence times of 48, 24, 12, and 4.8 s, respectively. The mass spectra obtained from cytochrome *c* digested at these different flow rates are shown in Figure 3-3. As seen in this figure, the digestion of cytochrome *c* was more efficient at lower flow rates as

evidenced by a larger number of peptide peaks in the mass spectrum. Mowse scores were 181 for

48 s residence time with 75% sequence coverage, 137 for 24 s residence time with 67% sequence

coverage, 128 for 12 s residence time with 59% sequence coverage, and 101 for 4.8 s residence

time with 42% sequence coverage.
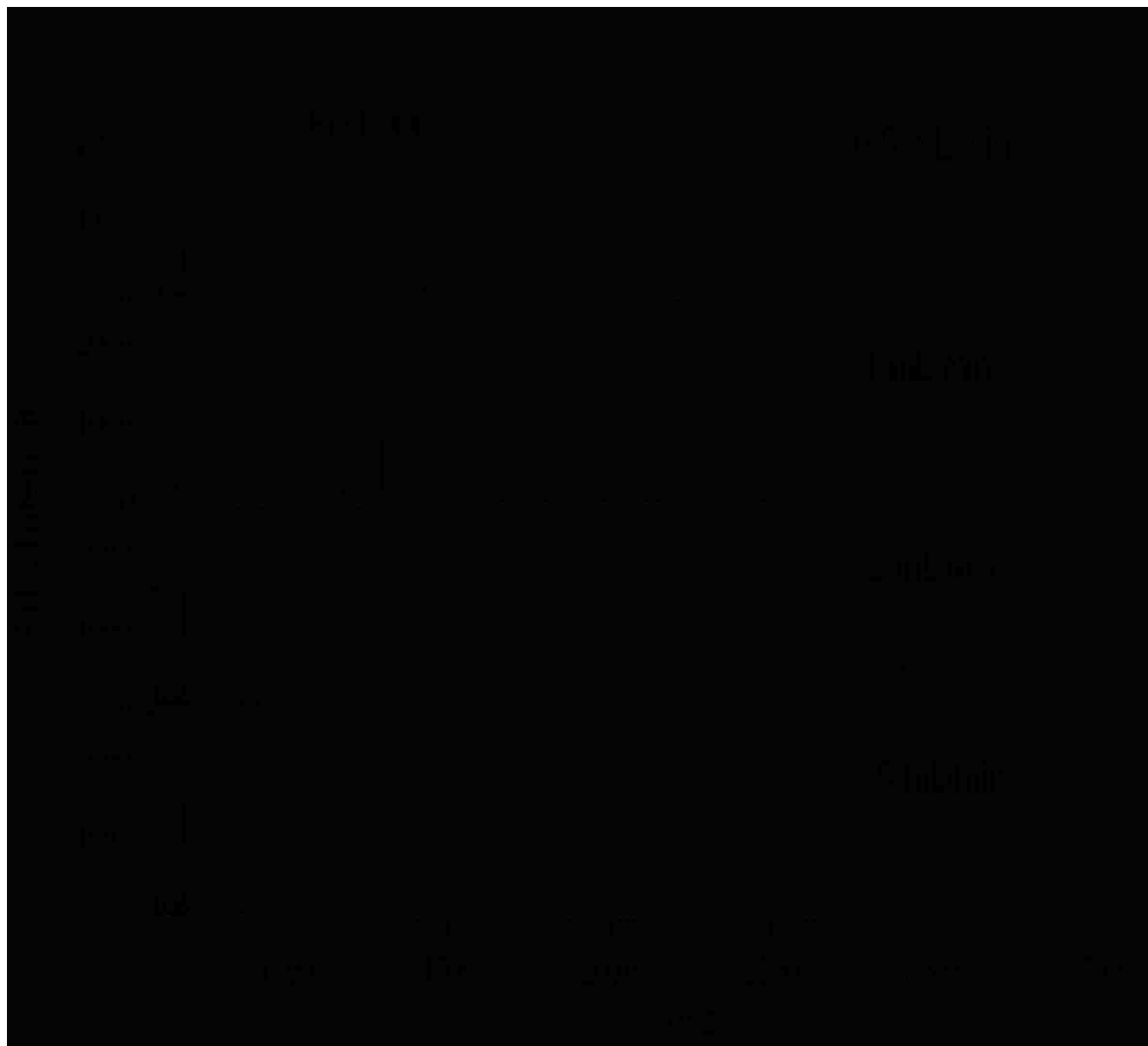
Figure 3-3. MALDI-TOF MS spectra obtained from digests of cytochrome *c* at different flow rates: 10 µM in 50 mM ammonium bicarbonate buffer; deposition time, 40, 20, 10, and 4 s for flow rate, 0.5, 1, 2, and 5 µL/min, respectively. Bradykinin is an internal standard. At low flow rate (long residence time) the intensity of peaks was larger compared to high flow rates.

The reaction rate for heterogeneous bioreactors is primarily determined by the mass transport of reactant to the surface and enzyme activity.[290, 291] In the open channel, mass transport plays a major role in determining overall reaction rate at higher flow velocities due to less frequent encounters between the solution-phase protein and the surface-immobilized enzyme.[40, 203] Slovakova *et al.* described a methodology for efficient digestion using a bioreactor packed with immobilized trypsin beads in order to reduce diffusional distances and increase the number of encounters between the reactant and substrate.[203] In their report, the sequence coverage of human growth hormone increased from 7% to 44% with increased residence time ranging from 141 s to 564 s.

In a previous study, Duan *et al*. reported increased digestion efficiency with greater residence time of cytochrome *c* in a monolithic enzymatic bioreactor prepared by *in situ* polymerization of acrylamide, *N*-acryloxysuccinimide, and ethylene dimethacrylate.[40] In their report, the sequence coverage of cytochrome *c* at a residence time of 7 s (1 µL/min) was 54.8%. In our system, 67% sequence coverage with the Mowse score of 137 at the flow rat of 1.0 µL/min (24 s residence time) was adequate to identify cytochrome *c* using an open channel reactor that did not require fabrication of a 3-D support network for the enzyme. In subsequent experiments reported herein, we utilized a flow rate of 1.0 µL/min since it produce a Mowse score adequate for protein identification.

3.4.3   Digestion Capacity of the Solid-Phase Open Channel Bioreactor

We next continuously monitored the peptides generated from a cytochrome *c* trypsin digest from the bioreactor at 20 s intervals to determine the stability of the bioreactor system. The immobilized trypsin was continuously exposed to a solution containing 10 µM cytochrome *c* prepared in 50 mM ammonium bicarbonate buffer at a flow rate of 1 µL/min. A total of 7 µL of 10 µM cytochrome *c* was flowed through the bioreactor using a syringe pump with

approximately 7 min of infusion. Twenty fractions were collected on the MALDI target plate and each fraction contained peptides from 3.3 pmol of cytochrome *c* injected into the reactor. The intensity and sequence coverage as a function of sampling interval obtained from the mass spectra data are shown in Figure 3-4. The intensity of the peak at *m/z* 1168, which is one of the major peptide peaks corresponding to residues 28-38 of cytochrome *c* (TGPNLHGLFGR), was normalized to the intensity of the internal standard, bradykinin (*m/z* 1060, 8.3 pmol) and this value was used as an indication of the extent of digestion. As seen in Figure 3-4a, the *m/z* 1168 peak was observed 40 s (including hold-up time of 18 s) after 0.4 µL of cytochrome *c* was injected into the bioreactor. The normalized peak intensity ratio reached a maximum after one minute and remained at that within the standard deviation of the measurement. During the continuous injection of cytochrome *c*, the peak intensity ratio was nearly the same, which indicates that the activity of trypsin covalently attached onto the PMMA surface remained high during this experiment. In Figure 3-4b, it can be seen that the sequence coverage of cytochrome *c* was 53% at 40 s. The fraction at 60 s had a sequence coverage of 67% and remained at this value during the rest of this experimental run. Note that this value is appropriate for confirmation of cytochrome *c* based on Mowse score. The fraction at 100 s did not produce significant differences from the fraction at 60 s. In contrast with in-solution digestion which cannot be reused, the solid phase bioreactor could be reused without noticeable loss of activity of immobilized enzyme.[44, 281, 292] During three independent experimental runs similar to that shown in Figure 3-4 using the same bioreactor, the activity remained relatively constant after rinsing the bioreactor with 50 mM ammonium bicarbonate between experimental runs. The memory effect of the bioreactor was checked between runs of cytochrome *c* solutions by collecting and analyzing the first spot. As can be seen in the figure, these blank spots did not result in any mass spectral peaks due to carryover.
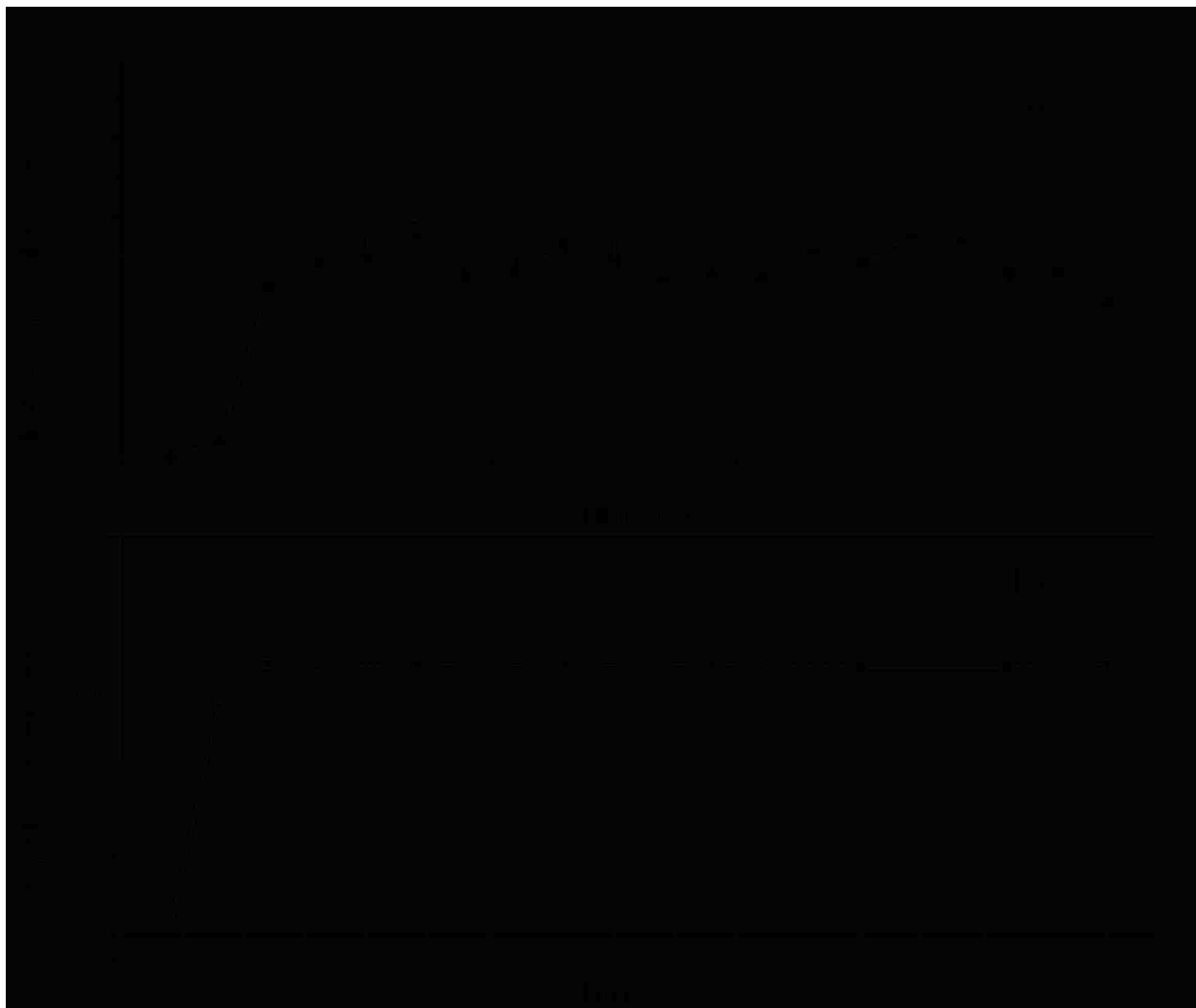
Figure 3-4. Evaluation of microfluidic chip performance for the digestion of cytochrome *c* as a function of time: a) intensity ratio of selected peak (*m/z* 1168) using internal standard, bradykinin (*m/z* 1060) and b) sequence coverage; 10 µM in 50 mM ammonium bicarbonate buffer; flow rate, 1 µL/min; deposition time, 20 s.

Typically, proteins are digested in solution at an enzyme-to-substrate molar ratio of 1:50 for 24 h of incubation.[30] When a relatively low enzyme-to-substrate molar ratio is employed, the enzymatic reaction has low efficiency;[30, 192] however, this low molar ratio is necessary to avoid excessive autodigestion of trypsin. Lazar *et al.* discussed the effects of trypsin concentration on the rate of digestion in solution.[192] In their work, in-solution digestion of various proteins was accomplished using enzyme-to-substrate molar ratios of 1:1 to 1:20 for 15 min to 24 h of

incubation. For the highest enzyme-to-substrate mole ratio (1:1), adequate digestion could be obtained after 15 min of digestion. The sequence coverage of cytochrome *c* at that mole ratio was 88-95% using ESI-TOF MS. In our experiment, 8 pmol trypsin was used for immobilization onto the surface of the UV-exposed microchannel. The amount of immobilized trypsin depends on the molecular size of trypsin and the surface density of the carboxylate group on the substrate. In a previous study, McCarley *et al*. described the effect of UV exposure time on carboxylic acid coverage on PMMA surfaces, which was determined to be 1×10^{-9} moles/cm^2 after an exposure time of 20 min.[206] Trypsin is a globular protein of 24 kDa with a diameter of about 4 nm.[179] If it is assumed that trypsin is attached to the PMMA surface in a monolayer, the quantity of trypsin immobilized on the surface of the bioreactor can be calculated by taking into account the carboxylic acid coverage, the size of trypsin, and the surface area. Using these values, it is found that the reactor contains 2.1 pmol trypsin. The 10 µM of cytochrome *c* used to test the performance of the bioreactor corresponds to 4 pmol protein, thus the enzyme-to-substrate mole ratio was nearly 1:2 for a single enzymatic reaction.

3.4.4   Effects of the Quantity of Cytochrome *c* on Sequence Coverage

Figure 3-5a shows the intensity ratio of peptide peaks normalized to the internal standard, bradykinin, obtained from different amounts of cytochrome *c*. The digest peak at *m/z* 1168 was normalized using the internal standard peak, which resulted from 8.3 pmol of bradykinin. As shown in Figure 3-5a, the intensity ratio increased with increasing quantity of cytochrome *c*. At 170 fmol of cytochrome *c* (Figure 3-5b), the peptide peaks indicated with asterisks were identified. The signal-to-noise ratio (SNR) of identified peaks was above 10 except for the peak at *m/z* 1633.3, where the SNR was 7. Below 0.66 pmol, the sequence coverage was 57% and it reached 67% at 3.3 pmol where the best sequence coverage was obtained. Above 3.3 pmol of

cytochrome c, the peak intensity ratio was saturated most likely due to longitudinal diffusion of

proteins at high concentration being restricted, reducing mass transport to the surface.[200]
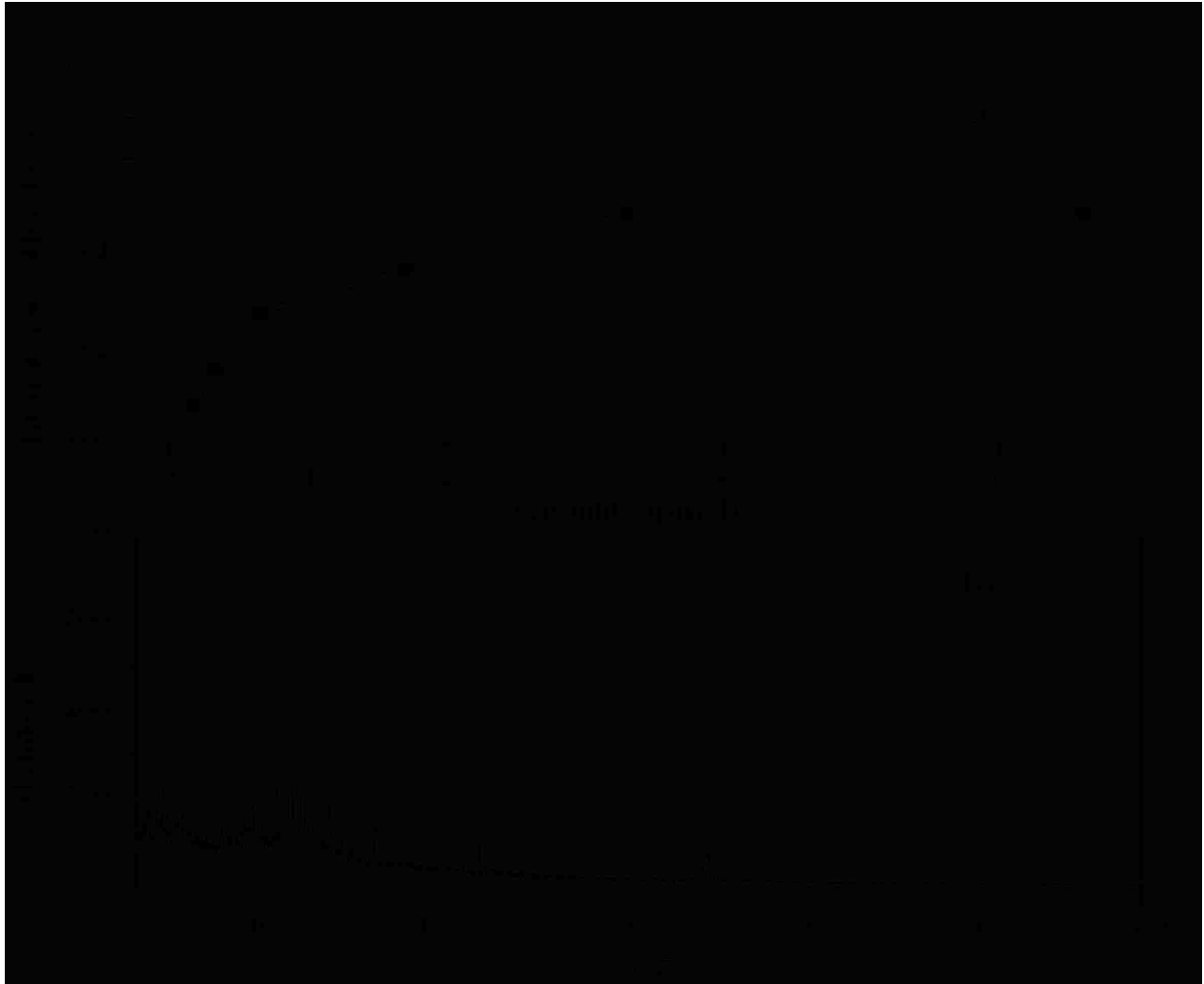
Figure 3-5. a) Effect of relative intensity for the tryptic digests of cytochrome *c* as a function of quantity in pmol: internal standard, bradykinin (*m/z* 1060); flow rate, 1 µL/min; deposition time, 20 s; b) MALDI-TOF mass spectrum of tryptic digest of 0.5 µM cytochrome *c* in 50 mM ammonium bicarbonate buffer (170 fmol).

3.4.5   Tryptic Digestion of Proteins

The performance of the bioreactor system was further evaluated for proteins with

different molecular weights and isoelectric points. The immobilized trypsin bioreactor was

exposed to solutions containing 10 µM BSA (66 kDa), 10 µM myoglobin (16.5 kDa), and 10 µM

phosphorylase *b* (97 kDa) prepared in 50 mM ammonium bicarbonate buffer. Each deposited

spot contained digested peptides from 3.3 pmol of protein infused at 1.0 µL/min flow rate and a

20 s deposition time. The mass spectra of the trypsin-digested proteins are shown in Figure 3-6.
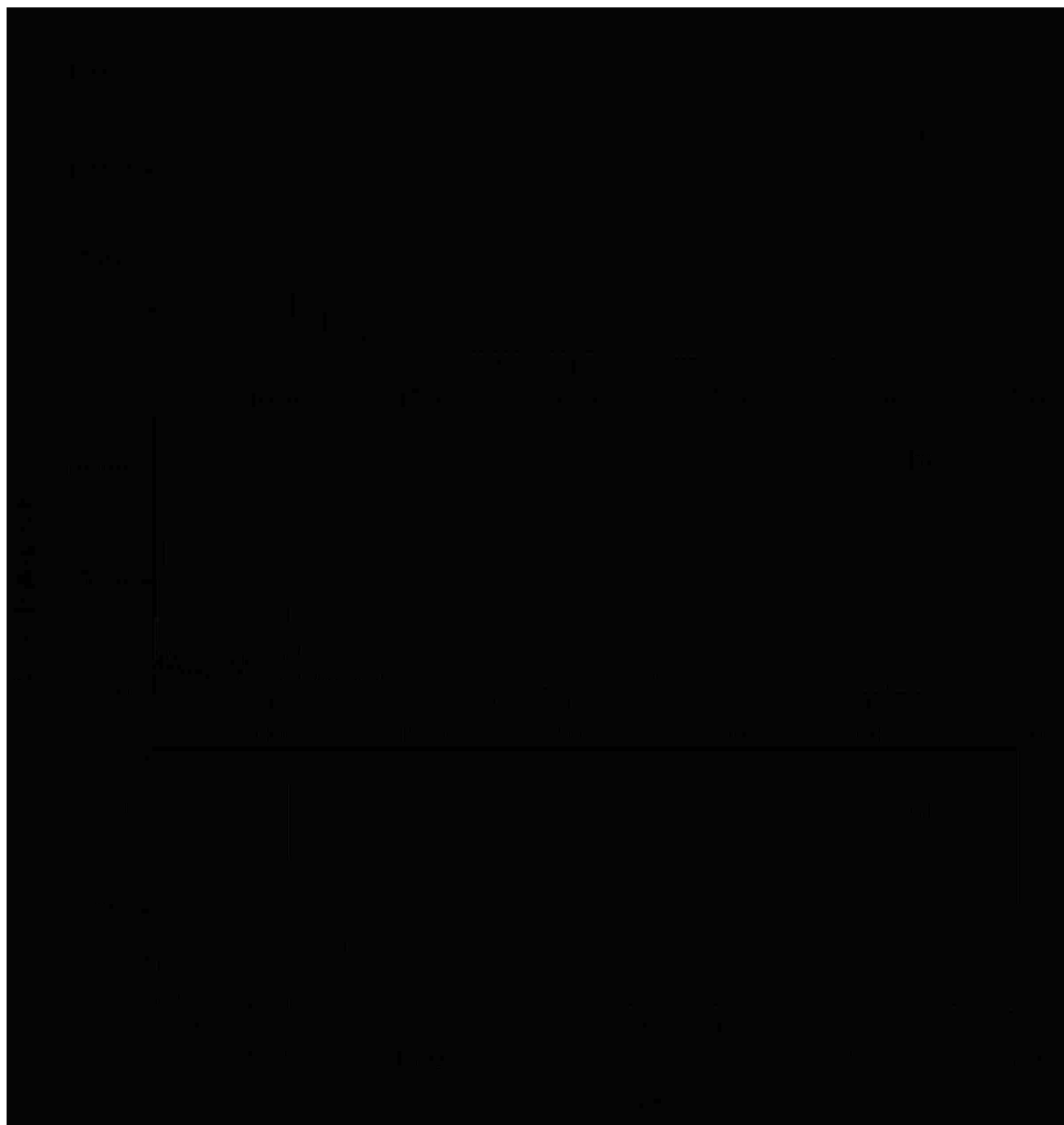
Figure 3-6. MALDI-TOF mass spectra of tryptic digests of a) BSA, b) myoglobin, and c) phosphorylase *b* using the automatic digestion chip. Proteins are 25 µM in 50 mM ammonium bicarbonate buffer; flow rate, 1 µL/min; deposition time, 20 s (3.3 pmol); Sequence coverage of BSA, myoglobin, and phosphorylase *b* was 35, 58, and 47 %, respectively.

The microfluidic chip coupled to the MALDI-TOF MS analysis produced an average sequence coverage of 35, 58, and 47% for BSA, myoglobin, and phosphorylase *b*, respectively. The probability-based Mowse score (P < 0.05) was 143 for BSA, 121 for myoglobin, and 319 for phosphorylase *b*. Based on sequence coverages and Mowse scores of these proteins, the identified peptides matched target proteins with high degree of certainty. Compared to cytochrome *c*, lower sequence coverage was obtained for these proteins which was likely due to their proteolysis-resistant structures.[191, 293] BSA is typically difficult to digest because its tertiary structure is stabilized by disulfide bonds. Myoglobin is also resistant to tryptic digestion at the stabilized hydrophobic interior and phosphorylase *b* has a relatively high molecular weight with a folded structure.

3.5 Summary

In the work described in this Chapter, the coupling of a PMMA microfluidic chip to MALDI-TOF MS was developed for an automated enzymatic digestion and droplet deposition system. This system integrates steps for proteomic analysis using MALDI-TOF MS such as digestion, mixing with a matrix solution, and depositing onto a MALDI target plate. Compared to several reported microfluidic devices for protein digestion that require reaction times of 3 to 10 min to achieve the desired sequence coverage,[193, 202, 203, 293] our automated digestion system affords comparable coverage after a residence time of less than 1 min. These results show that our microfluidic chip system coupled with a MALDI-TOF MS can be successfully applied to a wide range of proteins with high-throughput and sensitive detection of peptides for proteomic research.

CHAPTER 4. DEVELOPMENT OF AN EFFICIENT ON-CHIP DIGESTION SYSTEM FOR PROTEIN ANALYSIS USING MALDI-TOF MS[*]

The work reported in this chapter has been published in the *Analyst*.[294]

4.1 Overview

In this chapter the development of a micropost bioreactor operated with electrokinetically-driven flow interfaced to MALDI MS for the digestion of proteins is described. An increase in protein digestion efficiency was achieved by introducing micropost-structured channels, which have a higher surface area-to-volume ratio compared to open channel formats. The micropost bioreactor was created using hot embossing on PMMA disks from a mold master in a single step. Using this bioreactor, improved protein sequence coverage was obtained for various proteins tested.

4.2 Introduction

Most proteomic analyses rely on the combination of two-dimensional gel electrophoresis with MS for identification of complex protein mixtures.[8] An alternative, shotgun sequencing, uses multi-dimensional separation of proteolytic fragments generated from intact proteins followed by MS analysis and data base searching.[11] Effective separation tools with efficient digestion protocols are required to identify individual proteins for both multi-dimensional and shotgun approaches.[10] Furthermore, the sample preparation steps such as digestion, separation, and cleanup can be time consuming and labor-intensive.[141] Maintaining high sensitivity and high protein sequence coverage with low sample consumption and high throughput are the analytical challenges for the development of a fully automated proteomic analysis system.[142]

Efficient digestion of intact proteins is an indispensable component of systems for fast and accurate protein identification.[178, 179] To achieve optimal peptide identification, the

_____

*Reproduced by permission of The Royal Society of Chemistry.

efficiency of digestion must be maximized. Three different approaches are used for proteolytic protein digestion: in-gel,[180] in-solution,[30] and solid-phase bioreactor.[181] Among them a solid-phase bioreactor has many advantages in terms of fast response, low sample/reagent consumption, minimal sample loss, reduced autolysis of typsin, and a higher enzyme-to-substrate ratio.[189]

The digestion efficiency of solid-phase microreactors depends on the geometry of the reactor, the digestion temperature, the compositions of digestion solvents, and the transport velocity of the target protein through the reactor.[40, 191-193] Also, the digestion efficiency can be enhanced by physical means such as microwave energy[194] and ultrasound.[195, 196] One of the limitations associated with solid-phase reactors for digestion is their poor kinetics due to the slow mass transport of proteins to the reactor surface.[295] In contrast to in-solution digestion, proteins in a solid-phase microreactor must diffuse to the immobilized enzyme to undergo digestion. Therefore, optimized support geometries for the microreactors are required to reduce mass transfer limitations.[296-298]

The efficiency of digestion can be increased by moving from an open channel to a three-dimensional (3-D) format. This bioreactor type can improve digestion efficiency due to the high surface area-to-volume ratio resulting in reduced diffusion paths and an increase in the number of encounters between the substrate and immobilized enzyme.[203, 298] Various bioreactor types have been developed to improve digestion efficiency using 3-D formats, for example, reactors packed with typsin-loaded beads,[202] sol-gels,[44] and monolithic porous networks.[201] Fast and efficient digestion of proteins can be achieved with these 3-D approaches due to their higher surface area-to-volume ratio proteolysis reactions, which take between 5 s and 1 h with these geometries. Even though monolithic bioreactors provide fast reaction kinetics, relatively long times are required for preparation due to the multiple

75

steps.[44, 201, 204, 282] When monomers with different polarities are used for monolithic columns, the preparation of homogeneous supports is also hindered.[170]

In Chapter 3, a simple and fast digestion and deposition microfluidic device with an open-channel bioreactor operated by pressure-driven flow was described.[81] As indicated in the previous chapter, the limitation in this open channel bioreactor format was the relatively long diffusion distances, which resulted in a diffusion-limited digestion rate due to the relatively small diffusion constants of proteins. A 3-D structured bioreactor can be achieved by introducing microposts inside the open channel bioreactor. A micropost structured bioreactor can be manufactured in a simple fashion using micro-replication of a polymeric material from a mold master in a single step because it does not require bead packing or the formation of a polymer monolith within the channel. Also, inter-micropost distances are fixed, which provides reproducible devices because of the precise microfabrication processes.[299, 300] Furthermore, the support structures are fixed in the desired location within the device and can provide unrestricted substrate access to the immobilized enzyme.

Electrokinetically-driven flow inside a microchannel has many advantages over pressure-driven flow for bioreactor digestion. An electrokinetic flow eliminates the need for a mechanical pumping system, allows easy control of forward and reverse flow, and provides a flat flow profile in the microchannel.[275] In addition, the applied electric field can induce protein conformational changes, which can provide efficient enzymatic cleavage to aid in protein digestion.[293]

In this Chapter, we report on the fabrication, assembly, and testing of a novel trypsin immobilized PMMA microfluidic chip with micropost structured channels. The microfluidic chip was fabricated using hot embossing and trypsin was covalently immobilized on the surface of the PMMA microposts using a UV mediated surface modification protocol. This

system employed an electric field to transport proteins through the bioreactor and move the peptides from the enzymatic reactor directly onto a MALDI target. The electrokinetically-driven flow was used to deposit the chip effluent on a MALDI target plate using a robotic fraction collector system. Cytochrome *c* was used as a model protein for optimizing the performance of the system and for evaluating digestion efficiency in terms of sequence coverage. The performance of this system using molecular standard proteins such as bovine serum albumin, phosphorylase *b*, and β-casein was also demonstrated. Finally, intact *Escherichia coli (E. coli)* was used to demonstrate bacterial fingerprint analysis using this system.

4.3 Experimental

A mold master was prepared using micro-milling[267] and was subsequently used to replicate polymer microparts via hot embossing. The desired microfluidic network was designed using computer-aided design software. The mold master was used to replicate PMMA chips using hot embossing on PMMA disks that were 5 mm thick and 120 mm diameter.[2, 272, 273] The embossed microfluidic devices had a bioreactor consisting of a 4 cm long × 200 µm wide × 50 µm deep microfluidic channel populated with an array of 50 µm in diameter microposts with a 50 µm inter-post spacing. Figure 4-1 shows a photo of the micropost channel.

Figure 4-1. A photo of the micropost channel

Two reservoirs of approximately 1 mm in diameter were drilled for sample and matrix solution introduction. The enzyme attachment based on PMMA modification protocols was described in Chapter 2.[206]

The PMMA microfluidic chip was mounted in a microfraction collector system. Electrokinectically-driven flow was used for transporting the proteins through the bioreactor and the deposition of the resulting peptides along with a matrix solution onto the MALDI target plate. The PMMA chip was designed to fit into a stationary mount of a robotic fraction collector system (Probot, Dionex, Sunnyvale, CA); the MALDI plate translated in the xy plane for spot deposition. A photo of the assembled chip was shown in Figure 4-2.

The chip had a coaxial matrix and analyte mixing system with the analyte exiting the chip. To generate an electrokinetically-driven flow inside the bioreactor, platinum electrodes were inserted into a sample inlet (anode) and the end point (cathode) of the bioreactor, which was sealed in place using epoxy (see Figure 2-11). The analyte flowed through the interface capillary and the matrix through an outer tube using pressure driven flow. These eluents were mixed at the point of target deposition on the MALDI plate. The interface capillary was 1 cm in length and had an ID of 100 µm and an OD of 363 µm, which was surrounded by a 1 cm long stainless steel tube that was 500 µm ID and 1.5 mm OD. The capillary was inserted into a guide channel that was embossed into the chip and placed directly at the output end of the microreactor and, finally glued in place.

Solutions of cytochrome c, BSA, phosphorylase b, and β-casein in 50 mM ammonium bicarbonate buffer solution were infused through the microchannel at a field strength of 375 V/cm. MALDI matrix was added to the microchip reservoir hydrostatically with a syringe pump at a flow rate of 2 µL/min. The MALDI matrix solution consisted of 5 mg/mL CHCA

dissolved in 60% acetonitrile with 0.1% TFA. Eluent from the microchip was deposited onto

a 100 spot MALDI target plate for 10 s per spot.
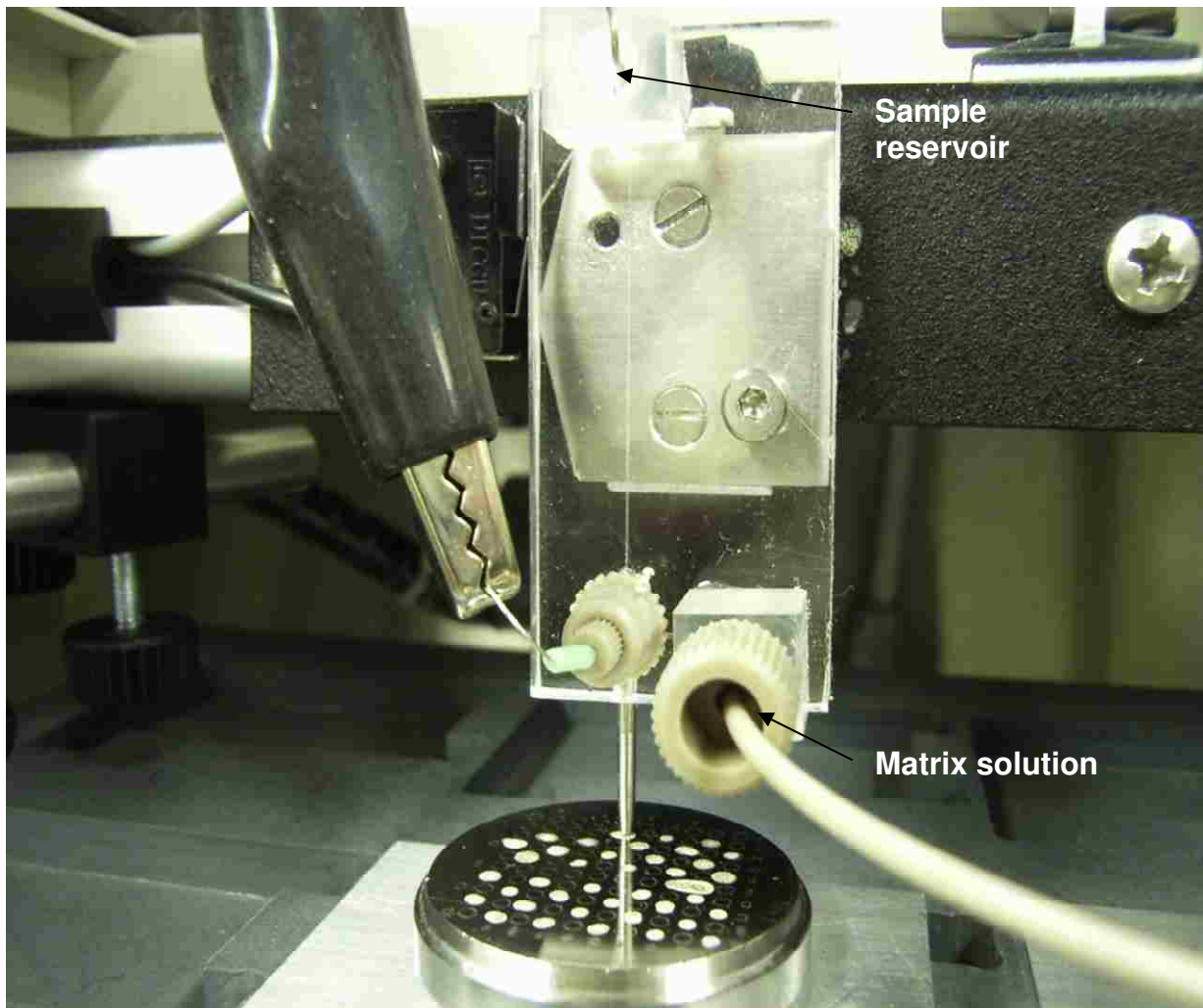
Figure 4-2. A photo of the micropost bioreactor attached on a robotic fraction collector for off-line MALDI MS detection.

4.4 Results

The bioreactor used in this study consisted of a microfluidic channel with 50 µm

diameter microposts with immobilized trypsin on the reactor walls, a matrix solution channel,

and two electrodes for generating the electrokinetic flow through the bioreactor and driving

the eluent of the bioreactor through the interface capillary. In our previous study, we used a 4

cm long open-channel bioreactor containing immobilized trypsin that had a total bioreactor volume of 400 nL with 16 mm^2 surface area.[81] In the current study, the total volume of the micropost reactor was 340 nL with a 22 mm^2 surface area. There were approximately 570 posts in the bioreactor, which increased the surface area-to-volume ratio of this chamber by 60% compared to the open channel reactor. This higher surface-to-volume ratio will increase the number of encounters between the protein and the surface bound enzyme due to reduced diffusional distances.

Cytochrome c was used as a model protein for evaluating the performance of the micropost bioreactor and droplet deposition system. A 10 µM cytochrome c solution in 50 mM ammonium bicarbonate buffer was moved through the bioreactor at a field strength of 375 V/cm. To evaluate the efficiency of fluid transfer between the bioreactor and the interface capillary (see Figure 2-11), a solution of cytochrome c was allowed to flow though the bioreactor for ~10 min without allowing matrix solution to flow into the sheath tube (see Figure 2-11b). This was followed by flowing a MALDI matrix solution through the outer sheath tube and the mixture was deposited directly on the MALDI plate in ten separate fractions for 30 s intervals (volume = 1 µL). MALDI analyses confirmed that each fraction deposited onto the target plate contained only matrix peaks and no discernable cytochrome c peaks were observed in the mass spectrum. From this analysis, we concluded that the leakage of sample into the sheath matrix flow was minimal.

The eluent from the bioreactor was combined with a MALDI matrix solution delivered by a syringe pump and the combined streams were spotted onto a MALDI target plate using a robotic fraction collector system. The deposition time was 10 s for each spot with a total volume ~0.5 µL, which consisted of the protein digest and the matrix solution mixed in a ratio of 1:2 (v/v) at a sample solution flow rate of 1 µL/min and a matrix solution

flow rate of 2 µL/min. The entire procedure of digestion, mixing with the matrix solution and deposition took less than 30 s to complete. The deposited spot sizes were 1.0 mm in diameter with a standard deviation of ± 0.1 mm. The hold-up volume of this system was estimated to be 80 nL, which resulted primarily from the interface capillary (100 µm ID × 10 mm long) used for deposition.
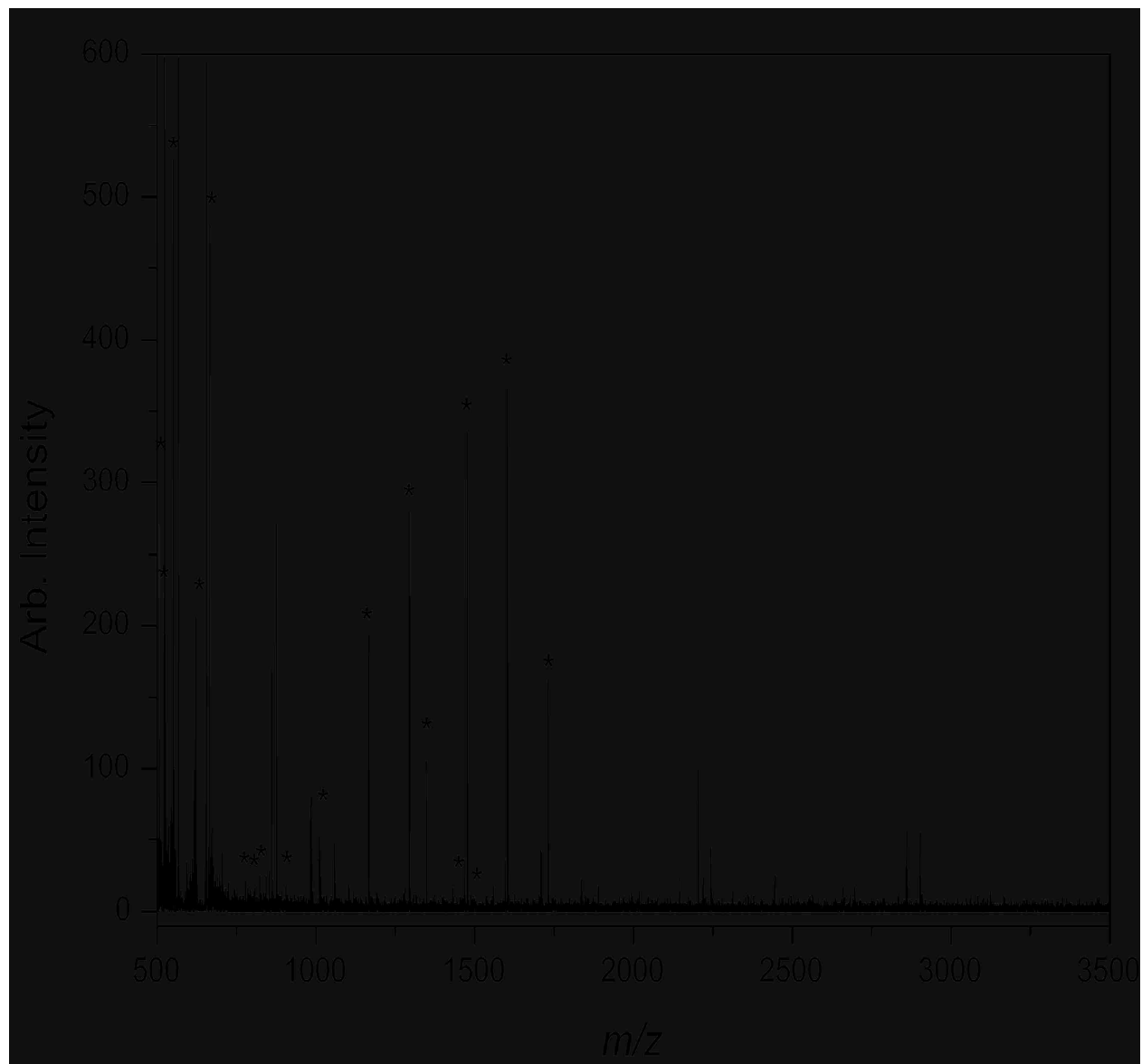

Figure 4-3. MALDI-TOF mass spectrum of the tryptic digest of cytochrome *c* from a fraction at 30 s: 20 µM in 50 mM ammonium bicarbonate buffer (pH 8.2); field strength, 375 V/cm; deposition time, 10 s; asterisks indicate identified peptide peaks.

Figure 4-3 shows a representative mass spectrum of a cytochrome *c* digest from a fraction obtained at 30 s after injection using MALDI-TOF in reflectron mode. A total of 19 fragments containing 101 out of the 104 possible amino acids of cytochrome *c* were obtained, producing a sequence coverage of 97%. This sequence coverage is significantly better than the 67% coverage obtained for an open channel bioreactor system with a similar residence time.[81] Peptide fragments were assigned on the basis of the MSDB database using the MASCOT search engine. The asterisks shown in Figure 4-3 indicate identified peptides. This sequence coverage identification process was evaluated using the probability-based Mowse (molecular weight search) score,[287, 288] which is defined as -10Log (*P*), where *P* is the probability that the match is a random event (*P* <0.05). In our search, using digested mass lists of cytochrome *c*, Mowse scores greater than 78 are considered significant identifiers of the target protein. The mass spectrum in Figure 4-3 corresponds to a Mowse score of 260; thus, the identified peptides matched the cytochrome *c* sequence with a high degree of certainty.

The apparent mobility, μ_{app}, of cytochrome *c* in the PMMA chip is the sum of the electroosmotic mobility, $\mu_{(EO)}$, and the electrophoretic mobility, $\mu_{(EP)}$, of cytochrome *c*. The apparent velocity at which the protein moves is governed by Equation 4-1;

$$\nu_{app} = \mu_{app}E = (\mu_{(EO)} + \mu_{(EP)})E \qquad (4\text{-}1)$$

where ν_{app} is the apparent velocity (cm/s) and E is the field strength (V/cm). The $\mu_{(EO)}$ of UV-exposed PMMA and the $\mu_{(EP)}$ of cytochrome *c* are 4.5×10^{-4} cm^2/Vs and 0.5×10^{-4} cm^2/Vs, respectively. From Equation 4-1, the apparent mobility was estimated to be 5.0×10^{-4} cm^2/Vs. Based on these parameters, a residence time was calculated as a function of field strength. For example, a field strength of 375 V/cm applied to the bioreactor produced

82

an apparent velocity of cytochrome *c* of 0.188 cm/s. Therefore, the residence time within the bioreactor at this field strength was approximately 21 s (0.188 cm/s on the 4 cm reactor). Also, a volumetric flow rate was estimated to 0.97 µL/min from the 0.34 µL reactor volume and 21 s residence time. Various field strengths were examined to find an optimal digestion condition for this microreactor. For field strengths of 250, 375, and 800 V/cm, the residence time was calculated to be 32, 21, and 10 s, respectively. The extent of sequence coverage decreased as the applied field strength increased. Mowse scores were 295 for a 32 s residence time with 100% sequence coverage, 260 for a 21 s residence time with 97% sequence coverage, and 165 for a 10 s residence time with 70% sequence coverage. A field strength of 375 V/cm was used in the remaining experiments to balance the processing time with high sequence coverage and high protein identification probability.

Figure 4-4 shows mass spectra obtained for different concentrations of cytochrome *c*. The immobilized trypsin bioreactor was exposed to solutions containing 0.5, 1.0, 2.0, 5.0, and 10 µM cytochrome *c* prepared in 50 mM ammonium bicarbonate buffer at identical bioreactor residence times of 21 s. Three replicate runs were obtained for each concentration. As shown in this figure, the number of peptide peaks increased with increasing cytochrome *c* concentration; the average sequence coverage was 41, 54, 64, 80, and 89% for concentrations of 0.5, 1.0, 2.0, 5.0, and 10 µM cytochrome *c*, respectively. Each deposited spot contained digested peptides from 0.08, 0.16, 0.32, 0.80, and 1.6 pmol of protein transported at a 375 V/cm field strength and a 10 s deposition time per spot. At 0.5 µM of cytochrome *c*, the lowest concentration tested, 7 peptide peaks generated from the tryptic digestion were identified. The probability-based Mowse score ($P < 0.05$) was 242 for 10 µM cytochrome *c*, 207 for 5 µM, 180 for 2 µM, 124 for 1 µM, and 96 for 0.5 µM.
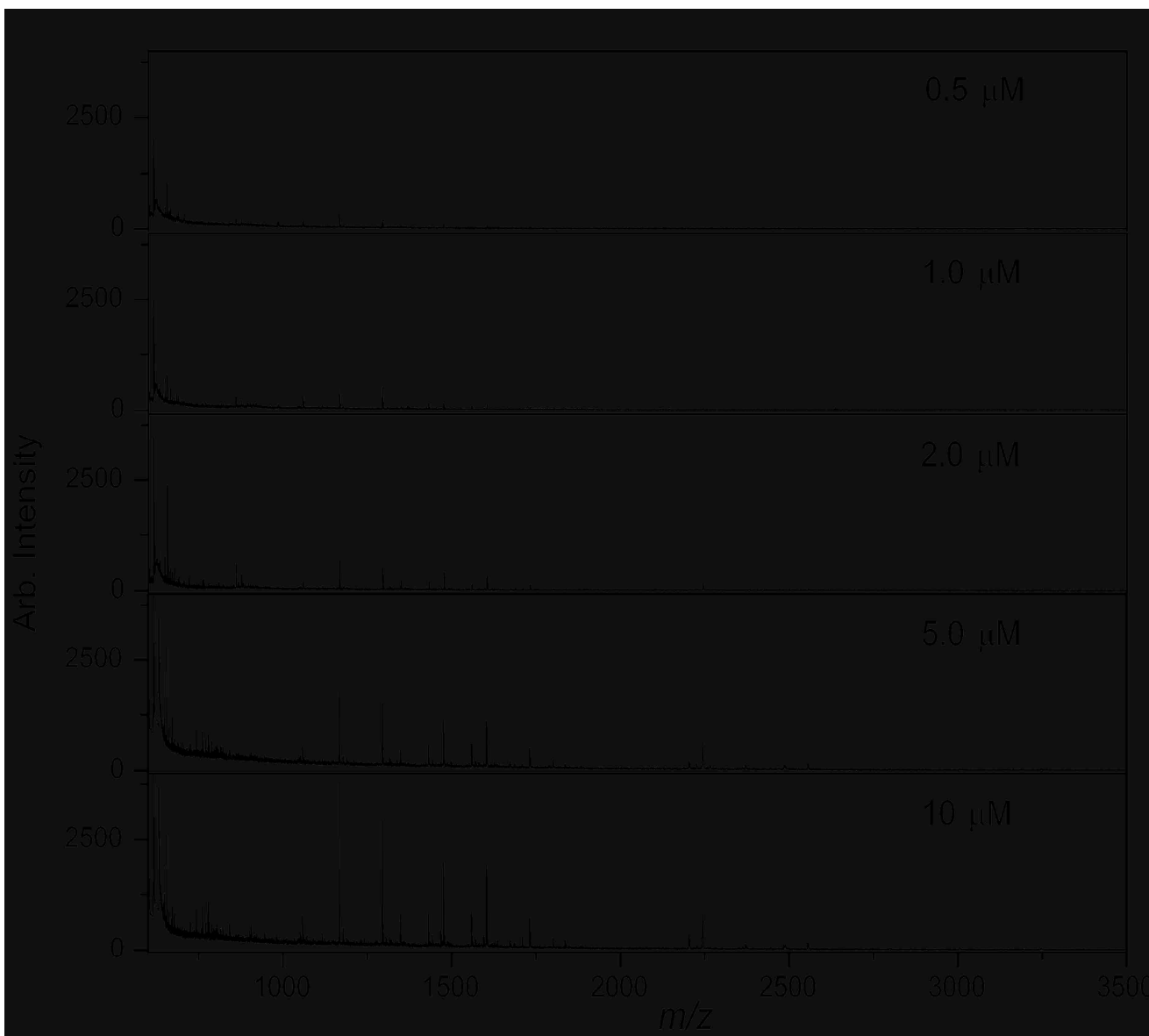
Figure 4-4. (a) MALDI-TOF mass spectra of tryptic digests of cytochrome *c* at different concentrations: 50 mM ammonium bicarbonate buffer (pH 8.2); field strength, 375 V/cm; deposition time, 10 s.

Figure 4-5 shows a comparison of the sequence coverage generated from the micropost and open channel bioreactor formats at different concentrations of cytochrome *c*. To compare these different reactors, an identical residence time of 21 s was selected. As can be seen in this figure, the sequence coverage increased with increasing concentration for both formats. However, for the open channel format, the sequence coverage gradually reached a

constant value above a concentration of 10 µM, most likely due to inadequate mass transport

to the enzyme-immobilized surface.[200] In contrast, the sequence coverage for the micropost

bioreactor was 90% at 10 µM concentration of cytochrome *c* and increased to 100% at 20

µM compared to only 65% at this same concentration for the open-channel format. At lower

concentrations, the rate of increase in the sequence coverage was substantially higher for the

micropost bioreactor compared to the open channel format, again likely due to the reduced

diffusional distances.
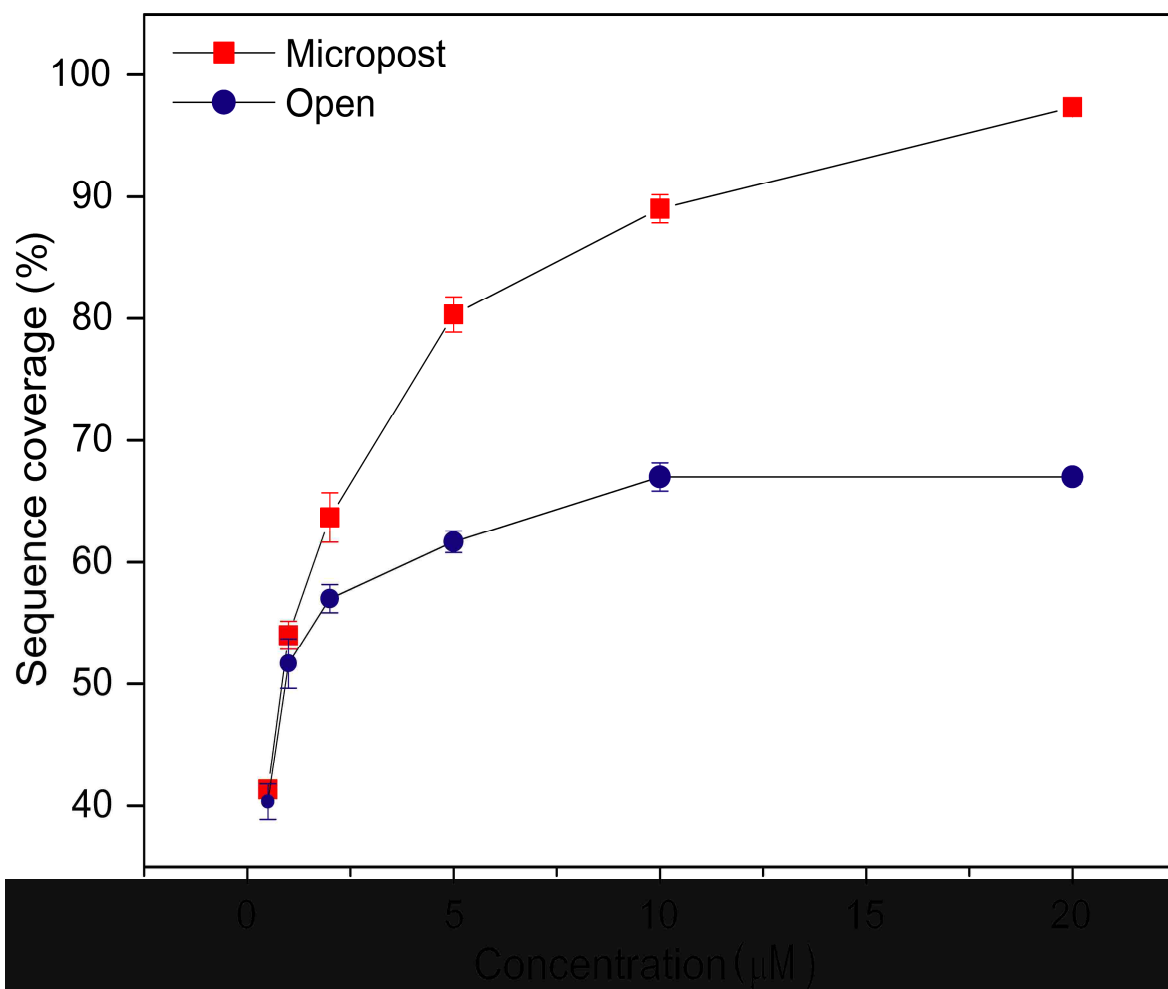
Figure 4-5. Sequence coverage for cytochrome *c* as a function of concentration for two bioreactor format; residence time, 21 s; ■ micropost channel, ● open channel.

The performance of the micropost bioreactor was also demonstrated for proteins with a range of molecular weights. For these studies, 10 μM BSA, 10 μM phosphorylase b, and 10 μM β-casein prepared in 50 mM ammonium bicarbonate buffer were infused electrokinetically into the bioreactor. The average residence times within the bioreactor at a field strength of 375 V/cm were measured at 24, 23, and 25 s for BSA, phosphorylase b, and β-casein, respectively. Each deposited spot contained peptides generated from approximately 1.42, 1.48, and 1.37 pmol for BSA, phosphorylase b, and β-casein, respectively, at 10 s deposition time. The mass spectra of the trypsin digested proteins are shown in Figure 4-6.
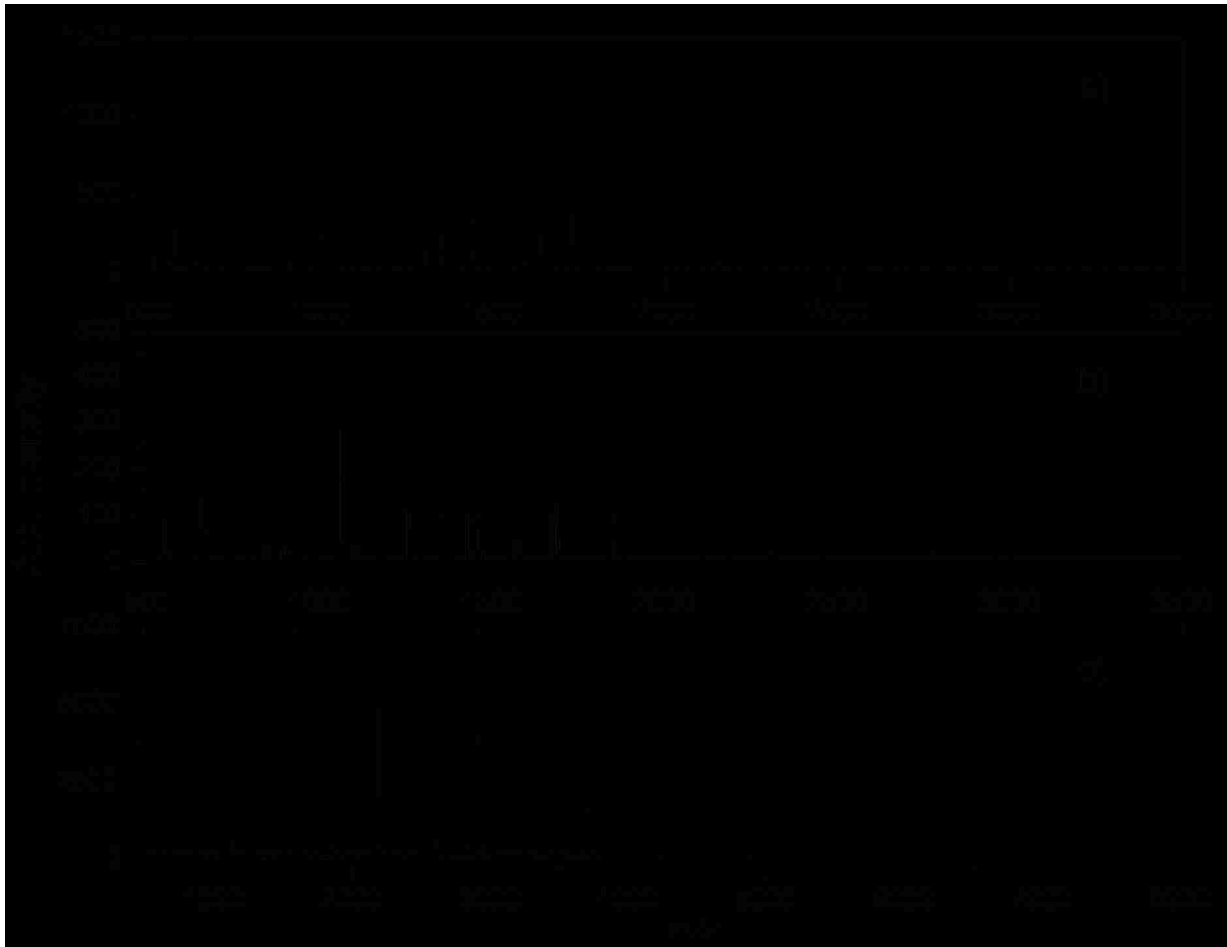
Figure 4-6. MALDI-TOF mass spectra of the tryptic digests of a) BSA, b) phophorylase b, and c) β-casein using the micropost bioreactor and electrokinetically-driven flow. Proteins are 10 μM in 50 mM ammonium bicarbonate buffer (pH 8.2); field strength, 375 V/cm; deposition time, 10 s. The sequence coverage for BSA, phosphorylase b and β-casein was 46, 63, and 79 %, respectively.

With five replicate experiments for each protein, the microfluidic chip analysis produced an average sequence coverage of 46, 63, and 79% for BSA, phosphorylase *b*, and β-casein, respectively. The probability-based Mowse score (P < 0.05) was 222 for BSA, 487 for phosphorylase *b*, and 258 for β-casein. Based on the sequence coverage and Mowse scores for these proteins, the identified peptides matched the target proteins with a high degree of certainty. Compared to the open channel bioreactor, 10% higher sequence coverages were obtained for all of the protein targets.

The micropost bioreactor was then used to investigate on-chip enzymatic digestion of intact bacterial cells.[301, 302] The bacterium *E. coli* was used to demonstrate the approach. A suspension of 1 mg/mL *E. coli* in 50 mM ammonium bicarbonate buffer was prepared and infused electrokinetically into the trypsin immobilized bioreactor. The eluent from the bioreactor was combined with the matrix solution; in this case, the matrix solution contained an internal standard of 5 µM insulin B-chain (MW = 3495.9). Figure 4-7a shows a MALDI mass spectrum of 1 µL intact *E. coli* deposited on a MALDI target plate. Peaks observed in the region below *m/z* 900 are from the matrix itself. Compared to the MALDI spectrum obtained from the on-chip tryptic digestion of *E. coli* shown in Figure 4-7b, several tryptic peptide peaks could be observed. The peaks marked with closed circles (●) correspond to peptides generated from the digestion of the aminoglycoside 3'-phosphotransferase type 1 protein derived from *E. coli*. The Mowse score for this protein was 142 with 57% sequence coverage based on MSDB database searches. Peaks marked with open circles (○) represent unidentified peaks from the tryptic digest of *E. coli*. Other peaks indicated by closed triangles (▲) were assigned to background ions arising from the intact *E. coli* cells.
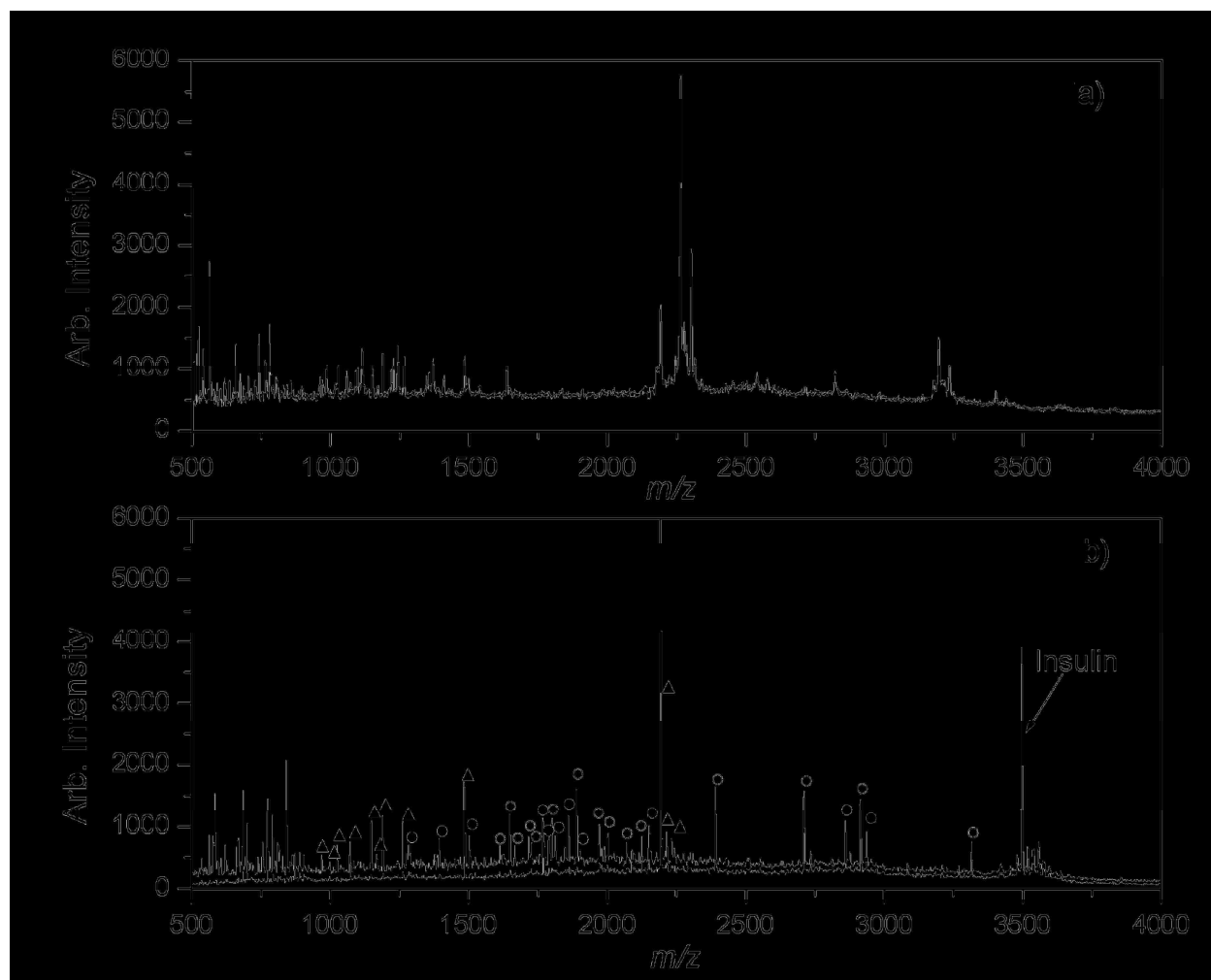
Figure 4-7. MALDI-TOF mass spectra of a) intact *E. coli* cells and b) tryptic digest of intact *E. coli* cells using the micropost and electrokinetically-driven flow format chip. Conditions were 1 mg/mL in 50 mM ammonium bicarbonate buffer (pH 8.2); field strength, 375 V/cm; deposition time, 10 s. ●, identified peptides from aminoglycoside 3'-phosphotransferase type 1 protein derived from *E. coli* with 57% sequence coverage; ○, unidentified peaks from tryptic digest of intact *E. coli* cells; ▲, background peaks from intact *E. coli* cells. Insulin was used as an internal standard.

4.5 Summary

In this chapter, the construction of a PMMA based micropost bioreactor was described for off-line MALDI-TOF MS analysis of digested proteins and its application to on-chip digestion of proteins with electrokinetically-driven flow. This system demonstrated the integration of steps for proteomic analysis using MALDI-TOF MS such as digestion, addition of

a matrix solution, and depositing onto a MALDI target plate. Our results showed that this novel

bioreactor design is well suited for proteomic analysis and that protein identification was

improved compared to an open channel format used previously.[81] Also, the current microfluidic

design offers a number of advantages compared to other solid-phase bioreactor formats in terms

of simple micro-replication of the reactor bed, highly reproducible production, and efficient

digestion. The micropost bioreactor required less than 200 nL of analyte deposited onto a

MALDI target, yet was capable of efficient protein identification. The bioreactor also brings the

capability for direct analysis of intact cells.

CHAPTER 5. SOLID-PHASE BIOREACTOR COUPLED TO MALDI-TOF MS USING CONTINUOUS SAMPLE DEPOSITION

5.1 Overview

In this chapter the use of continuous sample deposition for interfacing a solid-phase bioreactor to MALDI-TOF MS is described. In Chapters 3 and 4, the spotting deposition of digested peptides from a solid-phase bioreactor was described. Here, the continuous deposition interface demonstrates sample deposition with low volume. Tryptic peptides were formed in an on-chip bioreactor and continuously deposited onto a MALDI target plate using a motor-driven xyz stage. The MALDI target plate was modified by spin-coating a nitrocellulose solution containing a MALDI matrix on the surface prior to placing it on the xyz moving stage. Protein molecular weight standards were used to evaluate the performance of the continuous deposition chip. Deposition efficiency was improved without loss of protein sequence coverage compared to spot deposition.

5.2 Introduction

A low volume sample deposition interface with integrated proteomic analysis components such as sample cleanup, digestion, and separation is needed to meet the requirements for the fast and efficient identification of low abundance proteins. The most direct method for sample deposition is spotting using a robotic fraction collector. However, the primary difficulty with target spotting is the relatively large volume contained in a droplet from a small diameter capillary. The deposition volumes from this spotting manner range from 150 nL to 330 nL,[102] which can be a significant volume compared to peak volumes emanating from microfluidic components. It can also be difficult to control the spotting volume with high precision.

A range of different deposition strategies using microfluidic chips have been described for depositing small sample quantities onto MALDI targets. For example, a piezoelectric flow-through dispenser for depositing microfluidic chip eluent has been developed for the delivery of subnanoliter volumes to a MALDI target.[82] The dispenser was fabricated in wet etched silicon and was developed for interfacing a microchip with a high-density silicon nanovival target consisting of $300 \times 300 \times 20$ μm wells. The droplets generated by this dispenser ranged in size from 65 pL to 300 nL at a droplet frequency of 50 to 100 Hz with an attomole-level detection limit for proteins. Another chip deposition approach is electrospraying. In one such approach, a hydrophobic membrane electrospray deposition device was used to deposit the output of a polycarbonate microfluidic chip to a MALDI target.[83] The deposited volume by this chip was 70 nL with a detection limit of 3.5 fmol of angiotensin. Although low-volume sample deposition has been obtained with these approaches, they have not been combined with proteomic sample processing in a single chip.

The continuous deposition of flowing samples onto MALDI targets has been used to obtain small sample spots at low flow rates.[303-305] For example, deposition volume ranges of 1 - 40 nL/mm was achieved at sample flow rates of 0.1 – 2.5 μL/min using a continuous deposition system.[305] However, a continuous deposition technique has not been used for microfluidic deposition on a MALDI target. Continuous deposition interfaces provide a narrow and uniform sample trace, thereby concentrating analytes in a small area and improving the detection limit. A further benefit is the highly uniform deposition trace that results in a reproducible MALDI signal from position to position on the trace. In addition, when interfaced to a separation, the continuous deposition approach retains the separation resolution.

In this study, a microfluidic chip bioreactor was coupled with off-line MALDI-TOF MS using continuous sample deposition. The microfluidic chip channels were fabricated on a

poly(methyl methacrylate) (PMMA) plate with a micro-machined mold and hot embossing. The

MALDI target plate was coated with a nitrocellulose solution containing a MALDI matrix and

the chip eluent was directly deposited in a serpentine track using a multi-axis translation stage.

The proteins cytochrome c, myoglobin, β-casein, and bovine serum albumin were used to

evaluate the performance of the chip deposition system. The sequence coverage obtained by

continuous deposition was compared to the results of spot deposition.

5.3 Experimental

PMMA chips were fabricated using hot embossing with a molding tool prepared via

high-precision micromilling.[1, 267] A more complete description of the fabrication techniques used

in this study was given in Chapter 2. The microfluidic devices were constructed with a 4 cm long

× 200 µm wide × 50 µm deep microfluidic reactor containing an array of 50 µm diameter

cylindrical micropost support structures with a 50 µm inter-post spacing. The total reactor

volume of the bioreactor was 340 nL with 16 mm^2 surface area. A guide channel that was 0.5 cm

long × 370 µm wide × 370 µm deep was embossed into the chip at the output end of the

bioreactor to accept a PEEK capillary, which was used to transport samples to the MALDI target

plate. The PMMA chip was designed to fit into the stationary mount of a xyz stage (Newport,

Irvine, CA) for continuous deposition.

To assemble the microfluidic bioreactor, the PMMA surfaces were first activated by

exposing them and the cover slip to a UV lamp (254 nm; 15 mW cm^{-2}) for 20 min.[81] The

covalent attachment of the enzyme was based on PMMA surface modification protocols

developed in our laboratories.[81, 206] A 1-cm long PEEK capillary was inserted into the guide

channel on the UV-exposed PMMA substrate. After gluing the PEEK tube in place within the

PMMA substrate, the UV-exposed 0.125 mm PMMA cover slip was thermally annealed to the

substrate at 99°C for 20 min. The UV-modified channels were treated with a mixture of 5 mM

EDC and 5 mM sulfo-NHS solution for 15 min. Then, a 20 µM trypsin solution in a 100 mM

phosphate buffer (pH 7.0) was flowed through the bioreactor channel for 2 h. Following this

step, the bioreactor was ready for use or could be refrigerated for future use.

A schematic of the continuous deposition system is shown in Figure 2-12. The sample

was deposited along a series of circular areas on the 10×10 MALDI target. The size of a

circular well was 1 mm diameter, representing a 4 s deposition time at the stage moving speed of

250 µm/s. The target was moved in a 20 mm square single raster pattern on the target with 2 mm

spaced lanes. Deposition was optimized by controlling the speed of the xyz stage ranging from

0.25 mm/s to 1.0 mm/s with the flow rate of sample solution ranging from 25 nL/min to 1

µL/min. Cytochrome c, myoglobin, β-casein, and BSA were dissolved in 50 mM ammonium

bicarbonate buffer (pH 8.2) to 10 µM concentration. A syringe pump (Model 11, Harvard

Apparatus, MA) was used to deliver the sample to the microfluidic chip.

5.4 Results

Cytochrome c was used to characterize the continuous deposition of the digestion eluent

from a 10 µM protein solution continuously infused into the bioreactor. The deposited streak of

the digested cytochrome c solution was made along a 10×10 Bruker MALDI target plate at a

speed 15 mm/min and a sample flow rate of 50 nL/min; the deposition volume was 3.3 nL/mm.

The laser spot size was approximately 100 µm in diameter, which corresponded to a 400 ms

deposition time at a 250 µm/s stage velocity. The quantity deposited in each laser diameter was

3.3 fmol. The deposited trace width was approximately 200 µm and was laid out in a 20 mm

square raster pattern with a 2 mm distance between the 10 traces.

Various combinations of a stage velocity and a sample flow rate were examined to find

suitable deposition conditions for the microfluidic chip. The effect of sample flow was

investigated at rates between 25 and 1,000 nL/min. For a stage velocity of 250 µm/s (the lowest

93

speed for the system), the width of the trace increased with increasing sample flow rate. For example, at a flow rate of 1 µL/min, the trace was sufficiently broad that it overlapped the adjacent trace. At flow rates lower than 25 nL/min, the trace was not uniform. It was found that a sample flow rate of 50 nL/min resulted in the best compromise between trace width and uniformity.

Figure 5-1 shows representative mass spectra of a cytochrome *c* tryptic digest with the continuous deposition interface. Mass spectra were obtained with an average of 50 single-shots

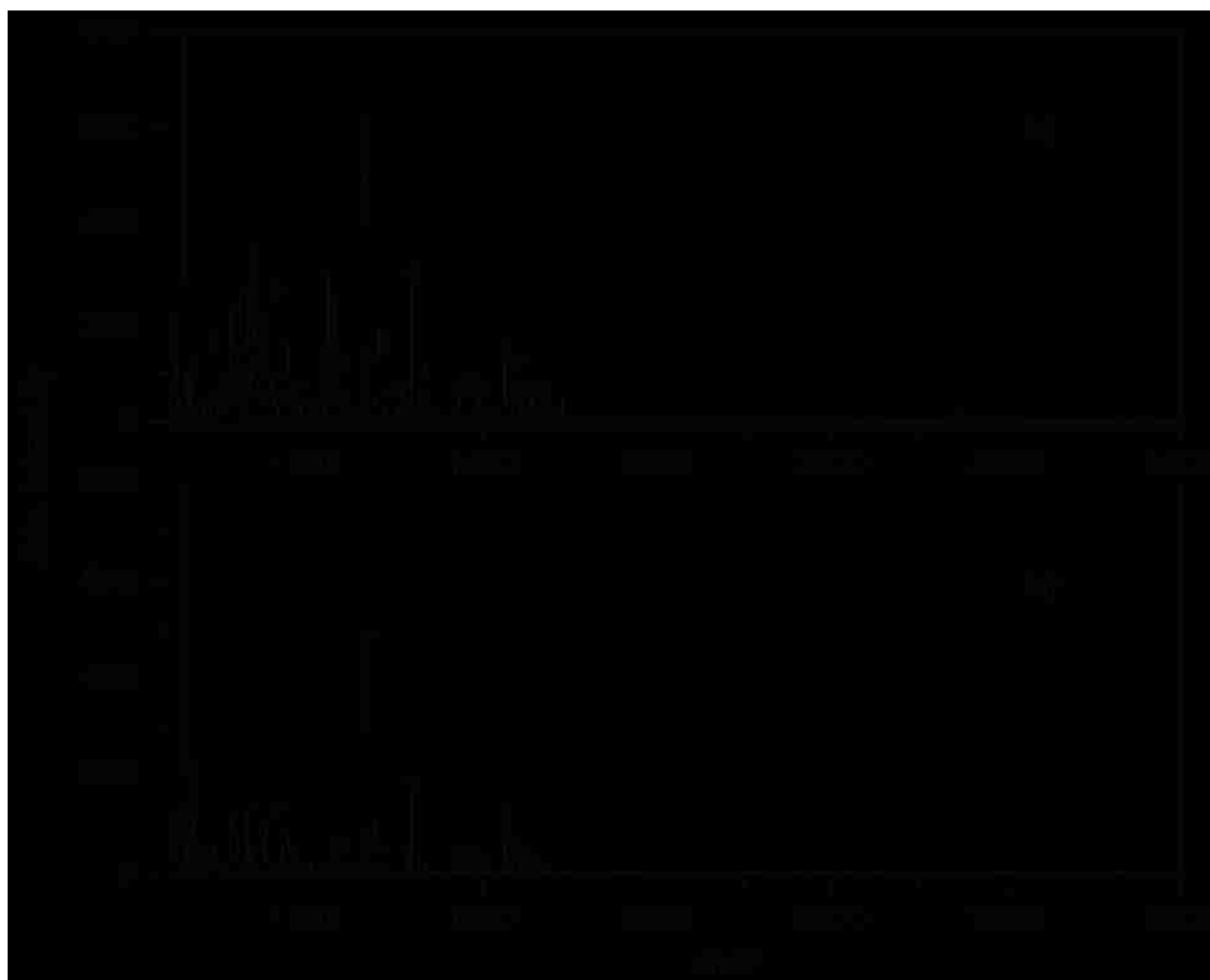**Figure 5-1.** MALDI-TOF mass spectra of a tryptic digest of cytochrome *c* using the micropost bioreactor and continuous deposition interface using a 10 µM protein concentration in 50 mM ammonium bicarbonate buffer (pH 8.2), stage velocity of 250 µm/s, deposition volume of 6.7 nL and 3.3 nL for sample flow rates of (a) 100 nL/min and (b) 50 nL/min, respectively. Asterisks indicate matched peptides.

from each portion of the sample trace. A 10 µM solution of cytochrome *c* was pumped through the bioreactor at 100 nL/min (Figure 5-1a) and 50 nL/min (Figure 5-1b), which resulted in residence times within the reactor of 200 s and 400 s, respectively. The sample was deposited at 250 µm/s stage speed. In Figure 5-1a, 13 tryptic peptides were identified for a sequence coverage of 75% and a 164 Mowse score. Peptide fragments were assigned on the basis of the MSDB database using the MASCOT search engine.[287] In Figure 5-1b a sequence coverage of 73% from 10 tryptic peptides and a Mowse score of 134 was obtained. Asterisks indicated in these spectra represent peptides identified from cytochrome *c*. Based on the Mowse score, the identified peptides matched the cytochrome *c* sequence with a high degree of certainty.

Additional proteins with different molecular weights and isoelectric points were used to test the performance of the continuous deposition chip device. The immobilized trypsin bioreactor was exposed to solutions containing 10 µM myoglobin (16.5 kDa), 10 µM β-casein (25 kDa), and 10 µM BSA (66 kDa) prepared in 50 mM ammonium bicarbonate buffer. The stage speed was 250 µm/s and the sample flow rates were 50 nL/min resulting in a residence times of 400 s within the bioreactor. The mass spectra of the trypsin digested proteins are shown in Figure 5-2. Each deposition contained digested peptides at 33 fmol/mm. In the figure, digested peptide peaks are indicated with asterisks. The peptide mass mapping results produced from these proteins at different flow rates are indicated in Table 5-1. The average sequence coverage was 62, 78, and 46% for myoglobin, β-casein, and BSA, respectively, and the probability-based Mowse score ($P < 0.05$) was 120 for myoglobin, 143 for β-casein, and 179 for BSA. Based on sequence coverages and Mowse scores of these proteins, the identified peptides matched target proteins with high degree of certainty.
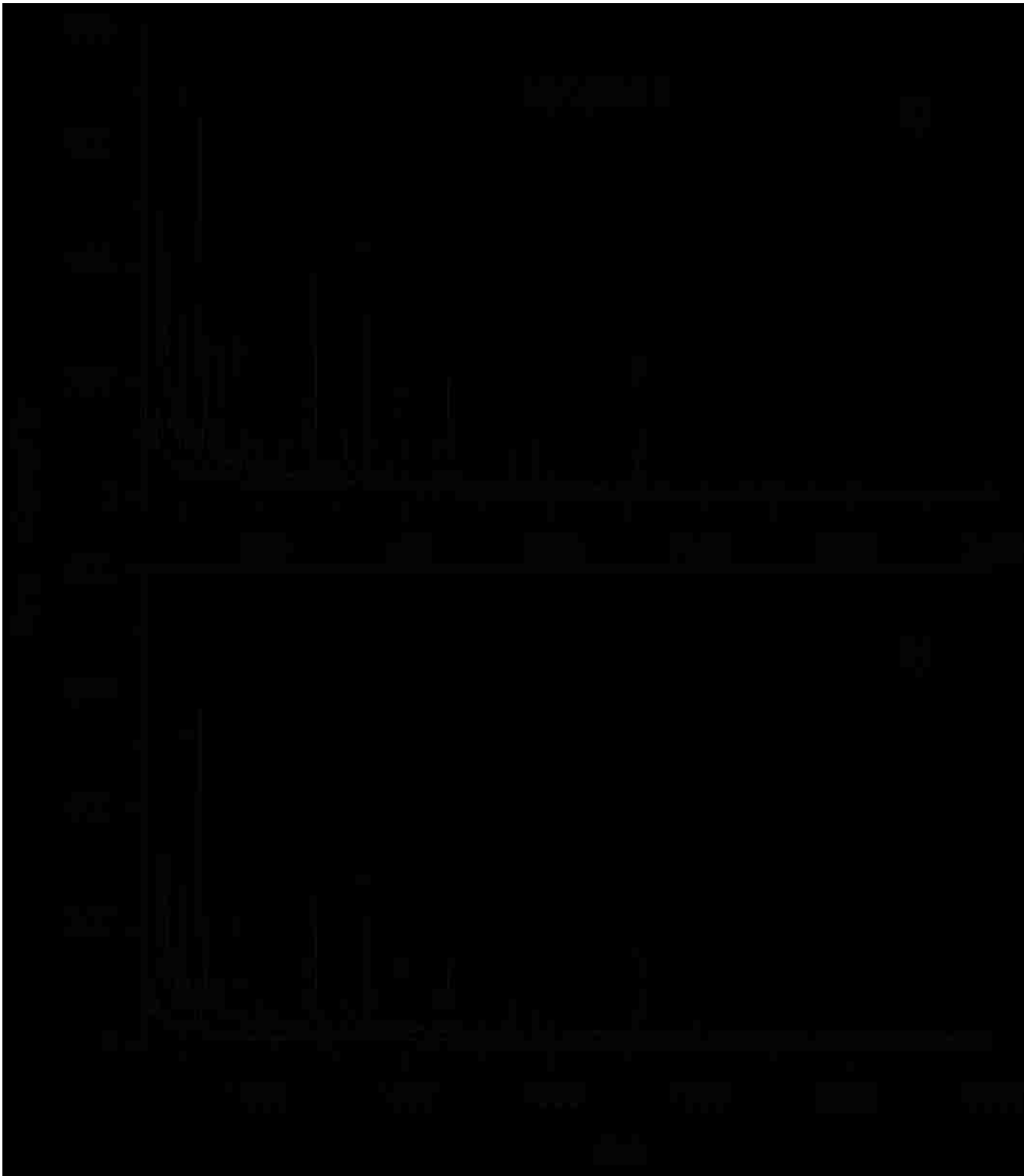
Figure 5-2. MALDI-TOF mass spectra of the tryptic digested myoglobin using the micropost bioreactor and continuous deposition interface a 10 μM protein concentration in 50 mM ammonium bicarbonate buffer (pH 8.2), stage velocity of 250 μm/s, deposition volume of 6.7 nL and 3.3 nL for sample flow rates of a) 100 nL/min and b) 50 nL/min, respectively. Asterisks indicates matched peptides.
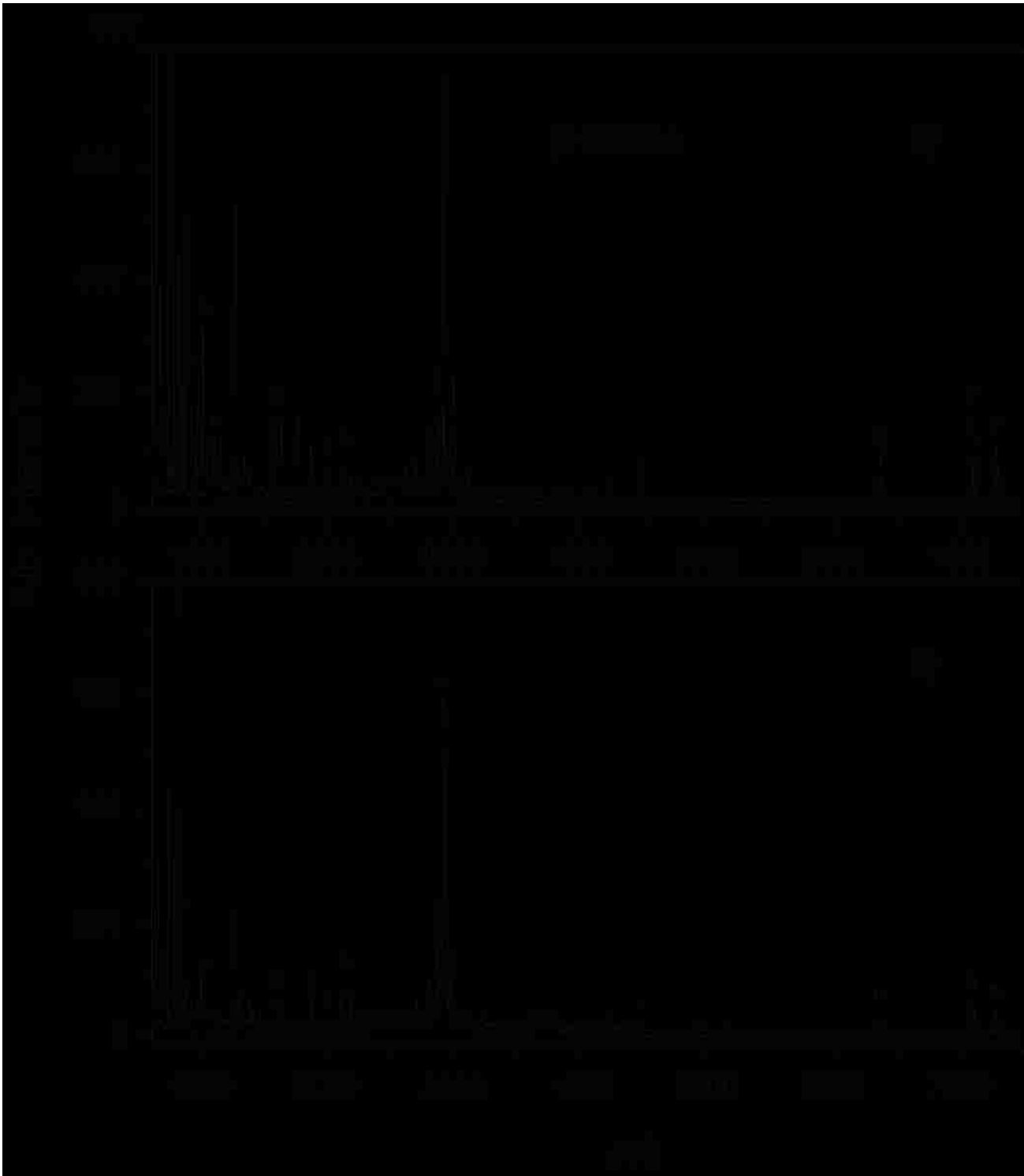
Figure 5-3. MALDI-TOF mass spectra of the tryptic digested β-casein using the micropost bioreactor and continuous deposition interface a 10 μM protein concentration in 50 mM ammonium bicarbonate buffer (pH 8.2), stage velocity of 250 μm/s, deposition volume of 6.7 nL and 3.3 nL for sample flow rates of a) 100 nL/min and b) 50 nL/min, respectively. Asterisks indicates matched peptides.

Figure 5-4. MALDI-TOF mass spectra of the tryptic digested BSA using the micropost bioreactor and continuous deposition interface a 10 μM protein concentration in 50 mM ammonium bicarbonate buffer (pH 8.2), stage velocity of 250 μm/s, deposition volume of 6.7 nL and 3.3 nL for sample flow rates of a) 100 nL/min and b) 50 nL/min, respectively. Asterisks indicates matched peptides.
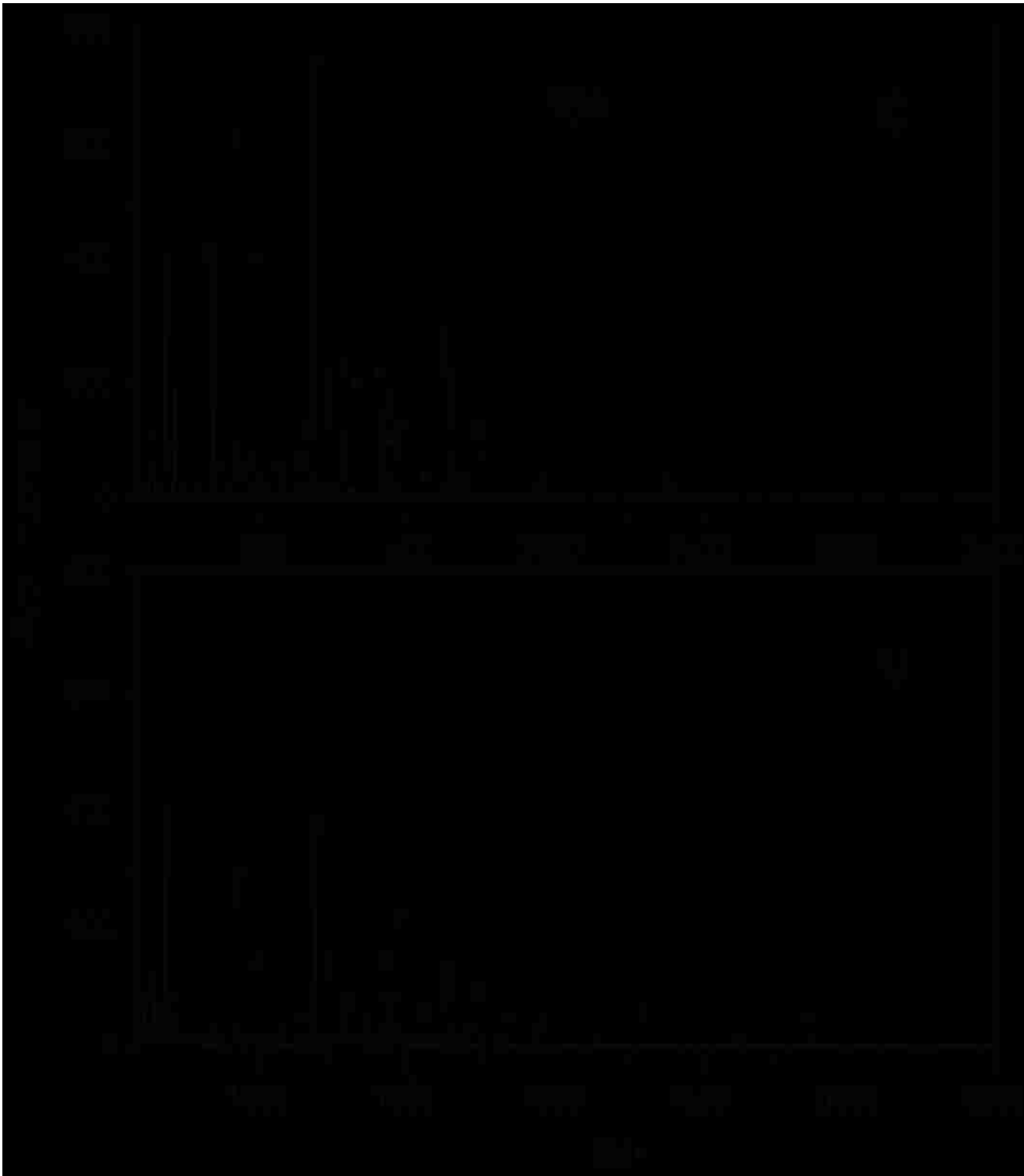
Table 5-1. Sequence coverage and MOWSE score of model protein identification.

Amounts (fmol/µm)	6.66				3.33			
Protein	Cyt-c	Myoglobin	β-Casein	BSA	Cyt-c	Myoglobin	β-Casein	BSA
Sequence coverage	75	69	79	50	73	62	78	46
MOWSE score	164	133	169	204	134	121	143	179

The performance of the continuous deposition interface was compared to the spot deposition interface using identical bioreactors. Figure 2-8 shows a schematic of the spot deposition interface described in Chapter 2.[81] A 10 µM cytochrome c solution in 50 mM ammonium bicarbonate buffer was infused into the bioreactor at a flow rate of 1 µL/min using a syringe pump. The deposition time for each droplet in the spotting deposition was 20 s and each drop had 330 nL of analyte solution. To achieve comparable residence times in the bioreactors, a flow rate of 50 nL/min with 400 s deposition time was used. The sample spot size for spot deposition was 1.5 mm diameter whereas a trace width of 200 µm was obtained for the continuous deposition. When the same lengths of each spot were compared, the areas of each spot were 0.3 mm^2 and 1.8 mm^2 for the continuous deposition and the spot deposition, respectively. Sampling times for each deposition technique were compared to evaluate deposition efficiency. Sampling time for MALDI analysis can be estimated by taking into account the surface area of a sample spot, the area of the laser spot, and its repetition rate. The nitrogen laser used for this experiment had a spot of 100 µm diameter with 2 Hz repetition rate. The sampling time (s) is calculated by Equation 5-1,

$$\text{Sampling time} = A_S / (A_L \times R) \qquad (5\text{-}1)$$

where A_S is the area of a sample spot (mm^2), A_L is the area of the laser spot (mm^2), and R is the repetition rate (s^{-1}). From this equation, the spot deposition and the continuous deposition required 115 s and 19 s to scan one spot, respectively. The analysis time for the continuous deposition is approximately 6 times faster as compared to the time for the spot deposition.

The results for peptide mass mapping with the two deposition methods are shown in Table 5-2. Continuous deposition resulted in better peptide mass mapping for all of the tested proteins compared to the spot deposition method even though the deposited spot contained a higher volume of analyte. Compared to the other microfluidic deposition interfaces, the piezoelectric dispenser approach yields droplets from 65 pL to 300 nL[82] and electrospray deposition results in spots of 70 nL,[83] this microfluidic device can collect similar or lower fraction volumes. To compare concentrations of the deposited samples in a unit area for the two deposition methods, equal quantities of a sample were deposited using a same chip. For 33 fmol cytochrome *c* deposited from a solution with a concentration of 10 μM, the spot size was approximately 1 mm diameter, or 42 fmol/mm^2. The continuous deposition trace contained an estimated 165 fmol/mm^2 at 250 μm/s stage speed, which increased the local concentration of the deposit by 300% compared to the spot deposition method.

Table 5-2. Comparison of the continuous deposition interface with spot deposition for bioreactor peptide mass mapping.

Deposition method	Deposited vol.(nL)	Spot area (mm^2)	Sequence coverage (%)			
			Cyt-c	Myoglobin	β-Casein	BSA
Continuous	3.30	0.3	73	62	78	46
Spot	330	1.8	67	58	72	35

5.5 Summary

We have described the coupling of a micropost bioreactor and continuous deposition device to MALDI-TOF MS for the detection of small quantities of tryptic peptides with improved protein identification. A uniform and narrow sample trace was obtained using a continuous deposition interface and the system reduced deposition volume 100-fold compared to droplet spotting. In addition to this deposition technology for low volume spotting of a sample, the microfluidic chip included a solid-phase microreactor for an on-chip digestion of low sample volumes. The continuous deposition interface achieved higher sequence coverage than the spot deposition for the identification of the proteins tested due to the increased local concentration.

CHAPTER 6. MICROFLUIDIC CULTURING OF BACTERIA WITH MALDI MASS SPECTROMETRY DETECTION

6.1 Overview

The goal of the research described in this chapter was to develop a microfluidic cell culturing device for bacterial identification with MALDI MS detection. Two independent culture chambers for a sample and a blank were contained in a single PMMA microfluidic chip. Different strains of *E. coli* were tested for the feasibility of using a microfluidic culturing device coupled with MALDI-TOF MS for whole cell analysis. Two channels, a sample channel and a culture medium channel, were connected to a culture chamber. *E. coli* cells were loaded into the culturing area without flushing out the nutrient medium due to the different depths of the sample and medium inlets. The culturing device was sealed with either a PMMA or a PDMS cover slip, and mass spectra of the bacteria were compared after culturing.

6.2 Introduction

New capabilities for quick and reliable identification of microorganisms are required for the detection of environmental pathogens and for clinical applications such as cancer screening, the detection of blood-borne pathogens, respiratory tract infections, and quality analysis of donated blood.[208-211] Cell culturing is an essential technique in biological research as well as in many important clinical applications.[212] Microfluidic devices for cell culturing have advantages over conventional cell culture methods in terms of low consumption of reagents, effective isolation from the outside, and precise control of the microenvironment.[220]

A variety of detection methods have been used for microfluidic cell culture devices including fluorescence and conductivity.[220] Although these methods offer rapid and sensitive detection, they have limited ability to discriminate among more than a few different species in flow cytometry with fluorescence detection. Also, dye-labeled antibodies must be developed for

each system. Polymerase chain reaction (PCR) has been developed for the rapid detection of target microorganisms; however, additional steps are often necessary to remove PCR-inhibitory substances present in samples before DNA amplification.[306] Further, PCR can give false negative results for mutant strains, as indicated by supporting evidence from other methods.[307, 308]

Mass spectrometry (MS) is a promising method for the detection of microorganisms because it is capable of rapid microorganism characterization through protein biomarkers.[309-313] Matrix-assisted laser desorption/ionization time-of-flight MS (MALDI-TOF MS) has been used for identification of bacteria for more than fifteen years.[312-318] The principle advantage of MALDI-TOF MS is speed: preparation and analysis of a whole-cell sample can take as little as five minutes.[11] This is in part due to its relatively high tolerance of impurities which leads to fewer preparation steps.[11, 13] Even though MALDI can be used to identify bacteria at the strain level, much of its speed advantage is lost when the bacteria are cultured with traditional techniques. Also, pathogenic bacteria can cause infections in human with only 10-100 cells; however, MALDI of bacteria requires a minimum of 1,000-10,000 cells.[319] Lack of spectral reproducibility is another limitation of MALDI.[312] Many factors affect the mass spectra, including the matrix, sample preparation, growth medium, and colony age.[320, 321] Small differences in growing conditions effect gene expression, changing the protein makeup.[322] Coupling MALDI MS analysis of intact cell with microfluidic culturing could create more consistent spectra as well as reduce the total processing time.

In this study, a simple microfluidic cell culture device with MALDI MS analysis is described for the identification of different strains of *E. coli*. Microfluidic cell culture chambers were fabricated on a PMMA plate from a mold master with a hot embossing method. To demonstrate the feasibility of this system, the microfluidic device was used for culturing several *E. coli* strains followed by off-line MALDI-TOF MS detection of the intact cells.

103

6.3 Experimental

Two independent culturing beds were fabricated on a poly(methyl methacrylate) (PMMA) microfluidic chip for side-by-side culturing of control and experimental bacteria samples. Each bed consisted of a 3 mm diameter and 300 μm deep circular microfluidic chamber with a volume of 2.1 μL. Different cover slips, either PMMA or PDMS, were used for sealing the PMMA culturing chip and were compared with each other. An *E. coli* cell line was cultured simultaneously in a Petri dish and on chip for comparison (See Figure 2-14 schematic). The 8 g/L nutrient broth culture medium was autoclaved at 121 ºC for 1 h for culturing the cell line in each culture chamber. Three different strains of *E. coli*, ATCC 9637, ATCC 11303, and ATCC 11775, were prepared with a concentration of 8×10^6 cells mL^{-1}. Figure 6-1 shows the procedure for cell culturing in the microfluidic chip. The culture medium was first added to the cell culture chamber through the Channel A. A 0.5 μL volume of the *E. coli* suspension was then loaded
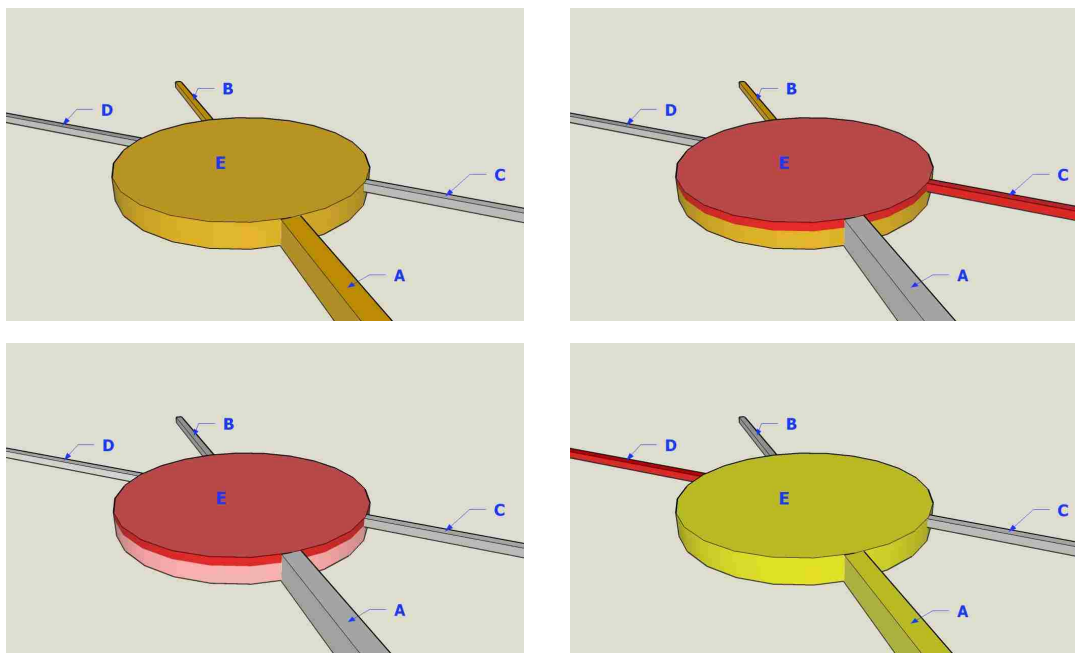

Figure 6-1. Procedure for chip culturing (clockwise from upper left); Filling the culture chamber (E) with nutrient broth (A→B); Infusing 0.5 μL of 8,000 cells/μL *E. coli* (C→B); Incubating at 39 ℃ for 24 h; Pumping out cultured *E. coli* (A→D) and depositing 1 μL of cultured *E. coli* onto a MALDI target.

into the culture chamber through the Channel C using a sterile syringe. After all of the reservoirs

were closed, the cell culture chip was placed in an incubator (G24, New Brunswick Scientific Co

Edison, NJ) at 37 ºC for 24 h. The cultured cells were pumped out using a syringe pump through

Channel A to Channel D and deposited onto a MALDI target through the capillary tube. To

assess cultured cell densities, a 1 µL volume of cultured cells was collected and three 10-fold

dilutions were made in HPLC-grade water. Cell counts were made using an Axiovert 200 M

microscope (Carl Zeiss, Jena, Germany).

6.4 Results

6.4.1 Device Design and Operation

To culture bacteria in a microfluidic device, sample and nutrient must be infused without

disturbing the bacteria already present in the culturing area. Different channel depths for sample

and culture medium solution were fabricated so that the bacteria could enter the culture area at

the top and the nutrient at the bottom. Figure 2-14 shows the schematic of cell culturing device.

The culturing area was contains 300 µm deep with a 2.1 µL active volume. The nutrient solution

entered the culturing chamber through a 300 µm deep inlet channel. The bacteria suspension was

then injected through a 100 µm deep inlet channel. In this manner, the cells were delivered to the

chamber without flushing out nutrient medium. The device thus provides a closed sterile

environment for bacteria.

6.4.2 Calibration Curve

The optical density (OD) of the bacterial suspensions was measured to estimate the

number of *E. coli* cells in each sample. Different amounts of *E. coli* ATCC 9637 ranging

between 1 µg/mL and 10 mg/mL were prepared in 10 mM phosphate buffered saline (pH 7.4).

The calibration curve was generated by measuring the optical density of each *E. coli* suspension

at 600 nm. The number of cells per µL in the each calibration suspension was estimated by

counting using a microscope after serial dilutions from the stock suspension of bacteria. Figure 6-2 shows the plot of OD at 600 nm according to suspended mass of *E. coli*. The plot is linear between 0.1 and 0.5 OD. The number of cells per μL can be related to the OD value.
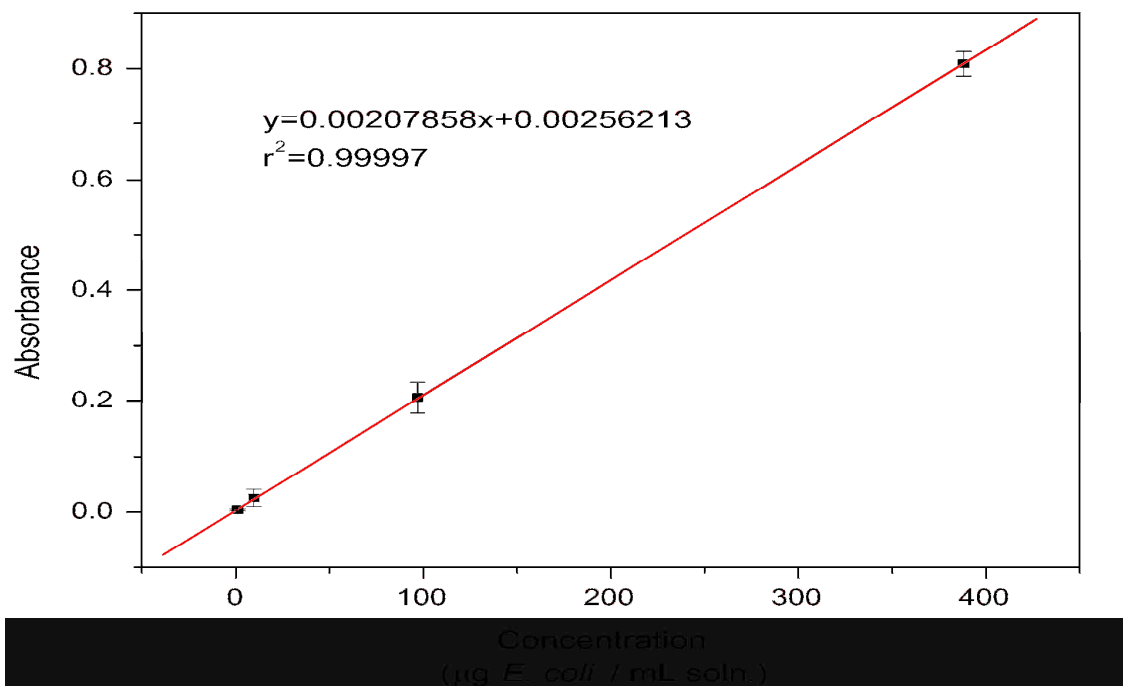

Figure 6-2. Plot of optical density at 600 nm for *E. coli* ATCC 9637 suspensions prepared in 10 mM phosphate buffer (pH 7.4) as a function of concentration.

Table 6-1 shows the relationship between the concentration and the number of cells. For example, 100 μg/mL of *E. coli* corresponds to approximately 81,000 cells/μL. An aliquot of each suspension was deposited onto a MALDI target to determine detection limit for intact *E. coli* cells. A 1 μL volume of each calibration solution was deposited on a MALDI target with a 2 μL of CHCA solution. Figure 6-3 shows the MALDI mass spectra of *E. coli* (ATCC 9637) obtained at various concentrations. As can be seen in this figure, the number of peaks and intensities increase with the number of cells. The detection limit of *E. coli* using our instrument is 10 μg/mL, which corresponds to 8,000 cells/μL. This concentration was selected as an initial concentration for *E. coli* bacteria culturing and compared to the results of *E. coli* in bulk.

Table 6-1. The relationship between *E. coli* concentrations and optical density (OD) and the corresponding number of cells for each concentration.

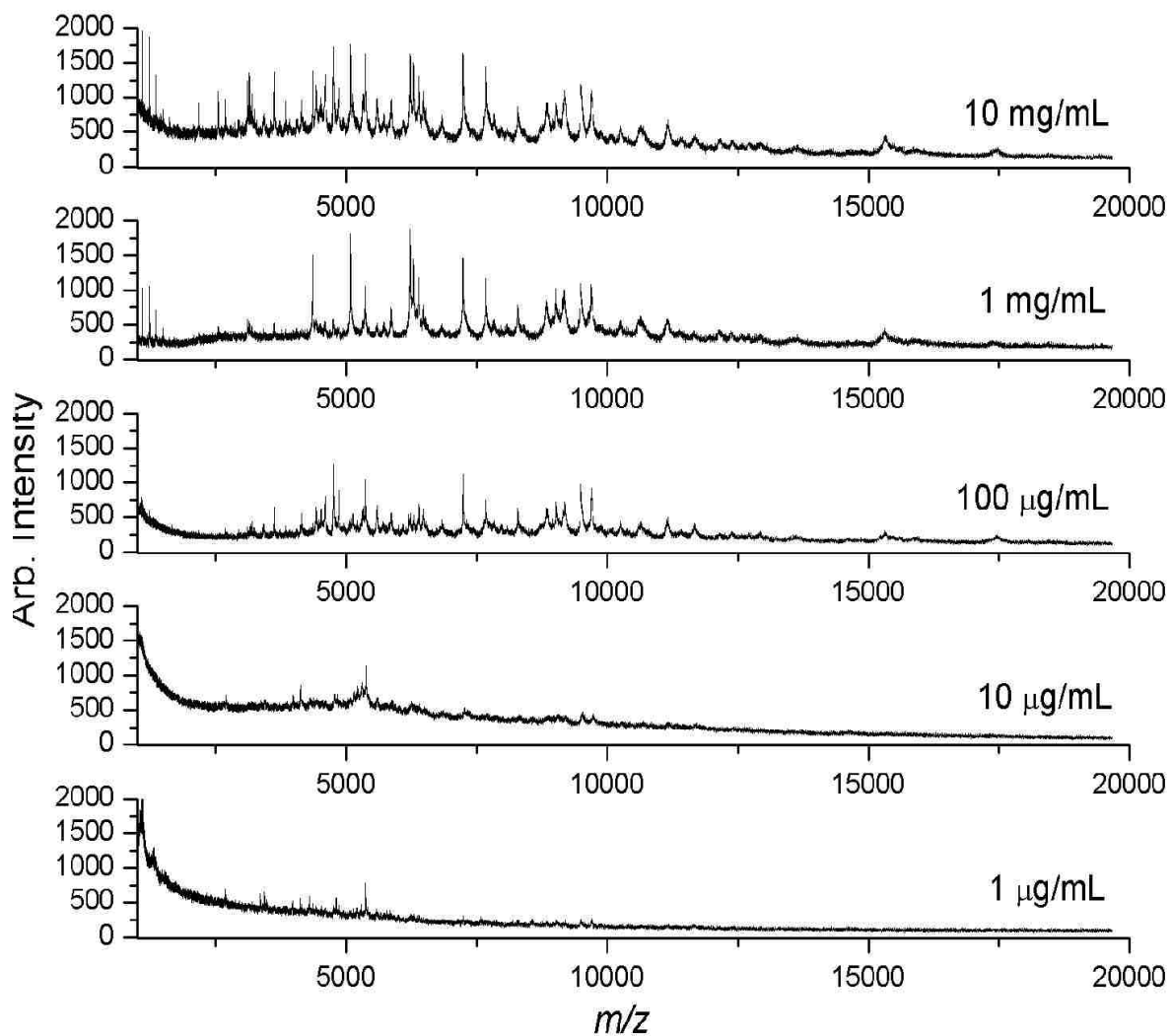| *E. coli* concentration (µg/mL)	Ave. cell count (µL^{-1}, n=5)	RSD (%)
1	742 ± 24	6.4
10	7,871 ± 434	5.5
100	81,367 ± 5183	3.3

Figure 6-3. MALDI-TOF mass spectra of *E. coli* ATCC 9637 at various concentrations in 10 mM phosphate buffer (pH 7.4); matrix, CHCA (2% TFA in water:acetonitrile(1:3, v/v)).

107

6.4.3 Cell Culture in PMMA Chip and MALDI Analysis

MALDI mass spectra were obtained before and after culturing on the chip. Initially, whole cell suspensions (8×10^6 cells mL^{-1} in broth) of three *E. coli* strains (9637, 11303, and 11775 from ATCC) were analyzed in CHCA matrix. A 1 µL aliquot of bacterial suspension (8000 cells / spot) was deposited on the MALDI target plate with 2 µL of CHCA. Figure 6-4 shows the mass spectra of the three strains before culturing.
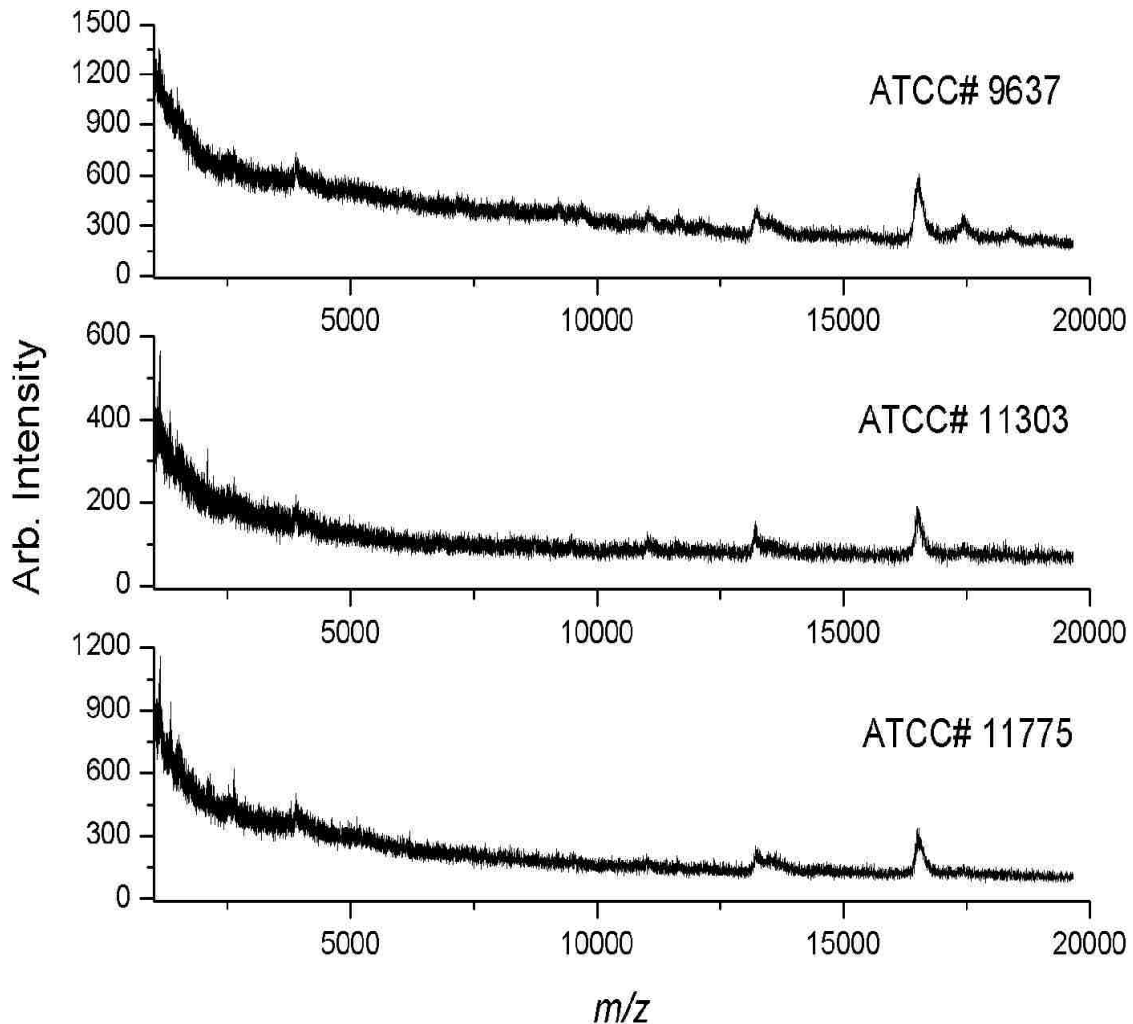

Figure 6-4. MALDI-TOF mass spectra of different strains of *E. coli* (8000 cells/µL in nutrient medium) before culturing. a) ATCC 9637; b) ATCC 11303; c) ATCC 11775.

Different peak patterns were observed for *E. coli* 9637 from ATCC compared to for *E. coli* 9637 obtained from Sigma (See Figure 6-3). The difference in mass spectra between these bacteria may have resulted from the fact that bacteria from ATCC are intended as a start culture; however, bacteria from Sigma are not. In Figure 6-4, some weak, broad peaks are observed but the mass spectra of the three strains are similar and cannot be distinguished from each another.

Using identical *E. coli* suspensions, cell culturing was performed in the microfluidic chips. Aliquots of *E. coli* 9637, 11303, and 11775 were seeded into different microfluidic culture beds with approximately 4000 cells by injecting 0.5 µL of each strain suspension (8,000 cells µL^{-1} × 0.5 µL). The chips were incubated at 37 ºC for 24 h, after which the cell suspension was flushed out and 1 µL was deposited onto a MALDI target plate. Another 1 µL of the suspension was collected and serially diluted to 1 mL with deionized water for cell counting. A 1 µL aliquot of the diluted sample was spotted onto a glass slide to count the cells using a microscope. The cell count was 150 ± 21 over five replicate experiments corresponding to approximately 1.50×10^5 cells µL^{-1}. Compared to the initial number of bacteria cells, the number of cultured bacteria increased by approximately 80-fold in the culturing chip.

The matrix CHCA was added to the sample deposits on the MALDI target followed by MS analysis. Representative mass spectra of different strains of *E. coli* are depicted in Figure 6-5. As shown in this figure, some peaks are common to all strains and were highly reproducible over five replicate runs. Several peaks in the mass spectra are unique to each strain. Because most intact proteins translated by bacterial genomes are in the mass range from 4 to 15 kDa,[319] the majority of peaks below 15 kDa in MALDI mass spectra of bacteria are likely from singly protonated proteins, which can be used for protein biomarkers.[313, 323] Peaks in the mass spectra that matched ribosomal proteins from *E. coli* using a RMID*b* search are the 9 peaks indicated with asterisks in Figure 6-5.
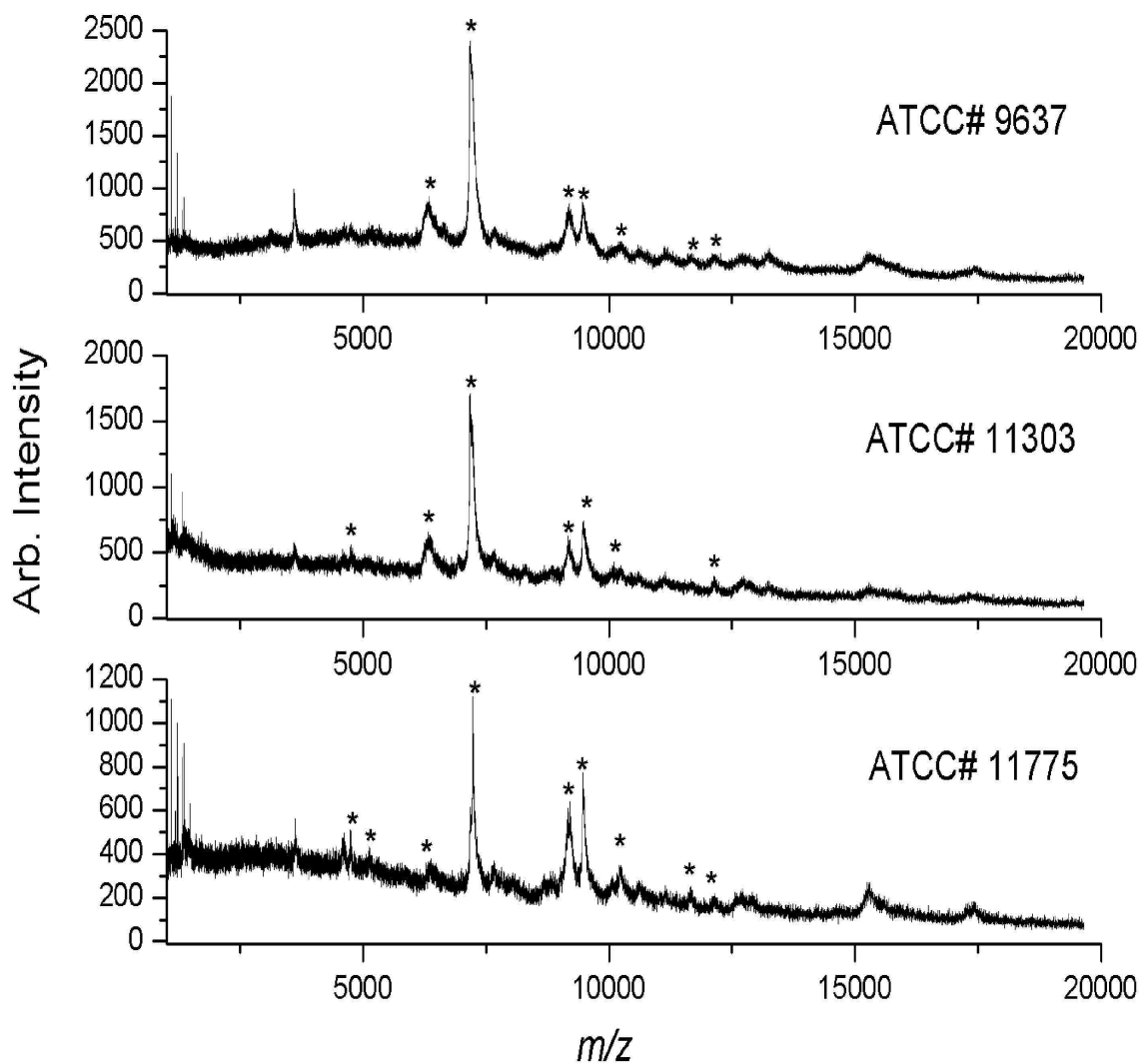
Figure 6-5. MALDI-TOF mass spectra of different strains of *E. coli* after 24 h culturing at 37℃ in PMMA microfluidic devices. a) ATCC 9637; b) ATCC 11303; c) ATCC 11775. Asterisks indicate matched peaks.

6.4.4　Cell Culture in PMMA Chip with PDMS Cover Slip and MALDI Analysis

　　　A PMMA chip with a PDMS cover was used for cell culturing. Figure 6-6 shows

representative MALDI-TOF MS spectra of ATCC 9637, ATCC 11303, and ATCC 11775 strains

of *E. coli* after 24 h culturing at 37 ℃ in a PMMA microfluidic device with a 1 mm thick PDMS

cover slip. Asterisks in the mass spectra indicate peaks matched using RMID*b* search. The

110

PMMA/PDMS chip resulted in 22 peaks matching database proteins from *E. coli*. Among them, peaks at *m/z* 4426, 4471, 7110, 8924, 10059, 11677, 12870, 13550, and 14272 were differently expressed according to the strains.
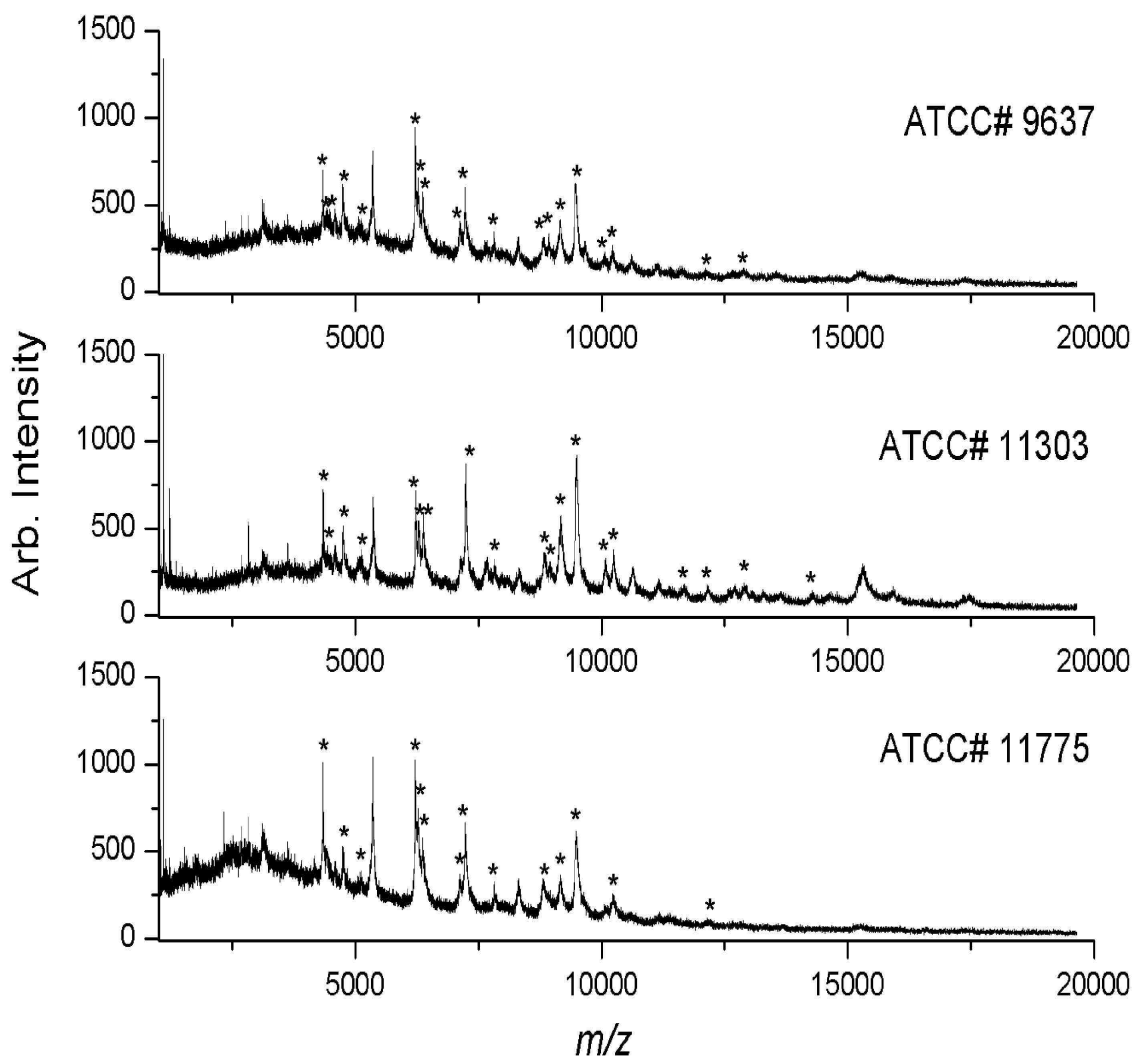

Figure 6-6. MALDI-TOF mass spectra of different strains of *E. coli* after 24 h culturing at 37 ℃ in PMMA microfluidic devices with PDMS cover. a) ATCC 9637; b) ATCC 11303; c) ATCC 11775. Asterisks indicate matched peaks.

To determine cell concentration in the PMMA/PDMS device, dilution and cell counting was performed as above. The number of *E. coli* was 155 ± 25 and the total number of bacteria

111

was approximately 1.55×10^5 cells μL^{-1}. From these results, there is no significant difference in bacteria growth based on the different materials for culturing. However, it was found that the PDMS cover slip resulted in more protein biomarkers compared to the PMMA cover. We hypothesize that the gas permeability of the PDMS cover resulted in higher quality mass spectra due to the aerobic conditions of the culture bed, which can change the proteins expressed during cell growth.[229, 324, 325]

6.5 Summary

In this chapter, the construction of a PMMA based micro-culture device was described for off-line MALDI-TOF MS detection. The feasibility of using a microfluidic culture device coupled with MALDI analysis was demonstrated for identification of *E. coli*. The mass spectral patterns associated with various strains were different, providing evidence that whole cell analysis using microfluidic cell culture coupled with MALDI-TOF MS can serve as a tool for bacterial identification. Three different strains of *E. coli* were cultured and fingerprint spectra distinguishing the strains were produced using this system. Peak intensities in the spectra as well as the number of peaks were enhanced using a PDMS cover slip. The current microfluidic design offers a number of advantages in terms of low sample consumption and nutrient medium, easy manipulation of the cultured cells, and a reproducible environment. Our results showed that this novel microfluidic culture chip coupled with MALDI MS was well suited for bacterial analysis and protein identification could improve analysis compared to ordinary cell culture platforms.

CHAPTER 7. DEVELOPMENT OF A CONTINUOUS CELL CULTURING DEVICE WITH TEMPERATURE CONTROL FOR BACTERIAL IDENTIFICATION

7.1 Overview

The work described in this chapter focuses on a microfluidic device for culturing with continuous perfusion of a medium for better cell growth by removing metabolite from a culture area. A polycarbonate membrane was embedded in the outlet of the culture chamber for changing the medium without the loss of cells. Also, a temperature-control system was developed to directly culture cells on the chip. The device was thermostatically heated and the medium was changed at 6 h intervals. The chip was inspected under a microscope and MALDI analysis to assess the extent of cell growth.

7.2 Introduction

In the past a decade, the interest in manipulation and detection of complex biological systems including living cells has increased with the development of microfabrication techniques.[220] Microfluidic devices are being used increasingly for biological analysis of samples such as DNA and proteins extracted from biological fluids and tissue.[326] The properties of microfluidic chips make them ideally suited to the analysis of biological samples on a cell-by-cell basis,[219, 227] primarily due to the fact that the dimensions of the fluidic channels are the range of 10 to 100 µm, which closely matches cellular dimensions.[228] This makes it possible to manipulate the cells individually as well as to minimize artifacts such as intracellular content dilution following lysis and the ability to capture specific cells from heterogeneous populations.[327] In addition to providing a suitable environment for cell analysis, microfabricated culture devices offer several other advantages over conventional culturing methods.[227] For example, they can operate at low fluid volumes and thereby have low sample and reagent consumption. The dimensions of the features of the culture chamber can be varied to any size for

batch production and disposability, which can eliminate the chances of cell contamination. Also, a microfluidic device allows for more precise control of cell growing conditions due to rapid heat and mass transfer in the microreactor. Moreover, harmful bacteria inside a culturing chip can be isolated from the outside due to its closed architecture.

Cells are particularly sensitive to their environment and an accurate identification depends on proper growth conditions such as adding nutrient, removing waste, and maintaining proper temperature and pH.[218] It is difficult to control the cell culture environment in a bulk system, which can result in conditions varying considerably during the growth of the culture. To maintain a consistent environment a careful control of conditions is required during cell culturing.[223, 224] By continuously infusing culture medium into the chamber, waste products can be effectively removed.[328] Various continuous perfusion methods have been developed for microfluidic culture devices.[233, 329, 330] Recirculating and non-recirculating modes are the two most widely used perfusion methods for microfluidic culture devices. In the recirculating mode,[331, 332] a confined volume of nutrient solution is circulated through the culturing area and the waste is diluted into the total nutrient volume. In a non-recirculating culture,[333, 334] waste can be eliminated by infusing the nutrient solution through the culture chamber and sending it directly to waste reservoir.

A microfluidic cell culture device containing continuous perfusion of medium will allow cells to grow in a favorable environment and thereby generate more consistent mass spectra when interfaced to MALDI-TOF MS. Also, a culturing chamber with continuous perfusion of fresh medium can use a fluidic manifold that incorporates microheaters to keep the temperature constant.

In this study, a PMMA culture chip with continuous perfusion of nutrient medium was developed for off-line MALDI-TOF MS. The culture chip was also integrated with a micropost

bioreactor. Culturing temperatures were controlled on the surface of the integrated chip device with a thermostatically controlled microheater. The *E. coli* strains, ATCC 9637, 11303, and 11775 were used to evaluate the performance of the continuous culture system. MALDI mass spectra with different culture times were compared. Finally, intact *E. coli* was directly digested in the bioreactor following on-chip culturing for fingerprint analysis.

7.3 Experimental

Chips were fabricated from PMMA using hot embossing with a molding die prepared by high-precision micromilling.[267] A more complete description of the fabrication methods used in this study has been described in Chapter 2. All culture components including capillary tubes and connectors were sterilized with UV light prior to use. Each cell strain was cultured simultaneously in a Petri dish and on the microfluidic chip for comparison. The 8 g/L nutrient broth of culture medium was autoclaved at 121 ºC for 1 h for culturing the cell line in each culture chamber. A photo of the microfluidic cell culturing device is shown in Figure 7-1. The device is composed of a culture bed, two external pumps, fluid microchannels, and three reservoirs. Also, micropost bioreactor was fabricated at the outlet of the culture chamber. The total volume of the micropost channel, which contained surface-immobilized trypsin, was 750 nL with 37.4 mm^2 surface area.

The culture medium was first added to the culture bed through the nutrient reservoir and 0.5 μL of an *E. coli* solution was then seeded in the culture bed at a concentration of 8×10^6 cells mL^{-1}. The pump was connected to the nutrient reservoir and transported the culture medium into the culture area and then to the waste reservoir.

All of reservoirs except the waste reservoir were then closed and the device was heated to a constant as 37 ºC. The nutrient medium was changed at 6 h intervals over the 24 h incubation time after which the cultured cells were washed by replacing the medium with 50 mM NH$_4$HCO$_3$

115

buffer through the continuous perfusion channel. The cells were delivered to a microscope slide through the capillary to assess the extent of cell growth. An additional aliquot of cultured cells was deposited onto a MALDI target plate for MALDI analysis. For digestion, the cultured cells were transferred hydrodynamically into the bioreactor by sealing the intact cell collection capillary outlet. Tryptic peptides generated from the bioreactor were deposited on a MALDI target for MALDI analysis.
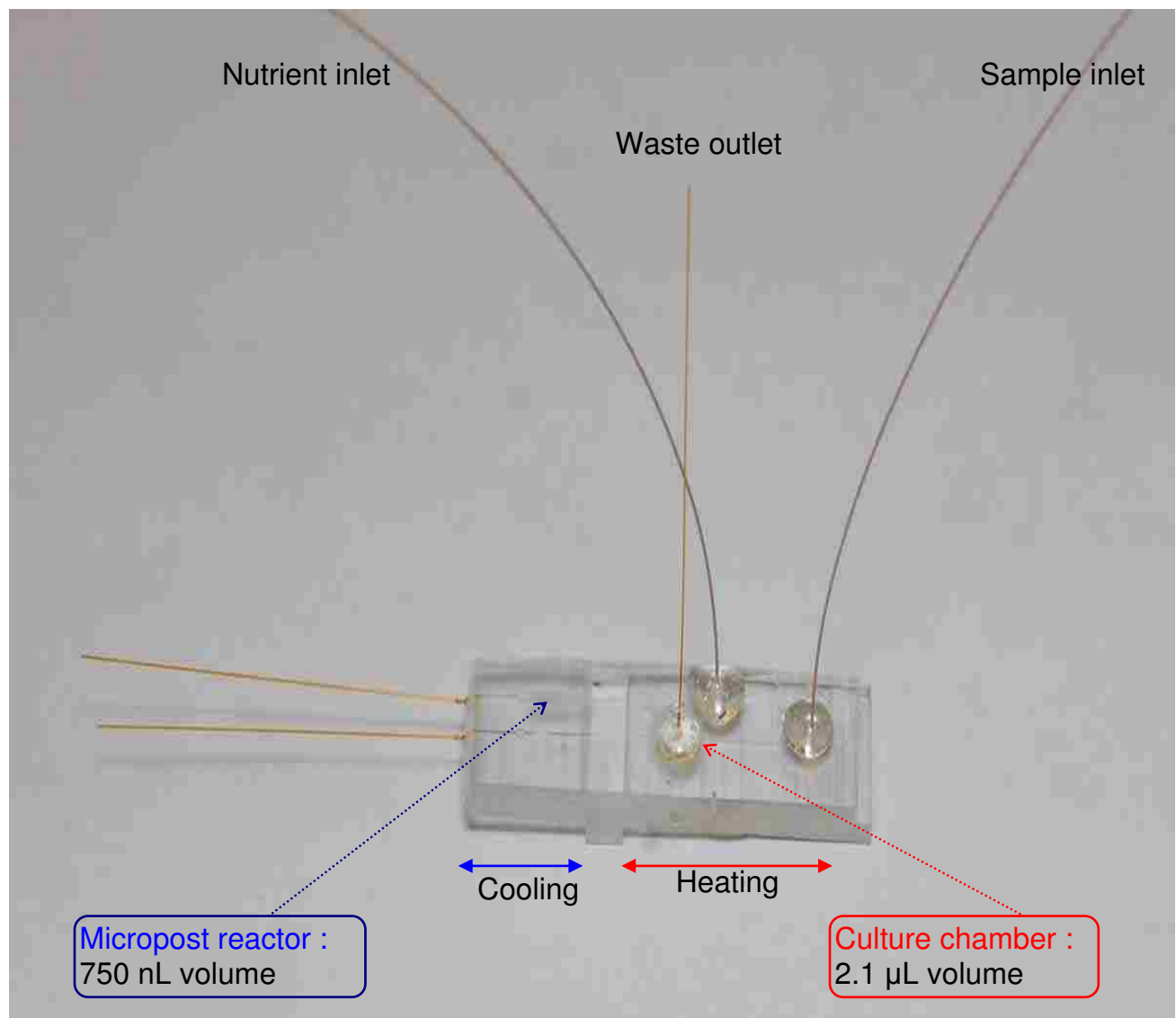

Figure 7-1. A photo of the microfluidic cell culturing device with continuous perfusion of medium and on-chip heating and cooling.

7.4 Results

Cell culturing was performed in the thermostatted PMMA culturing chips as described in

Chapter 2 for comparison with MALDI peak patterns of different *E. coli* strains. The thermostat

comprised a digitally controllable heater and cooler that were independently set. The

temperature precision of the system is ± 0.5 ℃ at 37 ℃ and ± 1 ℃ at 10 ℃ for the Kapton heater

and the Peltier cooler, respectively. The heating and cooling rates on the chip are 10 ℃/min and

2 ℃/min, respectively.

To culture the bacteria on-chip each of *E. coli* ATCC 9637, 11303, and 11775 were

seeded into different microfluidic culture beds with approximately 4000 cells each by injecting

0.5 μL of each strain solution (8,000 cells $μL^{-1}$ × 0.5 μL). Each *E. coli* strain was incubated in a

microfluidic culture device at 37 ºC for 24 h with the thermostatted system and the nutrient

medium solution was replaced through the polycarbonate (PC) membrane at an interval of 6 h.

After 24 h incubation, the cultured *E. coli* solution was flushed out and 1 μL of this solution was

deposited directly onto a MALDI target plate. Another 1 μL of the cultured solution was

collected and serially diluted to 1 mL with deionized water to quantify the number of cultured *E.

coli* bacteria. A 1 μL aliquot of this diluted sample was spotted onto a glass slide to count *E. coli*

directly using a microscope. The number of *E. coli* was 250 ± 35 over five replicate experiments.

The total number of bacteria in a culture chamber can be estimated to be approximately 2.5×10^{5}

cells $μL^{-1}$. Compared to the initial number of bacteria cells, the number of cultured bacteria

increased by approximately 130-fold in this PMMA culturing chip.

The MALDI matrix, CHCA, was added to the sample deposits on the MALDI target

followed by MALDI-TOF MS analysis. Representative mass spectra of different strains of *E.

coli* are depicted in Figure 7-2. As shown in this figure, several mass peaks are found in all

strains tested, which means *E. coli* can be grown in the temperature-controlled microfluidic

culture device. The peaks in the mass spectra were reproducible over five replicate analyses. In this figure, several protein peaks detected in the mass spectrum ranging from 4 to 15 kDa are conserved for each strain, and these might be used for protein biomarkers in the mass spectra of intact bacterial cells[323] since the mass spectral patterns of the *E. coli* strains tested are different. Peaks from the mass spectra were identified using a RMID*b* search; 8 peaks for ATCC 9637, 8 peaks for ATCC 11303, and 9 peaks for ATCC 11775 indicated with asterisks were matched with ribosomal proteins from *E. coli*. The identified peaks are listed in Table 7-1.
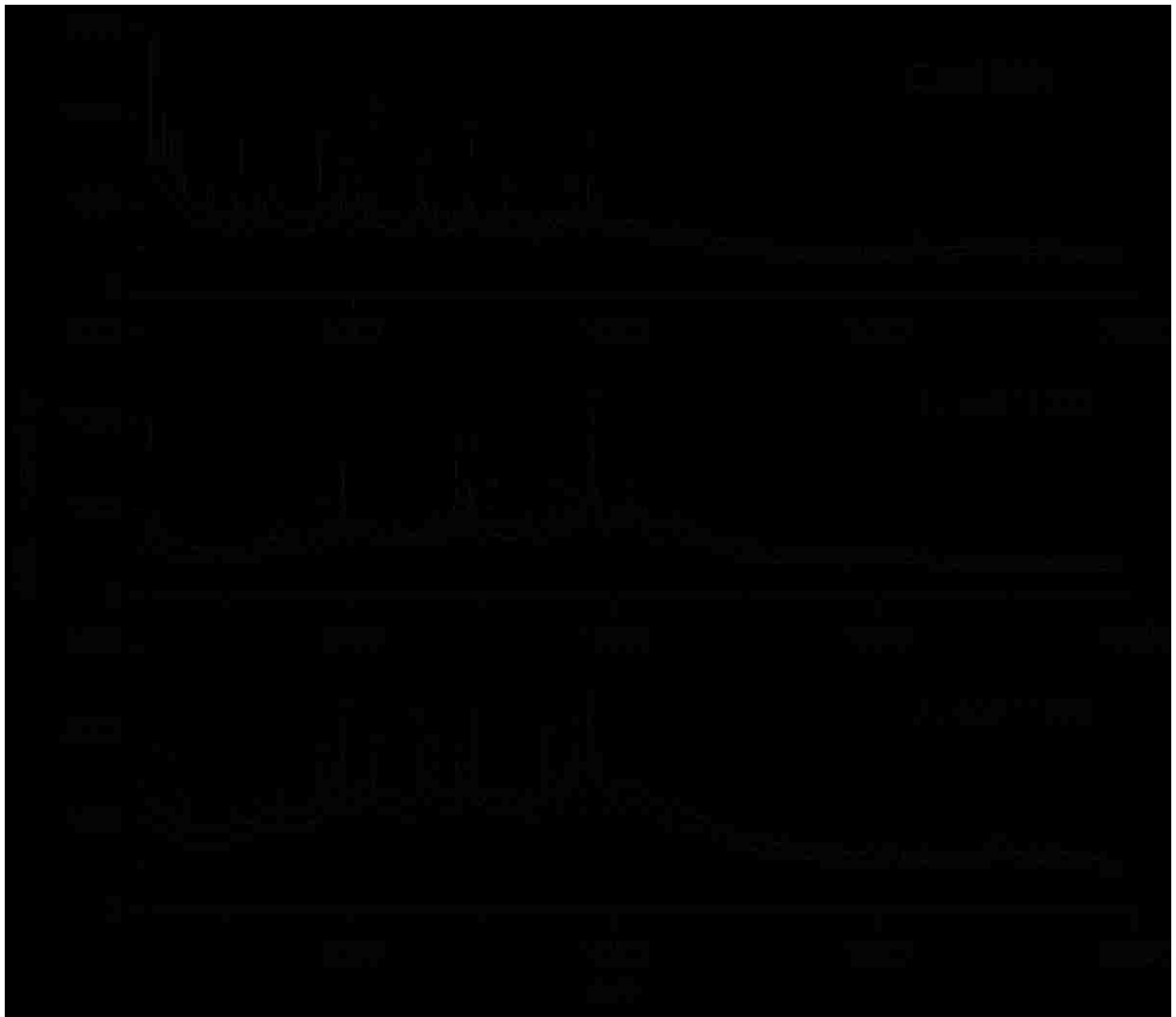
Figure 7-2. MALDI-TOF mass spectra of different strains of *E. coli* after 24 h culturing at 37℃ in a thermostatted PMMA microfluidic device. a) ATCC 9637; b) ATCC 11303; c) ATCC 11775. Asterisks indicate matched peaks

Among them, peaks at *m/z* 6315 and 7890 for ATCC 9637, peaks at *m/z* 4449, 7563, and 10265 for ATCC 111303, and peaks at *m/z* 6241 and 6411 for ATCC 11775 appeared to be differently expressed in the strains tested. These peaks might be useful for identification of different strains.

Table 7-1. Identified mass peaks in cultured *E. coli* (from Figure 7-2).

	Observed mass (*m/z*)															
Strain	4364	4449	4752	5097	5382	6241	6315	6411	6964	7258	7563	7890	8828	9192	9554	10265
9637	×		×	×	×		×			×		×		×	×	
11303		×							×	×	×		×	×	×	×
11775	×		×		×	×		×	×	×			×	×		

MALDI mass spectra from *E. coli* 9637 cultured after 6, 12, and 24 h of incubation are compared in Figure 7-3. The overall spectral patterns remained reproducibly consistent during incubation. Of the three culture times tested, 24 h gave the highest intensity of peaks and a significant number of peaks. As can be seen in this figure, at 12 and 24 h incubation time some mass peaks are missing while certain mass ranges within the spectra are similar. For example, after 24 h incubation, signal intensities at *m/z* 2825.5, 4364.0, 5382.1, 7258.7, and 9554.0 increased, suggesting that the proteins are differently expressed according to the incubation times. Even though a shorter incubation time (6 h) resulted in fewer peaks and lower peak intensities, some peaks might be used for protein biomarkers in the mass spectra of intact bacterial cells. From searches for intact protein masses and the identification of protein biomarkers of cultured *E. coli* cell at 6 h incubation time, the 6 peaks indicated with asterisks matched with ribosomal proteins from *E. coli*.
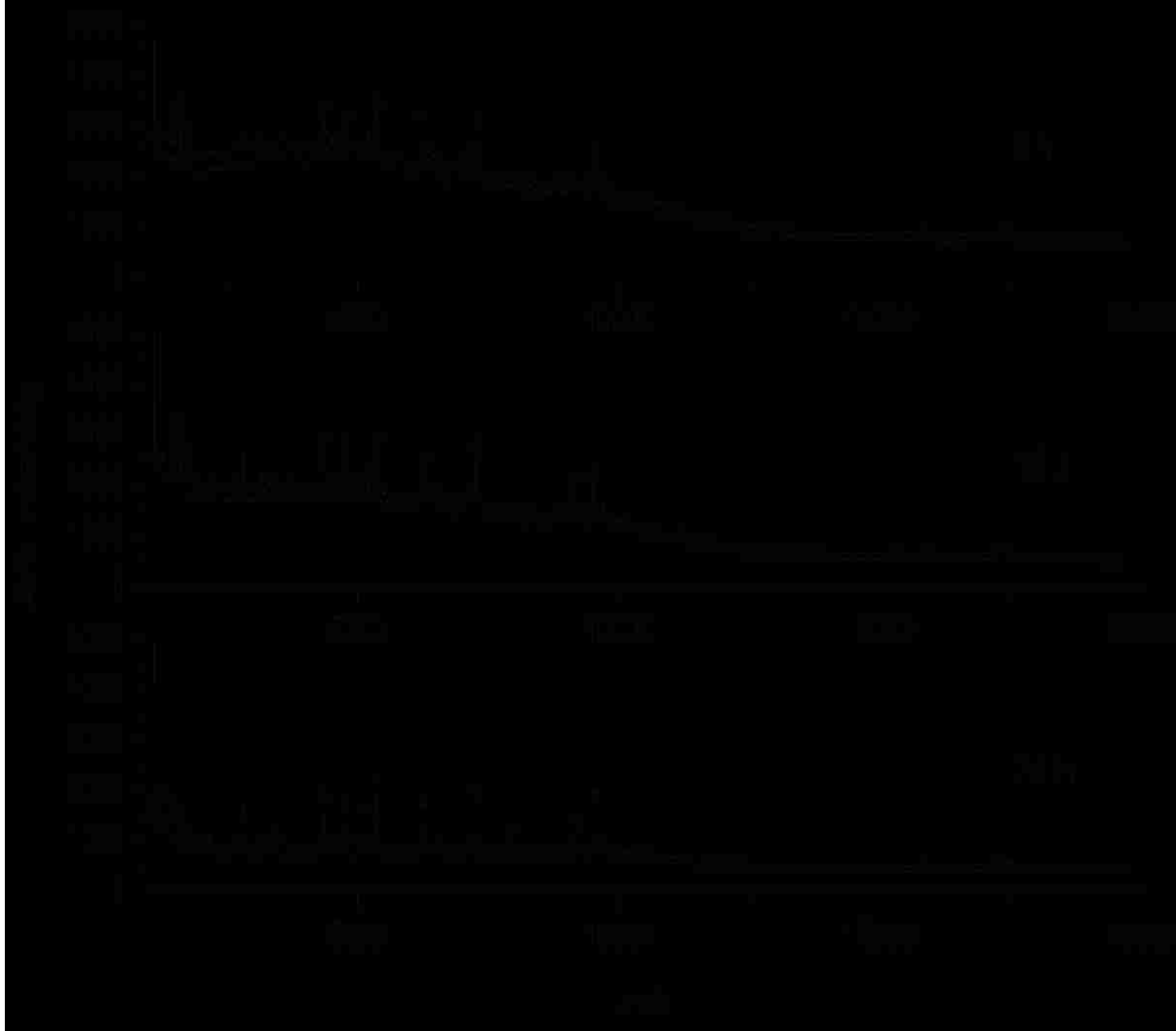
Figure 7-3. MALDI-TOF mass spectra of *E. coli* 9637 from the microfluidic culturing device with different growth times. Asterisks indicated matched peaks.

For the proteomic approach, a micropost bioreactor was prepared with a trypsin immobilized channel containing microposts after the culture chamber. *E. coli* (ATCC 9637) cells were cultured for 24 h and then washed with 5 μL of deionized water through the PC membrane. After the outlet of the waste reservoir was closed, 3 μL of a 100 mM phosphate buffer was infused into the culture chamber. The cultured *E. coli* solution was transferred into the micropost bioreactor and the flow was stopped for 5 min to allow time for digestion of proteins in cultured bacteria. After digestion, 1 μL was collected on a MALDI target. A representative MALDI mass spectrum of on-chip enzymatic digestion is shown in Figure 7-4.

120

Figure 7-4. MALDI –TOF mass spectrum of tryptic digest of *E. coli* 9637 from the culturing chamber. Asterisks indicated matched peaks.

As can be seen in this figure, several tryptic peptide peaks from *E. coli* were found. In our search using mass lists of *E. coli* digestion, Mowse scores greater than 58 are considered significant identifiers of the proteins in *E. coli* cells. The most significant protein hit is the cell shape determing protein homolog protein derived from *E. coli* (Q9R5Y8_ECOLI) in which 15 fragments among total 22 peaks in the spectum were matched. The peaks marked with closed circles (●) correspond to peptides generated from the digestion of the protein. The Mowse score for this protein was 153 with 53% sequence coverage based on MSDB database searches. Peaks marked with open circles (○) represent unidentified peaks from the tryptic digest of *E. coli*. Other peaks below *m/z* 1000 were assigned to background ions derived from the matrix. Table 7-2 shows matched all proteins with significant Mowse socres from the Mascot search results.

Table 7-2. Matched proteins with significant Mowse scores from search results.

Match	Accession	Mass	Score*	Description
1	Q9R5Y8_ECOLI	54839	153	Cell shape determining protein homolog (Fragment) - Escherichia coli.
2	CAA38206	91374	123	ECRNE NID - Escherichia coli
3	AAA23443	91374	122	ECOAMSG NID - Escherichia coli
4	CAA47818	114219	108	ECGAMS NID - Escherichia coli
5	S27311	118125	92	ribonuclease E (EC 3.1.4.-) - Escherichia coli (strain K-12)
6	F90811	118201	92	RNase E [imported] - Escherichia coli (strain O157:H7, substrain RIMD 0509952)
7	Q8FIP9_ECOL6	118272	92	Ribonuclease E (EC 3.1.4.-) - Escherichia coli O6
8	Q1RD73_ECOUT	118105	92	RNase E (EC 3.1.4.-) - Escherichia coli (strain UTI89 / UPEC)

*Protein scores greater than 58 are significant ($p < 0.05$)

7.5 Summary

In this chapter, the development of a PMMA culturing chip with continuous culture medium perfusion and thermostatic temperature control was described for off-line MALDI-TOF MS detection. This system demonstrated the integration of steps for bacterial identification using MALDI-TOF MS: cell culturing, digestion, and deposition onto a MALDI target plate. Three different strains of *E. coli* tested were cultured and fingerprint mass spectra distinguishing the strains were obtained using this system. In a test for the effect of culture time, 6 h incubation time could be acceptable for the bacterial identification procedure, which took shorter time compared to 24 h incubation time.

For proteomic analysis a micropost bioreactor after the culture area was used to investigate on-chip enzymatic digestion of proteins in cultured bacteria. The bioreactor brings the capability of an enhanced identification procedure for intact cells.

CHAPTER 8. CONCLUSIONS AND FUTURE DIRECTIONS

In this dissertation, the fabrication and use of microfluidic chips interfaced to MALDI mass spectrometry for proteomic applications was described. An automated digestion and droplet microfluidic device allows protein samples to be prepared for MALDI analysis. A micropost bioreactor was developed for the fast and efficient digestion of proteins. Continuous deposition was also used for low volume deposition. The microfluidic culturing devices were used to analyze cultured whole cells. The significance of this work lies in the ability of microfluidic devices for mass spectrometry to serve as a fast and effective analytical mean for proteomic samples.

In Chapter 3, a solid-phase bioreactor operated by a pressure-driven flow using a robotic fraction collector was used for off-line MALDI detection of protein samples. Here, the total sample preparation time was reduced from about 24 h required by a conventional digestion method to 40 s using the open-channel solid phase bioreactor. Also this bioreactor was demonstrated for proteins digestion and subsequently to deposit digested peptides with a matrix automatically on a MALDI target plate less than 1 min. The chip had a coaxial matrix and analyte mixing system, which combined the analyte with the matrix at the point of target deposition. It mixed digested peptides and the matrix more homogeneously, resulting in improved mass spectra. Microfluidic chips have been fabricated with micro-emitters combined with a ball inlet interface for on-line MALDI detection. However, the off-line MALDI approach incorporating an automated sample deposition interface had advantages of sensitivity and improved detection capabilities in a proteomics setting.

An approach to increase efficiency of digestion was developed. This approach was developed to address the problem of accurate protein identification from a complex sample. In a

solid-phase bioreactor, digestion efficiency depends on the geometry, digestion temperature, the compositions of digestion solvents, and the applied voltage. These parameters must be optimized to achieve fast and efficient digestion. Due to the precise microfabrication techniques various bioreactors with 3-D geometries can easily generated. The micropost bioreactor described in Chapter 4 provided highly reproducible micro-replication and efficient digestion by modifying the geometry of the open-channel bioreactor described in Chapter 3. Using this micropost bioreactor, the sequence coverage of proteins tested was improved compared to the open-channel format. In addition, proteins tested were identified with a high degree of certainty based on the high Mowse scores for the proteins, which means that the micropost bioreactor can be useful for accurate protein identification. The performance of the micropost bioreactor was extended to intact protein digestion in cells, giving rise to more applications for fast microorganism detection. This microfluidic device has the potential for use with chip-based separations using bottom-up proteomics as well as a shotgun proteomics of protein mixtures. One can also envision an on-chip 2-D separation (reversed phase plus ion exchange separation) for peptides that can be employed with the solid-phase digestion and deposition system.

Although we demonstrated the micropost bioreactor with MALDI-TOF MS to quickly digest intact proteins with high sequence coverage and high degree of certainty, the approach was still limited in application due to the relatively low abundances of proteins found in cells. For example, using the micropost bioreactor coupled with our MALDI mass spectrometer, the limit of quantification was 80 fmol for cytochrome *c* using a spotting deposition. In order to implement this interface, the limit of detection must be improved. One way this can be accomplished is with a hydrophobic MALDI target to obtain smaller deposited spot sizes.[335, 336] Under these conditions, the deposition volume can be reduced to achieve low volume fractions with a higher local concentration. Another way to address this issue is to utilize a continuous

deposition interface which has the potential for low volume sample deposition from the bioreactor,[303-305] thereby enhancing sensitivity.[23] An alternate sample deposition strategy, continuous deposition, was described in Chapter 5 for low-volume deposition. This continuous deposition interface offered a deposition volume 100-fold better than spotting deposition. Also, small sample deposits improved sensitivity due to an increase of local concentration of sample by more than 300% compared to the spotting deposition. A uniform sample trace was produced with a width which is similar to the ionization laser spot; thereby the operator does not need to search for a "sweet spot" in the sample. The continuous deposition interface can be interfaced to a separation but there are some additional requirements with this interface. The linear velocity of the solution needs to be balanced with the peak width of the separated plug.

A microfluidic device for more upstream proteomics was used to investigate microfluidic cell culturing chip for MALDI analysis. Three different strains of *E. coli* were cultured in the culturing chip and the mass spectral patterns associated with various strains were found to be different. Also, fingerprint mass spectra distinguishing strains were produced. These results showed that whole cell analysis using microfluidic cell culturing coupled with MALDI-TOF MS could serve as a tool for bacterial identification. This microfluidic culturing device can potentially be used for amplication of low abundance proteins in a cell. Collecting and preparing samples on this self-contained chip would extend the capabilities of MALDI-TOF to applications such as bacteria identification in clinical labs and water quality monitoring. To maintain a favorable environment for producing viable and consistent cell lines, a microfluidic cell culture device containing continuous perfusion of medium was developed by adding a polycarbonate membrane. Also a culturing area with continuous perfusion of fresh medium could be improved by modifying a chip manifold that incorporated a thermostatic temperature controller in place of an incubator to keep the temperature constant. Thus it could generate more consistent mass

spectra when interfaced to MALDI-TOF MS, and reduced the total detection time. Furthermore, a micropost bioreactor was fabricated at the end of the culture chamber to demonstrate the feasibility of an integrated chip for intact cell analysis. This integrated chip included dynamic culturing of bacteria cells using continuous perfusion of media, proteolytic digestion of cultured cells and deposition of generated peptides onto a MALDI target plate.

One of the future directions is the development of highly integrated microfluidic systems that contain multiple functional devices on a single wafer and incorporate a high density of microchannels and operational units. A proteomics chip is a fully integrated microfluidic platform that combines multiple functions on the same chip providing complete proteomic analysis and thus, fully automated analysis. Fully-integrated proteomic analysis chips do not yet exist; however, there have been several developments toward the integration of multiple processing steps into chips specifically for protein analyses. These devices will provide further automation capabilities and process integration into the sample processing pipeline. For example, developing an integrated system that can perform a solid phase extraction to isolate certain protein fractions, separation of the large number of protein components contained in the isolate using multi-dimensional separation, proteolytic digestion of the isolated proteins and then, deposition, either off-line or on-line, of these generated peptides for peptide-based mass fingerprinting would be very elegant. Integration of the entire proteomic processing pipeline will be necessary to promote high-throughput capabilities to enhance discovery-based projects and clinical applications of proteomics. While we have delineated the need for protein-type isolation using solid-phase extraction, further up-stream processing steps should be targeted for integration as well, such as cell isolation, culturing, and cell lysis. Lastly, high-throughput screening of proteomic samples for clinical diagnostics is a potential application area that could take advantage of these highly integrated and functional platforms.

126

REFERENCES

1.   Lee, J.; Soper, S. A.; Murray, K. K., Microfluidic chips for mass spectrometry-based proteomics. *J. Mass Spectrom.* **2009,** 44, 579-593.

2.   Lee, J.; Soper, S. A.; Murray, K. K., Microfluidics with MALDI Analysis for Proteomics - A Review. *Anal. Chim. Acta* **2009,** 649, 180-190.

3.   Abbott, A., A post-genomic challenge: learning to read patterns of protein synthesis. *Nature* **1999,** 402, 715-720.

4.   Harry, J. L.; Wilkins, M. R.; Herbert, B. R.; Packer, N. H.; Gooley, A. A.; Williams, K. L., Proteomics: Capacity versus utility. *Electrophoresis* **2000,** 21, 1071-1081.

5.   Quadroni, M.; James, P., Proteomics and automation. *Electrophoresis* **1999,** 20, 664-677.

6.   Anderson, N. L.; Matheson, A. D.; Steiner, S., Proteomics: applications in basic and applied biology. *Curr. Opin. Biotechnol.* **2000,** 11, 408-412.

7.   Haynes, P. A.; Roberts, T. H., Subcellular shotgun proteomics in plants: Looking beyond the usual suspects. *Proteomics* **2007,** 7, 2963-2975.

8.   Chait, B. T., Mass Spectrometry: Bottom-Up or Top-Down? *Science* **2006,** 314, 65-66.

9.   Egelhofer, V.; Gobom, J.; Seitz, H.; Giavalisco, P.; Lehrach, H.; Nordhoff, E., Protein Identification by MALDI-TOF-MS Peptide Mapping: A New Strategy. *Anal. Chem.* **2002,** 74, 1760-1771.

10.   Aebersold, R.; Mann, M., Mass spectrometry-based proteomics. *Nature* **2003,** 422, 198-207.

11.   Wu, C. C.; MacCoss, M. J., Shotgun proteomics: Tools for the analysis of complex biological systems. *Curr. Opin. Mol. Ther.* **2002,** 4, 242-250.

12.   Reid, G. E.; McLuckey, S. A., Top down protein characterization via tandem mass spectrometry. *J. Mass Spectrom.* **2002,** 37, 663-675.

13.   Marshall, A. G.; Hendrickson, C. L.; Jackson, G. S., Fourier transform ion cyclotron resonance mass spectrometry: A primer. *Mass Spectrom. Rev.* **1998,** 17, 1-35.

14.   Makarov, A., Electrostatic Axially Harmonic Orbital Trapping: A High-Performance Technique of Mass Analysis. *Anal. Chem.* **2000,** 72, 1156-1162.

15.   Aebersold, R.; Goodlett, D. R., Mass Spectrometry in Proteomics. *Chem. Rev.* **2001,** 101, 269-295.

16. Fenn, J. B.; Mann, M.; Meng, C. K.; Wong, S. F.; Whitehouse, C. M., Electrospray Ionization for Mass Spectrometry of Large Biomolecules. *Science* **1989,** 246, 64-71.

17. Domon, B.; Aebersold, R., Mass Spectrometry and Protein Analysis. *Science* **2006,** 312, 212-217.

18. Griffiths, W. J.; Jonsson, A. P.; Liu, S.; Rai, D. K.; Wang, Y., Electrospray and tandem mass spectrometry in biochemistry. *Biochem. J.* **2001,** 355, 545-561.

19. Hillenkamp, F.; Karas, M.; Beavis, R. C.; Chait, B. T., Matrix-assisted laser desorption/ionization mass spectrometry of biopolymers. *Anal. Chem.* **1991,** 63, 1193-1203.

20. Hardouin, J., Protein sequence information by matrix-assisted laser desorption/ionization in-source decay mass spectrometry. *Mass Spectrom. Rev.* **2007,** 26, 672-682.

21. Walker, K. L.; Chiu, R. W.; Monnig, C. A.; Wilkins, C. L., Off-Line Coupling of Capillary Electrophoresis and Matrix-Assisted Laser Desorption/Ionization Time-of-Flight Mass Spectrometry. *Anal. Chem.* **1995,** 67, 4197-4204.

22. Murray, K. K., Coupling matrix-assisted laser desorption/ionization to liquid separations. *Mass Spectrom. Rev.* **1997,** 16, 283-289.

23. Rejtar, T.; Hu, P.; Juhasz, P.; Campbell, J. M.; Vestal, M. L.; Preisler, J.; Karger, B. L., Off-Line Coupling of High-Resolution Capillary Electrophoresis to MALDI-TOF and TOF/TOF MS. *J. Proteome Res.* **2002,** 1, 171-179.

24. Collins, F. S.; Lander, E. S.; Rogers, J.; Waterston, R. H., Finishing the euchromatic sequence of the human genome. *Nature* **2004,** 431, 931-945.

25. Frö̈hlich, T.; Arnold, G. J., Proteome research based on modern liquid chromatography – tandem mass spectrometry: separation, identification and quantification. *J. Neural. Transm.* **2006,** 113, 973-994.

26. Corthals, G. L.; Wasinger, V. C.; Hochstrasser, D. F.; Sanchez, J.-C., The dynamic range of protein expression: A challenge for proteomic research. *Electrophoresis* **2000,** 21, 1104-1115.

27. Hancock, W. S.; Wu, S.-L.; Shieh, P., The challenges of developing a sound proteomics strategy. *Proteomics* **2002,** 2, 352-359.

28. Hunter, T. C.; Andon, N. L.; Koller, A.; John R. Yates, I.; Haynes, P. A., The functional proteomics toolbox: methods and applications *J. Chromatogr. B* **2002,** 782, 165-181.

29. Gygi, S. P.; Corthals, G. L.; Zhang, Y.; Rochon, Y.; Aebersold, R., Evaluation of two-dimensional gel electrophoresis-based proteome analysis technology. *Proc. Natl. Acad. Sci. USA* **2000,** 97, 9390-9395.

30.   Ru, Q. C.; Zhua, L. A.; Katenhusena, R. A.; Silbermana, J.; Brzeskia, H.; Liebmana, M.;
        Shriver, C. D., Exploring human plasma proteome strategies: High efficiency in-solution
        digestion protocol for multi-dimensional protein identification technology. *J.
        Chromatogr. A* **2006,** 1111, 175-191.

31.   Doucette, A.; Craft, D.; Li, L., Protein Concentration and Enzyme Digestion on
        Microbeads for MALDI-TOF Peptide Mass Mapping of Proteins from Dilute Solutions.
        Anal. Chem. **2000,** 72, 3355-3362.

32.   Zhoua, W.; B. Alex Merrickb; Khaledic, M. G.; Tomer, K. B., Detection and sequencing
        of phosphopeptides affinity bound to immobilized metal ion beads by matrix-assisted
        laser desorption/ionization mass spectrometry. *J. Am. Soc. Mass Spectrom.* **2000,** 11,
        273-282.

33.   Oda, Y.; Nagasu, T.; Chait, B. T., Enrichment analysis of phosphorylated proteins as a
        tool for probing the phosphoproteome. *Nat. Biotechnol.* **2001,** 19, 372-382.

34.   Wang, A.; Wu, C.-J.; Chen, S.-H., Gold Nanoparticle-Assisted Protein Enrichment and
        Electroelution for Biological Samples Containing Low Protein ConcentrationA Prelude
        of Gel Electrophoresis. *J. Proteome Res.* **2006,** 5, 1488–1492.

35.   Khandurina, J.; Guttman, A., Bioanalysis in microfluidic devices. *J. Chromatogr. A* **2002,**
        943, 159-183.

36.   Barry, R.; Ivanov, D., Microfluidics in biotechnology. *J. Nanotechnology* **2004,** 2, 2-6.

37.   Lazar, I. M.; Grym, J.; Foret, F., Microfabricated Devices: A New Sample Inroduction
        Approach to Mass Spectrometry. *Mass Spectrom. Rev.* **2006,** 25, 573-594.

38.   Sung, W.-C.; Makamba, H.; Chen, S.-H., Chip-based microfluidic devices coupled with
        electrospray ionization-mass spectrometry. *Electrophoresis* **2005,** 26, 1783-1791.

39.   Koster, S.; Verpoorte, E., A decade of microfluidic analysis coupled with electrospray
        mass spectrometry: An overview. *Lab Chip* **2007,** 7, 1394-1412.

40.   Duan, J.; Sun, L.; Liang, Z.; Zhang, J.; Wang, H.; Zhang, L.; Zhang, W.; Zhang, Y.,
        Rapid protein digestion and identification using monolithic enzymatic microreactor
        coupled with nano-liquid chromatography-electrospray ionization mass spectrometry. *J.
        Chromatogr. A* **2006,** 1106, 165-174.

41.   Mery, E.; Ricoul, F.; Sarrut, N.; Constantin, O.; Delapierre, G.; Garin, J.; Vinet, F., A
        silicon microfluidic chip integrating an ordered micropillar array separation column and a
        nano-electrospray emitter for LC/MS analysis of peptides. *Sens. Actuator B: Chemical*
        2008, 134, 438-446

42.   Ehlert, S.; Tallarek, U., High-pressure liquid chromatography in lab-on-a-chip devices.
        Anal. Bioanal. Chem. **2007,** 388, 517-520.

43. Mellors, J. S.; Gorbounov, V.; Ramsey, R. S.; Ramsey, J. M., Fully Integrated Glass Microfluidic Device for Performing High-Efficiency Capillary Electrophoresis and Electrospray Ionization Mass Spectrometry. *Anal. Chem.* **2008,** 80, 6881–6887.

44. Kato, M.; Sakai-Kato, K.; Jin, H.; Kubota, K.; Miyano, H.; Toyo'oka, T.; Dulay, M. T.; Zare, R. N., Integration of On-Line Protein Digestion, Peptide Separation, and Protein Identification Using Pepsin-Coated Photopolymerized Sol-Gel Columns and Capillary Electrophoresis/Mass Spectrometry. *Anal. Chem.* **2004,** 76, 1896-1902.

45. Staes, A.; Timmerman, E.; Damme, J. V.; Helsens, K.; Vandekerckhove, J.; Vollmer, M.; Gevaert, K., Assessing a novel microfluidic interface for shotgun proteome analysis. *J. Sep. Sci.* **2007,** 30, 1468-1476.

46. DeVoe, D. L.; Lee, C. S., Microfluidic technologies for MALDI-MS in proteomics. *Electrophoresis* **2006,** 27, 3559-3568.

47. Xu, Y.; Little, M. W.; Rousell, D. J.; Laboy, J. L.; Murray, K. K., Direct from Polyacrylamide Gel Infrared Laser Desorption/Ionization. *Anal. Chem.* **2004,** 76, 1078-1082.

48. Xu, Y.; Little, M. W.; Murray, K. K., Interfacing Capillary Gel Microfluidic Chips with Infrared Laser Desorption Mass Spectrometry. *J. Am. Soc. Mass Spectrom.* **2006,** 17, 469-474.

49. Fujita, M.; Hattori, W.; Sano, T.; Baba, M.; Someya, H.; Miyazaki, K.; Ken'ichi Kamijo, K. T., Hisao Kawaura High-throughput and high-resolution two dimensional mapping of pI and m/z using a microchip in a matrix- assisted laser desorption/ionization time-of-flight mass spectrometer. *J. Chromatogr. A* **2006,** 1111, 200-205.

50. Bakry, R.; Bonn, G. K.; Mair, D.; Svec, F., Monolithic porous polymer layer for the separation of peptides and proteins using thin-layer chromatography coupled with MALDI-TOF-MS. *Anal. Chem.* **2007,** 79, (2), 486-493.

51. Mok, M. L.-S.; Hua, L.; Phua, J. B.-C.; Wee, M. K. T.; Sze, N. S.-K., Capillary isoelectric focusing in pseudo-closed channel coupled to matrix assisted laser desorption/ionization mass spectrometry for protein analysis. *Analyst* **2004,** 129, 109-110.

52. Xue, Q.; Foret, F.; Dunayevskiy, Y. M.; Zavracky, P. M.; McGruer, N. E.; Karger, B. L., Multichannel Microchip Electrospray Mass Spectrometry. *Anal. Chem.* **1997,** 69, 426-430.

53. Ramsey, R. S.; Ramsey, J. M., Generating Electrospray from Microchip Devices Using Electroosmotic Pumping. *Anal. Chem.* **1997,** 69, 1174-1178.

54. Lazar, I. M.; Ramsey, R. S.; Sundberg, S.; Ramsey, J. M., Subattomole-Sensitivity Microchip Nanoelectrospray Source with Time-of-Flight Mass Spectrometry Detection. *Anal. Chem.* **1999,** 71, 3627-3631.

55. Yang, Y.; Li, C.; Lee, K. H.; Craighead, H. G., Coupling on-chip solid-phase extraction to electrospray mass spectrometry through an integrated electrospray tip. *Electrophoresis* **2005,** 26, 3622-3630.

56. Rohner, T. C.; Rossier, J. S.; Girault, H. H., Polymer Microspray with an Integrated Thick-Film Microelectrode. *Anal. Chem.* **2001,** 73, 5353-5357.

57. Xue, Q.; Dunayevskiy, Y. M.; Foret, F.; Karger, B. L., Integrated multichannel microchip electrospray ionization mass spectrometry: analysis of peptides from on-chip tryptic digestion of melittin. *Rapid Commun. Mass spectrom.* **1997,** 11, 1253-1256.

58. Li, J.; Thibault, P.; Bings, N. H.; Skinner, C. D.; Wang, C.; Colyer, C.; Harrison, J., Integration of Microfabricated Devices to Capillary Electrophoresis-Electropsray Mass Spectrometry Using a Low Dead Volume Connection: Application to Rapid Analyses of Proteolytic Digests. *Anal. Chem.* **1999,** 71, 3036-3045.

59. Barnidge, D. R.; Nilsson, S.; Markides, K. E., A Design for Low-Flow Sheathless Electrospray Emitters. *Anal. Chem.* **1999,** 71, 4115-4118.

60. Figeys, D.; Ning, Y.; Aebersold, R., A Microfabricated Device for Rapid Protein Identification by Microelectrospray Ion Trap Mass Spectrometry. *Anal. Chem.* **1997,** 69, 3153-3160.

61. Bings, N. H.; Wang, C.; Skinner, C. D.; Colyer, C. L.; Thibault, P.; Harrison, D. J., Microfluidic Devices Connected to Fused-Silica Capillaries with Minimal Dead Volume. *Anal. Chem.* **1999,** 71, 3292-3296.

62. Zhang, B.; Liu, H.; Karger, B. L.; Foret, F., Microfabricated Devices for Capillary Electrophoresis-Electrospray Mass Spectrometry. *Anal. Chem.* **1999,** 71, 3258-3264.

63. Oleschuk, R. D.; Harrison, D. J., Analytical microdevices for mass spectrometry. *Trends Anal. Chem.* **2000,** 19, 379-388.

64. Zhang, B.; Foret, F.; Karger, B. L., A Microdevice with Integrated Liquid Junction for Facile Peptide and Protein Analysis by Capillary Electrophoresis/Electrospray Mass Spectrometry. *Anal. Chem.* **2000,** 72, 1015-1022.

65. Wachs, T.; Henion, J., Electrospray Device for Coupling Microscale Separations and Other Miniaturized Devices with Electrospray Mass Spectrometry. *Anal. Chem.* **2001,** 73, 632-638.

66. Yin, H.; Killeen, K.; Brennen, R.; Sobek, D.; Werlich, M.; Goor, T. v. d., Microfluidic Chip for Peptide Analysis with an Integrated HPLC Column, Sample Enrichment Column, and Nanoelectrospray Tip. *Anal. Chem.* **2005,** 77, 527-533.

67. Schilling, M.; Nigge, W.; Rudzinski, A.; Neyer, A.; Hergenröder, R., A new on-chip ESI nozzle for coupling of MS with microfluidic devices. *Lab Chip* **2004,** 4, 220-224.

68. Svedberg, M.; Veszelei, M.; Axelsson, J.; Vangbo, M.; Nikolajeff, F., Poly(dimethylsiloxane) microchip: microchannel with integrated open electrospray tip. *Lab Chip* **2004,** 4, 322-327.

69. Kameoka, J.; Orth, R.; Ilic, B.; Czaplewski, D.; Wachs, T.; Craighead, H. G., An Electrospray Ionization Source for Integration with Microfluidics. *Anal. Chem.* **2002,** 74, 5897-5901.

70. Tang, K.; Lin, Y.; Matson, D. W.; Kim, T.; Smith, R. D., Generation of Multiple Electrosprays Using Microfabricated Emitter Arrays for Improved Mass Spectrometric Sensitivity. *Anal. Chem.* **2001,** 73, 1658-1663.

71. Schultz, G. A.; Corso, T. N.; Prosser, S. J.; Zhang, S., A Fully Integrated Monolithic Microchip Electrospray Device for Mass Spectrometry. *Anal. Chem.* **2000,** 72, 4058-4063.

72. Licklider, L.; Wang, X.-Q.; Desai, A.; Tai, Y.-C.; Lee, T. D., A Micromachined Chip-Based Electrospray Source for Mass Spectrometry. *Anal. Chem.* **2000,** 72, 367-375.

73. Xie, J.; Miao, Y.; Shih, J.; He, Q.; Liu, J.; Tai, Y.-C.; Lee, T. D., An Electrochemical Pumping System for On-Chip Gradient Generation. *Anal. Chem.* **2004,** 76, 3756-3763.

74. Xie, J.; Shih, J.; Lin, Q.; Yang, B.; Tai, Y.-C., Surface micromachined electrostatically actuated micro peristaltic pump. *Lab Chip* **2004,** 4, 495-501.

75. Xie, J.; Miao, Y.; Shih, J.; Tai, Y.-C.; Lee, T. D., Microfluidic Platform for Liquid Chromatography-Tandem Mass Spectrometry Analysis of Complex Peptide Mixtures. *Anal. Chem.* **2005,** 77, 6947-6953.

76. VanPelt, C. K.; Zhang, S.; Henion, J. D., Characterization of a Fully Automated Nanoelectrospray System with Mass Spectrometric Detection for Proteomic Analysis. *J. Biomol. Tech.* **2002,** 13, 72-84.

77. Yin, H.; Killeen, K., The fundamental aspects and applications of Agilent HPLC-Chip. *J. Sep. Sci.* **2007,** 30, 1427-1434.

78. Vollmer, M.; Hörth, P.; Rozing, G.; Couté, Y.; Grimm, R.; Hochstrasser, D.; Sanchez, J.-C., Multi-dimensional HPLC/MS of the nucleolar proteome using HPLC-chip/MS. *J. Sep. Sci.* **2006,** 29, 499-509.

79. Fortier, M.-H.; Bonneil, E.; Goodley, P.; Thibault, P., Integrated Microfluidic Device for Mass Spectrometry-Based Proteomics and Its Application to Biomarker Discovery Programs. *Anal. Chem.* **2005,** 77, 1631–1640.

80. Nägele, E.; Vollmer, M., Coupling of nanoflow liquid chromatography to matrix-assisted laser desorption/ionization mass spectrometry: real-time liquid chromatography run mapping on a MALDI plate. *Rapid Commun. Mass Spectrom.* **2004,** 18, 3008-3014.

81. Lee, J.; Musyimi, H. K.; Soper, S. A.; Murray, K. K., Development of an Automated Digestion and Droplet Deposition Microfluidic Chip for MALDI-TOF MS. *J. Am. Soc. Mass Spectrom.* **2008,** *19*, 964-972.

82. Ekström, S.; Önnerfjord, P.; Nilsson, J.; Bengtsson, M.; Laurell, T.; Marko-Varga, G., Integrated Microanalytical Technology Enabling Rapid and Automated Protein Identification. *Anal. Chem.* **2000,** 72, 286-293.

83. Wang, Y.-X.; Zhou, Y.; Balgley, B. M.; Cooper, J. W.; Lee, C. S.; DeVoe, D. L., Electrospray interfacing of polymer microfluidics to MALDI-MS. *Electrophoresis* **2005,** 26, 3631-3640.

84. Zhang, X.; Narcissea, D. A.; Murray, K. K., On-line single droplet deposition for MALDI mass spectrometry. *J. Am. Soc. Mass Spectrom.* **2004,** 15, 1471-1477.

85. Murray, K. K.; Russell, D. H., Liquid Sample Introduction for Matrix-Assisted Laser Desorption Ionization. *Anal. Chem.* **1993,** 65, 2534-2537.

86. Murray, K. K.; Russell, D. H., Aerosol matrix-assisted laser desorption ionization mass spectrometry. *J. Am. Soc. Mass Spectrom.* **1994,** 5, 1-9.

87. Fei, X.; Murray, K. K., On-Line Coupling of Gel Permeation Chromatography with MALDI Mass Spectrometry. *Anal. Chem.* **1996,** 68, 3555-3560.

88. Brivio, M.; Fokkens, R. H.; Verboom, W.; Reinhoudt, D. N.; Tas, N. R.; Goedbloed, M.; Berg, A. v. d., Integration Microfluidic System Enabling (Bio)chemical Reactions with On-Line MALDI-TOF Mass Spectrometry. *Anal. Chem.* **2002,** 74, 3972-3976.

89. Brivio, M.; Tas, N. R.; Goedbloed, M. H.; Gardeniers, H. J. G. E.; Verboom, W.; Berg, A. v. d.; Reinhoudt, D. N., A MALDI-chip integrated system with a monitoring window. *Lab Chip* **2005,** 5, 378-381.

90. Musyimi, H. K.; Narcisse, D. A.; Zhang, X.; Stryjewski, W.; Soper, S. A.; Murray, K. K., Online CE-MALDI-TOF MS Using a Rotating Ball Interface. *Anal. Chem.* **2004,** 76, 5968-5973.

91. Musyimi, H. K.; Guy, J.; Narcisse, D. A.; Soper, S. A.; Murray, K. K., Direct coupling of polymer-based microchip electrophoresis to online MALDI-MS using a rotating ball inlet. *Electrophoresis* **2005,** 26, 4703-4710.

92. Li, L.; Wang, A. P. L.; Coulson, L. D., Continuous-flow matrix-assisted laser desorption ionization mass spectrometry. *Anal. Chem.* **1993,** 65, 493-495.

93. Preisler, J.; Foret, F.; Karger, B. L., On-Line MALDI-TOF MS Using a Continuous Vacuum Deposition Interface. *Anal. Chem.* **1998,** 70, 5278-5287.

94. Ørsnes, H.; Graf, T.; Bohatka, S.; Degn, H., Rotating ball inlet for continuous mass spectrometric monitoring of aqueous solutions. *Rapid Commun. Mass spectrom.* **1998,** 12, 11-14.

95. Ørsnes, H.; Graf, T.; Degn, H.; Murray, K. K., A Rotating Ball Inlet for On-Line MALDI Mass Spectrometry. *Anal. Chem.* **2000,** 72, 251-254.

96. Liu, J.; Tseng, K.; Garcia, B.; Lebrilla, C. B.; Mukerjee, E.; Collins, S.; Smith, R., Electrophoresis Separation in Open Microchannels. A Method for Coupling Electrophoresis with MALDI-MS. *Anal. Chem.* **2001,** 73, 2147-2151.

97. Jacksén, J.; Frisk, T.; Redeby, T.; Parmar, V.; Wijngaart, W. v. d.; Stemme, G.; Emmer, Å., Off-line integration of CE and MALDI-MS using a closed-open-closed microchannel system. *Electrophoresis* **2007,** 28, 2458-2465.

98. Zhang, H.; Stoeckli, M.; Andren, P. E.; Caprioli, R. M., Combining solid-phase preconcentration, capillary electrophoresis and off-line matrix-assisted laser desorption/ionization mass spectrometry: intracerebral metabolic processing of peptide E in vivo. *J. Mass Spectrom.* **1999,** 34, 377-383.

99. Wang, J.; Ma, M.; Chen, R.; Li, L., Enhanced Neuropeptide Profiling via Capillary Electrophoresis Off-Line Coupled with MALDI FTMS. *Anal. Chem.* **2008,** 80, 6168-6177.

100. Müller, R.; Marchetti, M.; Kratzmeier, M.; Elgass, H.; Kuschel, M.; Zenker, A.; Allmaier, G., Comparison of planar SDS-PAGE, CGE-on-a-chip, and MALDI-TOF mass spectrometry for analysis of the enzymatic de-N-glycosylation of antithrombin III and coagulation factor IX with PNGase F. *Anal. Bioanal. Chem.* **2007,** 389, 1859-1868.

101. Tseng, K.; Liu, J.; Lebrilla, C. B.; Collins, S. D.; Smith, R. L., Fabrication and design of open microchannels for capillary electrophoresis separations and matrix-assisted laser/desorption mass spectroscopy analysis. *Proceedings of SPIE-The International Society for Optical Engineering* **1999,** 3606, 137-148.

102. Hsieh, S.; Dreisewerd, K.; Schors, R. C. v. d.; Jiménez, C. R.; Stahl-Zeng, J.; Hillenkamp, F.; Jorgenson, J. W.; Geraerts, W. P. M.; Li, K. W., Separation and Identification of Peptides in Single Neurons by Microcolumn Liquid Chromatography-Matrix-Assisted Laser Desorption/Ionization Time-of-Flight Mass Spectrometry and Postsource Decay Analysis. *Anal. Chem.* **1998,** 70, 1847-1852.

103. Miliotis, T.; Kjellström, S.; Nilsson, J.; Laurell, T.; Edholm, L.-E.; Marko-Varga, G., Capillary liquid chromatography interfaced to matrix-assisted laser desorption/ionization time-of-flight mass spectrometry using an on-line coupled piezoelectric flow-through microdispenser. *J. Mass Spectrom.* **2000,** 35, 369-377.

104.   Lou, X.; Dongen, L. J. v., Direct sample fraction deposition using electrospray in narrow-bore size-exclusion chromatography/matrix-assisted laser desorption/ionization time-of-flight mass spectrometry for polymer characterization. *J. Mass Spectrom.* **2000,** 35, 1308-1312.

105.   Guo, X.; Chan-Park, M. B.; Yoon, S. F.; Chun, J.-h.; Hua, L.; Sze, N. S.-K., UV Embossed Polymeric Chip for Protein Separation and Identification Based on Capillary Isoelectric Focusing and MALDI-TOF-MS. *Anal. Chem.* **2006,** 78, 3249-3256.

106.   Krone, J. R.; Nelson, R. W.; Dogruel, D.; Williams, P.; Granzow, R., BIA/MS: Interfacing Biomolecular Interaction Analysis with Mass Spectrometry. *Anal. Biochem.* **1997,** 244, 124-132.

107.   Nelson, R. W.; Krone, J. R.; Jansson, O., Surface plasmon resonance biomolecular interaction analysis mass spectrometry. 1. Chip-based analysis. *Anal. Chem.* **1997,** 69, 4363-4368

108.   Nelson, R. W.; Nedelkov, D.; Tubbs, K. A., Biomolecular Interaction Analysis Mass Spectrometry. *Anal. Chem.* **2000,** 72, 404A-411A.

109.   Nedelkov, D.; Nelson, R. W., Practical considerations in BIA/MS: optimizing the biosensor-mass spectrometry interface. *J. Mol. Recognit.* **2000,** 13, 140-145.

110.   Nedelkov, D.; Nelson, R. W., Exploring the limit of detection in biomolecular interaction analysis mass spctrometry (BIA/MS): detection of attomole amounts of native proteins present in compelex biological mixtures. *Biosens. Bioelectron* **2001,** 16, 1071-1078.

111.   Nedelkov, D.; Nelson, R. W., Analysis of human urine protein biomarkers via biomolecular interaction analysis mass spectrometry. *Am. J. Kidney Dis.* **2001,** 38, 481-487.

112.   Natsume, T.; Taoka, M.; Manki, H.; Kume, S.; Isobe, T.; Mikoshiba, K., Rapid analysis of protein interactions: On-chip micropurification of recombinant protein expressed in *Esherichia coli*. *Proteomics* **2002,** 2, 1247-1253.

113.   Nedelkov, D., Development of Surface Plasmon Resonance Mass Spectrometry Array Platform. *Anal. Chem.* **2007,** 79, 5987-5990.

114.   Harrison, D. J.; Manz, A.; Fan, Z.; Luedi, H.; Widmer, H. M., Capillary Electrophoresis and Sample Injection Systems Integrated on a Planar Glass Chip. *Anal. Chem.* **1992,** 64, 1926-1932.

115.   Jacobson, S. C.; Hergenroder, R.; Koutny, L. B.; Warmack, R. J.; Ramsey, J. M., Effects of Injection Schemes and Column Geometry on the Performance of Microchip Electrophoresis Devices. *Anal. Chem.* **1994,** 66, 1107-1113.

116.   Effenhauser, C. S.; Manz, A.; Widmer, H. M., Manipulation of Sample Fractions on a Capillary Electrophoresis Chip. *Anal. Chem.* **1995,** 67, 2284-2287.

117.   Schmalzing, D.; Adourian, A.; Koutny, L.; Ziaugra, L.; Matsudaira, P.; Ehrlich, D., DNA Sequencing on Microfabricated Electrophoretic Devices. *Anal. Chem.* **1998,** 70, 2303-2310.

118.   Jacobson, S. C.; Hergenroder, R.; Koutny, L. B.; Ramsey, J. M., High-Speed Separations on a Microchip. *Anal. Chem.* **1994,** 66, 1114-1118.

119.   Jacobson, S. C.; Moore, A. W.; Ramsey, J. M., Fused Quartz Substrates for Microchip Electrophoresis. *Anal. Chem.* **1995,** 67, 2059-2063.

120.   Ssenyange, S.; Taylor, J.; Harrison, D. J.; McDermott, M. T., A Glassy Carbon Microfluidic Device for Electrospray Mass Spectrometry. *Anal. Chem.* **2004,** 76, 2393-2397.

121.   Lion, N.; Rohner, T. C.; Dayon, L.; Arnaud, I. L.; Damoc, E.; Youhnovski, N.; Wu, Z.-Y.; Roussel, C.; Josserand, J.; Jensen, H.; Rossier, J. S.; Przybylski, M.; Girault, H. H., Microfluidic systems in proteomics. *Electrophoresis* **2003,** 24, 3533-3562.

122.   Becker, H.; Gärtner, C., Polymer microfabrication methods for microfluidic analytical applications. *Electrophoresis* **2000,** 21, 12-26.

123.   Becker, H.; Locascio, L. E., Polymer microfluidic devices. *Talanta* **2002,** 56, 267-287.

124.   Shadpour, H.; Musyimi, H.; Chen, J.; Soper, S. A., Physiochemical properties of various polymer substrates and their effects on microchip electrophoresis performance. *J. Chromatogr. A* **2006,** 1111, 238-251.

125.   Kopp, M. U.; Mello, A. J. d.; Manz, A., Chemical Amplification: Continuous-Flow PCR on a Chip. *Science* **1998,** 280, 1046-1048.

126.   McKnight, T. E.; Culbertson, C. T.; Jacobson, S. C.; Ramsey, J. M., Electroosmotically Induced Hydraulic Pumping with Integrated Electrodes on Microfluidic Devices. *Anal. Chem.* **2001,** 73, 4045-4049.

127.   Liu, Y.; Xue, Y.; Ji, J.; Chen, X.; Kong, J.; Yang, P.; Girault, H. H.; Liu, B., Gold Nanoparticle Assembly Microfluidic Reactor for Efficient On-line Proteolysis. *Mol Cell Proteomics* **2007,** 6, 1428-1436.

128.   Li, J. M.; Liu, C.; Qiao, H. C.; Zhu, L. Y.; Chen, G.; Dai, X. D., Hot embossing/bonding of a poly(ethylene terephthalate) (PET) microfluidic chip. *J. Micromech. Microeng.* **2008,** 18, 1-10.

129.   Waters, L. C.; Jacobson, S. C.; Kroutchinina, N.; Khandurina, J.; Foote, R. S.; Ramsey, J. M., Microchip Device for Cell Lysis, Multiplex PCR Amplification, and Electrophoretic Sizing. *Anal. Chem.* **1998,** 70, 158-162.

130.   Weigl, B. H.; Yager, P., Microfluidic Diffusion-Based Separation and Detection. *Science* **1999,** 283, 346-347.

131.   Colyer, C. L.; Tang, T.; Chiem, N.; Harrison, D. J., Clinical potential of microchip capillary electrophoresis systems. *Electrophoresis* **1997,** 18, 1733-1741.

132.   Dodge, A.; Brunet, E.; Chen, S.; Goulpeau, J.; Labas, V.; Vinh, J.; Tabeling, P., PDMS-based microfluidics for proteomic analysis. *Analyst* **2006,** 131, 1122-1128.

133.   Locascio, L. E.; Perso, C. E.; Lee, C. S., Measurement of electroosmotic flow in plastic imprinted microfluid devices and the effect of protein adsorption on flow rate. *J. Chromatogr. A* **1999,** 857, 275-284.

134.   Soper, S. A.; Henry, A. C.; Vaidya, B.; Galloway, M.; Wabuyele, M.; McCarley, R. L., Surface modification of polymer-based microfluidic devices. *Anal. Chim. Acta* **2002,** 470, 87-99.

135.   Gaudioso, J.; Craighead, H. G., Characterizing electroosmotic flow in microfluidic devices. *J. Chromatogr. A* **2002,** 971, (1-2), 249-253.

136.   Bi, H.; Meng, S.; Li, Y.; Guo, K.; Chen, Y.; Kong, J.; Yang, P.; Zhong, W.; Liu, B., Deposition of PEG onto PMMA microchannel surface to minimize nonspecific adsorption. *Lab Chip* **2006,** 6, 769-775.

137.   Křenková, J.; Foret, F., Immobilized microfluidic enzymatic reactors. *ELectrophoresis* **2004,** 25, 3550-3563.

138.   Tian, H.; Brody, L. C.; Landers, J. P., Rapid Detection of Deletion, Insertion, and Substitution Mutations via Heteroduplex Analysis Using Capillary- and Microchip-Based Electrophoresis. *Genome Res.* **2000,** 10, 1403-1413.

139.   Erickson, D.; Sinton, D.; Li, D., Joule heating and heat transfer in poly(dimethylsiloxane) microfluidic systems. *Lab Chip* **2003,** 3, 141-149.

140.   Ibáñez, A. J.; Muck, A.; Svatoš, A., Dissipation of charge on MALDI-TOF polymeric chips using an electron-acceptor: analysis of proteins. *J. Mass Spectrom.* **2007,** 42, 634-640.

141.   Nägele, E.; Vollmer, M.; Hörth, P., Two-dimensional nano-liquid chromatography–mass spectrometry system for applications in proteomics. *J. Chromatogr. A* **2003,** 1009, 197-205.

142.   Li, J.; LeRiche, T.; Tremblay, T.-L.; Wang, C.; Bonneil, E.; Harrison, D. J.; Thibault, P., Application of Microfluidic Devices to Proteomics Research. *Mol Cell Proteomics* **2002,** 1, 157-168.

143.   Freire, S. L. S.; Wheeler, A. R., Proteome-on-a-chip: Mirage, or on the horizon? *Lab Chip* **2006,** 6, 1415-1423.

144.	Lion, N.; Gellon, J.-O.; Jensen, H.; Girault, H. H., On-chip protein sample desalting and preparation for direct coupling with electrospray ionization mass spectrometry. *J. Chromatogr. A* **2003,** 1003, 11-19.

145.	Gustafsson, M.; Hirschberg, D.; Palmberg, C.; rnvall, H. J.; Bergman, T., Integrated Sample Preparation and MALDI Mass Spectrometry on a Microfluidic Compact Disk. *Anal. Chem.* **2004,** 76, 345-350.

146.	Hirschberg, D.; Tryggvason, S.; Gustafsson, M.; Bergman, T.; Swedenborg, J.; Hedin, U.; Jörnvall, H., Identification of Endothelial Proteins by MALDI-MS Using a Compact Disc Microfluidic System. *The Protein Journal* **2004,** 23, 263-271.

147.	Hirschberg, D.; Jägerbrink, T.; Samskog, J.; Gustafsson, M.; Ståhlberg, M.; Alvelius, G.; Husman, B.; Carlquist, M.; Jörnvall, H.; Bergman, T., Detection of Phosphorylated Peptides in Proteomic Analyses Using Microfluidic Compact Disk Technology. *Anal. Chem.* **2004,** 76, 5864-5871.

148.	Ekström, S.; Wallman, L.; Helldin, G.; Nilsson, J.; Marko-Varga, G.; Laurell, T., Polymeric integrated selective enrichment target (ISET) for solid-phase-based sample preparation in MALDI-TOF MS. *J. Mass Spectrom.* **2007,** 42, 1445-1452.

149.	Wheeler, A. R.; Moon, H.; Bird, C. A.; OgorzalekLoo, R. R.; Kim, C.-J.; Loo, J. A.; Garrell, R. L., Digital Microfluidics with In-Line Sample Purification for Proteomics Analyses with MALDI-MS. *Anal. Chem.* **2005,** 77, 534-540.

150.	Wheeler, A. R.; Moon, H.; Kim, C.-J.; Loo, J. A.; Garrell, R. L., Electrowetting-Based Microfluidics for Analysis of Peptides and Proteins by Matrix-Assisted Laser Desorption/Ionization Mass Spectrometry. *Anal. Chem.* **2004,** 76, 4833-4838.

151.	Nichols, K. P.; Gardeniers, H. J. G. E., A Digital Microfluidic System for the Investigation of Pre-Steady-State Enzyme Kinetics Using Rapid Quenching with MALDI-TOF Mass Spectrometry. *Anal. Chem.* **2007,** 79, 8699-8704.

152.	Ehlert, S.; Kraiczek, K.; Mora, J.-A.; Dittmann, M.; Rozing, G. P.; Tallarek, U., Separation Efficiency of Particle-Packed HPLC Microchips. *Anal. Chem.* **2008,** 80, 5945-5950.

153.	Ishida, A.; Yoshikawa, T.; Natsume, M.; Kamidate, T., Reversed-phase liquid chromatography on a microchip with sample injector and monolithic silica column. *J. Chromatogr. A* **2006,** 1132, 90-98.

154.	Kutter, J. P., Current developments in electrophoretic and chromatographic separation methods on microfabricated devices. *Trends Anal. Chem.* **2000,** 19, 352-353.

155.	Rossier, J. S.; Schwarz, A.; Reymond, F.; Ferrigno, R.; Bianchi, F.; Girault, H. H., Microchannel networks for electrophoretic separations. *Electrophoresis* **1999,** 20, 727-731.

156. Rossier, J.; Reymond, F.; Michel, P. E., Polymer microfluidic chips for electrochemical and biochemical analyses. *Electrophoresis* **2002,** 23, 858-867.

157. Liu, Y.; Foote, R. S.; Jacobson, S. C.; Ramsey, R. S.; Ramsey, J. M., Electrophoretic Separation of Proteins on a Microchip with Noncovalent, Postcolumn Labeling. *Anal. Chem.* **2000,** 72, 4608-4613.

158. Bousse, L.; Mouradian, S.; Minalla, A.; Yee, H.; Williams, K.; Dubrow, R., Protein Sizing on a Microchip. *Anal. Chem.* **2001,** 73, 1207-1212.

159. Culbertson, C. T.; Jacobson, S. C.; Ramsey, J. M., Microchip Devices for High-Efficiency Separations. *Anal. Chem.* **2000,** 72, 5814-5819.

160. Throckmorton, D. J.; Shepodd, T. J.; Singh, A. K., Electrochromatography in Microchips: Reversed-Phase Separation of Peptides and Amino Acids Using Photopatterned Rigid Polymer Monoliths. *Anal. Chem.* **2002,** 74, 784-789.

161. Li, Y.; DeVoe, D. L.; Lee, C. S., Dynamic analyte introduction and focusing in plastic microfluidic devices for proteomic analysis. *Electrophoresis* **2003,** 24, 193-199.

162. Figeys, D.; Pinto, D., Proteomics on a chip: Promising developments. *Electrophoresis* **2001,** 22, 208-216.

163. Deng, Y.; Zhang, H.; Henion, J., Chip-Based Quantitative Capillary Electrophoresis/Mass Spectrometry Determination of Drugs in Human Plasma. *Anal. Chem.* **2001,** 73, 1432-1439.

164. Wang, H.; Hanash, S., Multi-dimensional liquid phase based separations in proteomics. *J. Chromatogr. B* **2003,** 787, 11-18.

165. Oleschuk, R. D.; Shultz-Lockyear, L. L.; Ning, Y.; Harrison, D. J., Trapping of Bead-Based Reagents within Microfluidic Systems: On-Chip Solid-Phase Extraction and Electrochromatography. *Anal. Chem.* **2000,** 72, 585-590.

166. Hjertén, S.; Liao, J.-L.; Zhang, R., High-performance liquid chromatography on continuous polymer beds *J. Chromatogr. A* **1989,** 473, 273-275.

167. Tennikova, T. B.; Svec, F.; Belenkii, B. G., High-Performance Membrane Chromatography. A Novel Method of Protein Separation. *J. Liq. Chromatogr.* **1990,** 13, 63-70.

168. Svec, F.; Frechet, J. M. J., Continuous Rods of Macroporous Polymer as High-Performance Liquid Chromatography Separation Media. *Anal. Chem.* **1992,** 54, 820-822.

169. Svec, F.; Huber, C. G., Monolithic materials: Promises, challenges, achievements. *Anal. Chem.* **2006,** 78, 2100-2107.

170.   Eeltink, S.; Hilder, E. F.; Geiser, L.; Svec, F.; Fréchet, J. M. J.; Rozing, G. P.; Schoenmakers, P. J.; Kok, W. T., Controlling the surface chemistry and chromatography properties of methyacrylate-ester-based monolithic capillary colums via photografting. *J. Sep. Sci.* **2007,** 30, (3), 407-413.

171.   Ro, K. W.; Nayak, R.; Knapp, D. R., Monolithic media in microfluidic devices for proteomics. *Electrophoresis* **2006,** 27, 3547 - 3558.

172.   Ro, K. W.; Liu, J.; Knapp, D. R., Plastic microchip liquid chromatography-matirx-assiated laser desorption/ionization mass spectrometry using monolithic columns. *J. Chromatogr. A* **2006,** 1111, 40-47.

173.   Busch, K. L., Mass spectrometric detectors for samples separated by planar electrophoresis. *J. Chromatogr. A* **1995,** 692, 275-290

174.   Gusev, A. I.; Proctor, A.; Rabinovich, Y. I.; Hercules, D. M., Thin-Layer Chromatography Combined with Matrix-Assisted Laser Desorption/Ionization Mass Spectrometry. *Anal. Chem.* **1995,** 67, 1805-1814.

175.   Ivleva, V. B.; Elkin, Y. N.; Budnik, B. A.; Moyer, S. C.; O'Connor, P. B.; Costello, C. E., Coupling Thin-layer Chromatography with vibrational cooling Matrix-Assisted Laser Desorption/Ionization Fourier Transform Mass Spectrometry for the Analysis of Ganglioside Mixtures. *Anal. Chem.* **2004,** 76, 6484-6491.

176.   Dreisewerd, K.; Müthing, J.; Rohlfing, A.; Meisen, I.; Vukelić, Ž.; Peter-Katalinić, J.; Hillenkamp, F.; Berkenkamp, S., Analysis of Gangliosides Directly from Thin-Layer Chromatography Plates by Infrared Matrix Laser Desorption/Ionization Orthogonal Time-of-Flight Spectrometry with a Glycerol Matrix. *Anal. Chem.* **2005,** 77, 4098-4107.

177.   Salo, P. K.; Vilmunen, S.; Salomies, H.; Ketola, R. A.; Kostiainen, R., Two-Dimensional Ultra-Thin-Layer Chromatography and Atmospheric Pressure Matrix-Assisted Laser Desorption/Ionization Mass Spectrometry in Bioanalysis. *Anal. Chem.* **2007,** 79, 2101-2108.

178.   Ethier, M.; Hou, W.; Duewel, H. S.; Figeys, D., The Proteomic Reactor: A Microfluidic Device for Processing Minute Amounts of Protein Prior to Mass Spectrometry Analysis. *J. Proteome Res.* **2006,** 5, 2754-2759.

179.   Liu, Y.; Zhong, W.; Meng, S.; Kong, J.; Lu, H.; Yang, P.; Girault, H. H.; Liu, B., Assembly-Controlled Biocompatible Interface on a Microchip: Strategy to Highly Efficient Proteolysis. *Chem. Eur. J.* **2006,** 12, 6585-6591.

180.   Rosenfeld, J.; Capdevielle, J.; Guillemot, J. C.; Ferrara, P., In-gel digestion of proteins for internal sequence analysis after one- or two-dimensional gel electrophoresis. *Anal. Biochem.* **1992,** 203, 173-179.

181. Huang, Y.; Shan, W.; Liu, B.; Liu, Y.; Zhang, Y.; Zhao, Y.; Lu, H.; Tang, Y.; Yang, P., Zeolite nanoparticle modified microchip reactor for efficient protein digestion. *Lab Chip* **2006,** 6, 534-539.

182. Kumarathasan, P.; Mohottalage, S.; Goegan, P.; Vincent, R., An optimized protein in-gel digest method for reliable proteome characterization by MALDI–TOF–MS analysis. *Anal. Biochem.* **2005,** 346, 85-89.

183. Wilm, M.; Shevchenko, A.; Houthaeve, T.; Breit, S.; Schweigerer, L.; Fotsis, T.; Mann, M., Femtomole sequencing of proteins from polyacrylamide gels by nano-electrospray mass spectrometry. *Nature* **1996,** 379, 466-469.

184. Gharahdaghi, F.; Weinberg, C. R.; Meagher, D. A.; Imai, B. S.; Mische, S. M., Mass spectrometric identification of proteins from silver-stained polyacrylamide gel: A method for the removal of silver ions to enhance sensitivity. *Electrophoresis* **1999,** 20, 601-605.

185. Klammer, A. A.; MacCoss, M. J., Effects of Modified Digestion Schemes on the Identification of Proteins from Complex Mixtures. *J. Proteome Res.* **2006,** 5, 695-700.

186. Lundell, N.; Schreitmüller, T., Sample Preparation for Peptide Mapping - A Pharmaceutical Quality-Control Perspective. *Anal. Biochem.* **1999,** 266, 31-47.

187. Schaefer, H.; Chamrad, D. C.; Marcus, K.; Reidegeld, K. A.; Blüggel, M.; Meyer, H. E., Tryptic transpeptidation products observed in proteome analysis by liquid chromatography-tandem mass spectrometry. *Proteomics* **2005,** 5, 846-852.

188. Massolini, G.; Calleri, E., Immobilized trypsin systems coupled on-line to separation methods: Recent developments and analytical applications. *J. Sep. Sci.* **2005,** 28, 7-21.

189. Duan, J.; Liang, Z.; Yang, C.; Zhang, J.; Zhang, L.; Zhang, W.; Zhang, Y., Rapid protein identification using monolithic enzymatic microreactor and LC-ESI-MS/MS. *Proteomics* **2006,** 6, 412-419.

190. Slysz, G. W.; Lewis, D. F.; Schriemer, D. C., Detection and Identification of Sub-nanogram Levels of Protein in a NanoLC-Trypsin-MS System. *J. Proteome Res.* **2006,** 5, 1959-1966.

191. Strader, M. B.; Tabb, D. L.; Hervey, W. J.; Pan, C.; Hurst, G. B., Efficient and Specific Trypsin Digestion of Microgram to Nanogram Quantities of Proteins in Organic-Aqueous Solvent Systems. *Anal. Chem.* **2006,** 78, 125-134.

192. Lazar, I. M.; Ramsey, R. S.; Ramsey, J. M., On-Chip Proteolytic Digestion and Analysis Using "Wrong-Way-Round" Electrospray Time-of-Flight Mass Spectrometry. *Anal. Chem.* **2001,** 73, 1733-1739.

193. Sim, T. S.; Kim, E.-M.; Joo, H. S.; Kim, B. G.; Kim, Y.-K., Application of a temperature-controllable microreactor to simple and rapid protein identification using MALDI-TOF MS. *Lab Chip* **2006,** 6, 1056-1061.

194. Pramanik, B. N.; Mirza, U. A.; Ing, Y. H.; Liu, Y.-H.; Bartner, P. L.; Weber, P. C.; Bose, A. K., Microwave-enhanced enzyme reaction for protein mapping by mass spectrometry: A new approach to protein digestion in minutes. *Protein Sci.* **2002,** 11, 2676-2687.

195. López-Ferrer, D.; Capelo, J. L.; Vázquez, J., Ultra Fast Trypsin Digestion of Proteins by High Intensity Focused Ultrasound. *J. Proteome Res.* **2005,** 4, 1569-1574.

196. López-Ferrer, D.; Hixson, K. K.; Smallwood, H.; Squier, T. C.; Petritis, K.; Smith, R. D., Evaluation of a High-Intensity Focused Ultrasound-Immobilized Trypsin Digestion and 18O-Labeling Method for Quantitative Proteomics. *Anal. Chem.* **2009,** 81, 6272-6277.

197. Liu, J.; Lin, S.; Qi, D.; Deng, C.; Yang, P.; Zhang, X., On-chip enzymatic microreactor using trypsin-immobilized superparamagnetic nanoparticles for highly efficient proteolysis. *J. Chromatogr. A* **2007,** 1176, 169-177.

198. Park, Z.-Y.; Russell, D. H., Thermal Denaturation: A Useful Technique in Peptide Mass Mapping. *Anal. Chem.* **2000,** 72, 2667–2670.

199. Ho, S. Y.; Mittal, G. S.; Cross, J. D., Effects of high field electric pulses on the activity of selected enzymes. *J. Engineer.* **1997,** 31, 69-84.

200. Nesmelova, I. V.; Skirda, V. D.; Fedotov, V. D., Generalized concentration dependence of globular protein self-diffusion coefficients in aqueous solutions. *Biopolymers* **2002,** 63, 132-140.

201. Peterson, D. S.; Rohr, T.; Svec, F.; Fréchet, J. M. J., Enzymatic Microreactor-on-a-Chip: Protein Mapping Using Trypsin Immobilized on Porous Polymer Monoliths Molded in Channels of Microfluidic Devices. *Anal. Chem.* **2002,** 74, 4081-4088.

202. Wang, C.; Oleschuk, R.; Ouchen, F.; Li, J.; Thibault, P.; Harrison, D. J., Integration of immobilized trypsin bead beds for protein digestion within a microfluidic chip incorporating capillary electrophoresis separations and an electrospray mass spectrometry interface. *Rapid Commun. Mass Spectrom.* **2000,** 14, 1377-1383.

203. Slovakova, M.; Minc, N.; Bilkova, Z.; Smadja, C.; Faigle, W.; Fütterer, C.; Taverna, M.; Viovy, J.-L., Use of self assembled magnetic beads for on-chip protein digestion. *Lab Chip* **2005,** 5, 935-942.

204. Xie, S.; Svec, F.; Fréchet, J. M. J., Design of reactive porous polymer supports for high throughput bioreactors: Poly(2-vinyl-4,4-dimethylazlactone-co-acrylamide-co-ethylene dimethacrylate) monoliths. *Biotechnol. Bioeng.* **1999,** 62, 30-35.

205. Svec, F., Less common applications of monoliths: I. Microscale protein mapping with proteolytic enzymes immobilized on monolithic supports. *Electrophoresis* **2006,** 27, 947-961.

206. McCarley, R. L.; Vaidya, B.; Wei, S.; Smith, A. F.; Patel, A. B.; Feng, J.; Murphy, M. C.; Soper, S. A., Resist-Free Patterning of Surface Architectures in Polymer-Based Microanalytical Devices. *J. Am. Chem. Soc.* **2005,** 127, 842-843.

207. Qi, S.; Liu, X.; Ford, S.; Barrows, J.; Thomas, G.; Kelly, K.; McCandless, A.; Lian, K.; Goettert, J.; Soper, S. A., Microfluidic devices fabricated in poly(methyl methacrylate) using hot-embossing with integrated sampling capillary and fiber optics for fluorescence detection. *Lab Chip* **2002,** 2, 88-95.

208. Demirev, P. A.; Fenselau, C., Mass Spectrometry for Rapid Characterization of Microorganisms. *Annu. Rev. Anal. Chem.* **2008,** 1, 71-93.

209. Croston, G. E., Functional cell-based uHTS in chemical genomic drug discovery. *Trends Biotechnol.* **2002,** 20, 110-115.

210. Chanda, S. K.; Caldwell, J. S., Fulfilling the promise: drug discovery in the post-genomic era. *Drug Discov. Today* **2003,** 8, 168-174.

211. Umezawa, Y., Assay and screening methods for bioactive substances based on cellular signaling pathways. *Rev. Mol. Biotechnol.* **2002,** 82, 357-370.

212. Kempner, M. E.; Felder, R. A., A review of cell culture automation. *J. Assoc. Lab. Autom.* **2002,** 7, 56-62.

213. Monod, J., The growth of baterial cultures. *Annu. Rev. Microbiol.* **1949,** 3, 371-394.

214. Novick, A., Growth of bacteria. *Annu. Rev. Microbiol.* **1955,** 9, 97-110.

215. Pritchard, R. H., Review Lecture: On the Growth and Form of a Bacterial Cell *Philos. Trans. R Soc Lond B Biol Sci.* **1974,** 267, 303-336.

216. Black, J. G., *Microbiology : principles and explorations* 7ed.; Wiley: Hoboken, 2008; p 968.

217. Walker, G. M.; Ozers, M. S.; Beebe, D. J., Insect Cell Culture in Microfluidic Channels. *Biomed. Microdevices* **2002,** 4, 161-166.

218. Meyvantsson, I.; Beebe, D. J., Cell culture models in microfluidic systems. *Annu. Rev. Anal. Chem.* **2008,** 1, 423-449.

219. El-Ali, J.; Sorger, P. K.; Jensen, K. F., Cells on chips. *Nature* **2006,** 442, 403-411.

220. Yi, C.; Li, C.-W.; Ji, S.; Yang, M., Microfluidics technology for manipulation and analysis of biological cells. *Anal. Chim. Acta* **2006,** 560, 1-23.

221. Rhee, S. W.; Taylor, a. M.; Tu, C. H.; Cribbs, D. H.; Cotman, C. W.; Jeon, N. L., Patterned cell culture inside microfluidic devices. *Lab Chip* **2005,** 5, 102-107.

222. Sakamoto, C.; Yamaguchi, N.; Nasu, M., Rapid and simple quantification of bacterial cells by using a microfluidic device. *Appl. Environ. Microbiol.* **2005,** 71, 1117-1121.

223. Mahoney, M. J.; Chen, R. R.; Tan, J.; Saltzman, W. M., The influence of microchannels on neurite growth and architecture. *Biomaterials* **2005,** 26, 771-778.

224. Yeon, J. H.; Park, J.-K., Microfluidic cell culture systems for cellular analysis. *Biochip J.* **2007,** 1, 17-27.

225. Stangegaard, M.; Petronis, S.; Jørgensen, A. M.; Christensen, C. B. V.; Dufva, M., A biocompatible micro cell culture chamber (μCCC) for the culturing and on0line monitoring of eukaryote cells. *Lab Chip* **2006,** 6, 1045-1051.

226. Hung, P. J.; Lee, P. J.; Sabounchi, P.; Aghdam, N.; Lin, R.; Lee, L. P., A novel high aspect ratio microfluidic design to provide a stable and uniform microenvironment for cell growth in a high throughput mammalian cell culture array. *Lab Chip* **2005,** 5, 44-48.

227. Andersson, H.; Berg, A. v. d., Microfluidic devices for cellomics: a review. *Sens. Actuator B* **2003,** 92, 315-325.

228. Price, A. K.; Culbertson, C. T., Chemical Analysis of Single Mammalian Cells with Microfluidics. *Anal. Chem.* **2007,** 79, 2614-2621.

229. Walker, G. M.; Zeringue, H. C.; Beebe, D. J., Microenvironment design considerations for cellular scale studies. *Lab Chip* **2004,** 4, 91-97.

230. Mukhopadhyay, R., When PDMS isn't the best. *Anal. Chem.* **2007,** 79, 3248-3253.

231. Klapperich, C. M., Microfluidic diagnostics: time for industry standards. *Expert Rev. Med. Devices* **2009,** 6, 211-213.

232. Groisman, A.; Lobo, C.; Cho, H.; Campbell, J. K.; Dufour, Y. S.; Stevens, A. M.; Levchenko, A., A microfluidic chemostat for experiments with bacterial and yeast cells. *Nat. Methods* **2005,** 2, 685-689.

233. Zhang, Z.; Boccazzi, P.; Choi, H.-G.; Perozziello, G.; Sinskey, A. J.; Jensen, K. F., Microchemostat-microbial continuous culture in a polymer-based, instrumented microbioreactor. *Lab Chip* **2006,** 6, 906-913.

234. Huang, P. J.; Lee, P. J.; Sabounchi, P.; Aghdam, N.; Lin, R.; Lee, L. P., A novel high aspect ratio microfluidic design to provide a stable and uniform microenvironment for cell growth in a high throughput mammalian cell culture array. *Lab Chip* **2005,** 5, 44-48.

235. Tanaka, K., The Origin of Macromolecule Ionization by Laser Irradiation (Nobel Lecture). *Angew. Chem. Int. Ed Engl* **2003,** 42, 3860-3870.

236. Fenn, J. B., Electrospray Wings for Molecular Elephants (Nobel Lecture). *Angew. Chem. Int. Ed Engl* **2003,** 42, 3871-3894.

237.   Bonk, T.; Humeny, A., MALDI-TOF-MS Analysis of Protein and DNA. *Neuroscientist* **2001,** 7, 6-12.

238.   Dreisewerd, K., The Desorption Process in MALDI. *Chem. Rev.* **2003,** 103, 395-426.

239.   Hillenkamp, F.; Karas, M., The MALDI Process and Method. In *MALDI MS: A Practical Guide to Instrumentation, Method and Application*, Hillenkamp, F.; Peter-Katalini, J., Eds. Wiley-VHC: 2007; pp 1-28.

240.   Karas, M.; Hillenkamp, F., Laser desorption ionization of proteins with molecular masses exceeding 10,000 daltons. *Anal. Chem.* **1988,** 60, 2299-2301.

241.   Zenobi, R.; Knochenmuss, R., Ion formation in MALDI mass spectrometry. *Mass Spectrom. Rev.* **1998,** 17, 337-366.

242.   Reinarda, M. S.; Johnston, M. V., Ion Formation Mechanism in Laser Desorption Ionization of Individual Nanoparticles. *J. Am. Soc. Mass Spectrom.* **2008,** 19, 389-399.

243.   Bahr, U.; Karas, M.; Hillenkamp, F., Analysis of biopolymers by matrix-assisted laser desorption/ionization (MALDI) mass spectrometry. *Fresenius. J. Anal. Chem.* **1994,** 348, 783-791.

244.   Vestal, M. L., Modern MALDI time-of-flight mass spectrometry. *J. Mass Spectrom.* **2009,** 44, 303-317.

245.   Cotter, R. J., *Time-of-Flight Mass Spectrometry: Instrumentation and Applications in Biological Research* ACS: Washington D.C., 1997.

246.   Weickhardt, C.; Moritz, F.; Grotemeyer, J., Time-of-flight mass spectrometry: State-of the-art in chemical analysis and molecular science. *Mass Spectrom. Rev.* **1996,** 15, 139-162.

247.   Boesl, U.; Weinkauf, R.; Schlag, E. W., Reflectron time-of-flight mass spectrometry and laser excitation for the analysis of neutrals, ionized molecules and secondary fragments. *Int. J. Mass Spectrom. Ion Proc.* **1992,** 112, 121-166.

248.   Fei, X.; Wei, G.; Murray, K. K., Aerosol MALDI with a Reflectron Time-of-Flight Mass Spectrometer. *Anal. Chem.* **1996,** 68, 1143–1147.

249.   Birkinshaw, K., Fundamentals of Focal Plane Detectors. *J. Mass Spectrom.* **1997,** 32, 795-806.

250.   Birkinshaw, K.; Langstaff, D. P., The Ideal Detector. *Rapid Commun. Mass spectrom.* **1996,** 10, 1675-1676.

251. Langstaff, D. P.; Birkinshaw, K., The dependence of the resolving power and sensitivity of a discrete electrode detector array on the proximity of a microchannel-plate electron multiplier. *Rapid Commun. Mass spectrom.* **1995,** 9, 703-706.

252. Hill, J. A.; Biller, J. E.; Biemann, K., A variable dispersion array detector for a tandem mass spectrometer. *Int. J. Mass Spectrom. Ion Proc.* **1991,** 111, 1-25.

253. Matsuura, S.; Umebayashi, S.; Okuyama, C.; Oba, K., Characteristics of the Newly Developed MCP and Its Assembly. *IEEE Ttrans.* **1985,** 32, 350 - 354

254. Madou, M. J., *Fundamentals of Microfabrications: The Science of Miniaturization.* 2nd ed.; CRC Press: Boca Raton, 2002.

255. Ford, S. M.; Davies, J.; Kar, B.; Qi, S. D.; Mcwhorter, S.; Soper, S. A.; Malek, C. K., Micromachining in Plastics Using X-Ray Lithography for the Fabrication of Micro-Electrophoresis Devices. *J. Biomech. Eng. ASME* **1999,** 121, 13-21.

256. Belloy, E.; Pawlowski, A.-G.; Sayah, A.; Gijs, M. A. M., Microfabrication of high-aspect ratio and complex monolithic structures in glass. *J. Microelectromech. Syst.* **2002,** 11, 521-527.

257. Bien, D. C. S.; Rainey, P. V.; Mitchell, S. J. N.; Gamble, H. S., Characterization of masking materials for deep glass micromachining. *J. Micromech. Microeng.* **2003,** 13, S34-S40.

258. Hierlemann, A.; Brand, O.; Hagleitner, C.; Baltes, H., Microfabrication techniques for chemical/biosensors. *Proc. IEEE* **2003,** 91, 839-863.

259. Verpoorte, E.; Rooij, N. F. D., Microfluidics Meets MEMS. *Proc. IEEE* **2003,** 91, 930-953.

260. Esch, M. B.; Kapur, S.; Irizarry, G.; Genova, V., Influence of master fabrication techniques on the characteristics of embossed microfluidic channels. *Lab Chip* **2003,** 3, 121-127.

261. Hupert, M. L.; Guy, W. J.; Llopis, S. D.; Shadpour, H.; Rani, S.; Nikitopoulos, D. E.; Soper, S. A., Evaluation of micromilled metal mold masters for the replication of microchip electrophoresis devices. *Microfluid Nanofluid* **2007,** 3, 1-11.

262. Boone, T. D.; Fan, Z. H.; Hooper, H. H.; Ricco, A. J.; Tan, H.; Williams, S. J., Plastic advances microfluidic devices. *Anal. Chem.* **2002,** 74, 78A-86A.

263. Friedrich, C. R.; Vasile, M. J., Development of the Micromilling Prolcess for High-Aspect-Ratio Microstructures. *J. Microelectromech. Syst.* **1996,** 5, 33-38.

264. Friedrich, C. R.; Vasile, M. J., The micromilling process for high aspect ratio microstructures. *Microsystem Technol.* **1996,** 2, 144-148.

265. Roberts, M. A.; Rossier, J. S.; Bercier, P.; Girault, H., UV Laser Machined Polymer Substrates for the Development of Microdiagnostic Systems. *Anal. Chem.* **1997,** 69, 2035 -2042.

266. Srinivasan, R., Controlled degradation and ablation of polymer surfaces by ultraviolet laser radiation. *Polym. Degrad. Stab.* **1987,** 17, 193-203.

267. Soper, S. A.; Ford, S. M.; Qi, S.; McCarley, R. L.; Kelly, K.; Murphy, M. C., Polymeric Microelectro-Mechanical Systems. *Anal. Chem.* **2000,** 72, 642A-651A.

268. Rizvi, N. H.; Apte, P., Developments in laser micro-machining techniques. *J. Mater. Process. Tech.* **2002,** 127, 206-210.

269. Kathuria, Y. P.; Tsuboi, A., Excimer laser process technology for micro-machining. *Proceedings of the International Symposium on Micro Machine and Human Science* **1994,** 5, 153-160.

270. Martynova, L.; Locascio, L. E.; Gaitan, M.; Kramer, G. W.; Christensen, R. G.; MacCrehan, W. A., Fabrication of Plastic Microfluid Channels by Imprinting Methods. *Anal. Chem.* **1997,** 69, 4783-4789.

271. Ford, S. M.; Kar, B.; McWhorter, S.; Davies, J.; Soper, S. A.; Klopf, M.; Calderon, G.; Saile, V., Microcapillary electrophoresis devices fabricated using polymeric substrates and X-ray lithography. *J. Microcolumn Sep.* **1998,** 10, 413-422.

272. Ford, S. M.; Davies, J.; Kar, B.; Qi, S. D.; McWhorter, S.; Soper, S. A.; Malek, C. K., Micromachining in plastics using X-ray lithography for the fabrication of micro-electrophoresis devices. *J. Biomech. Eng.-Trans. ASME* **1999,** 121, (1), 13-21.

273. Ford, S. M.; Kar, B.; McWhorter, S.; Davies, J.; Soper, S. A.; Klopf, M.; Calderon, G.; Saile, V., Microcapillary electrophoresis devices fabricated using polymeric substrates and X-ray lithography. *J. Microcolumn Sep.* **1998,** 10, (5), 413-422.

274. Blanco, F. J.; Berganzo, J.; Garcia, J.; Mayora, K.; Calle, A.; Lechuga, L. M., 3-D polymeric microfluidic devices for BioMOEMS applications. *Proc. SPIE* **2005,** 5839, 127-137.

275. Bruin, G. J. M., Recent developments in electrokinetically driven analysis on microfabricated devices. *Electrophoresis* **2000,** 21, 3931-3951.

276. Wang, X.; Cheng, C.; Wang, S.; Liu, S., Electroosmotic pumps and their applications in microfluidic systems. *Microfluid Nanofluid* **2009,** 6, 145-162.

277. Witek, M. A.; Wei, S.; Vaidya, B.; Adams, A. A.; Zhu, L.; Stryjewski, W.; McCarley, R. L.; Soper, S. A., Cell transport *via* electromigration in polymer-based microfluidic devices. *Lab Chip* **2004,** 4, 464-472.

278.	Barlow, G. H.; Margoliash, E., Electrophoretic Behavior of Mammalian-type Cytochrome *c*. *J. Biol. Chem.* **1966,** 241, 1473-1477.

279.	Coohill, T. P.; Sagripanti, J.-L., Overview of the Inactivation by 254 nm Ultraviolet Radiation of Bacteria with Particular Relevance to Biodefense. *Photochem. Photobiol.* **2008,** 84, 1084-1090.

280.	Duffy, D. C.; McDonald, J. C.; Schueller, O. J. A.; Whitesides, G. M., Rapid Prototyping of Microfluidic Systems in Poly(dimethylsiloxane). *Anal. Chem.* **1998,** 70, 4974-4986.

281.	Liu, Y.; Lu, H.; Zhong, W.; Song, P.; Kong, J.; Yang, P.; Girault, H. H.; Liu, B., Multilayer-Assembled Microchip for Enzyme Immobilization as Reactor Toward Low-Level Protein Identification. *Anal. Chem.* **2006,** 78, 801-808.

282.	Peterson, D. S.; Rohr, T.; Svec, F.; Fréchet, J. M. J., High-Throughput Peptide Mass Mapping Using a Microdevice Containing Trypsin Immobilized on a Porous Polymer Monolith Coupled to MALDI TOF and ESI TOF Mass Spectrometers. *J. Proteome Res.* **2002,** 1, 563-568.

283.	Chen, M.; Cook, K. D.; Kheterpal, I.; Wetzel, R., A Triaxial Probe for On-line Proteolysis Coupled with Hydrogen/Deuterium Exchange-Electrospray Mass Spectrometry. *J. Am. Soc. Mass Spectrom.* **2007,** 18, 208-217.

284.	Havliš, J.; Thomas, H.; Šebela, M.; Shevchenko, A., Fast-Response Proteomics by Accelerated In-Gel Digestion of Proteins. *Anal. Chem.* **2003,** 75, 1300-1306.

285.	Russell, W. K.; Park, Z.-Y.; Russell, D. H., Proteolysis in Mixed Organic-Aqueous Solvent Systems: Applications for Peptide Mass Mapping Using Mass Spectrometry. *Anal. Chem.* **2001,** 73, 2682-2685.

286.	Park, Z.-Y.; Russell, D. H., Identification of Individual Proteins in Complex Protein Mixtures by High-Resolution, High-Mass-Accuracy MALDI TOF-Mass Spectrometry Analysis of In-Solution Thermal Denaturation/Enzymatic Digestion. *Anal. Chem.* **2001,** 73, 2558-2564.

287.	Perkins, D. N.; Pappin, D. J. C.; Creasy, D. M.; S.Cottrell, J., Probability-based protein identification by searching sequence databases using mass spectrometry data. *Electrophoresis* **1999,** 20, 3551-3567.

288.	Henkin, J. A.; Jennings, M. E.; Matthews, D. E.; Vigoreaux, J. O., Mass Processing-An Improved Technique for Protein Identification with Mass Spectrometry Data. *J. Biomol. Tech.* **2004,** 15, 230-237.

289.	Bigwarfe, P. M. J.; Wood, T. D., Effect of ionization mode in the analysis of proteolytic protein digests. *Int. J. Mass Spectrom.* **2004,** 234, 185-202.

290.	Seong, G. H.; Heo, J.; Crooks, R. M., Measurement of Enzyme Kinetics Using a Continuous-Flow Microfluidic System. *Anal. Chem.* **2003,** 75, 3161-3167.

291. Koh, W.-G.; Pishkoa, M., Immobilization of multi-enzyme microreactors inside microfluidic devices. *Sens. Actuator B-Chem.* **2005,** 106, 335-342.

292. Xi, F.; Wu, J.; Jia, Z.; Lin, X., Preparation and characterization of trypsin immobilized on silica gel supported macroporous chitosan bead. *Process Biochem.* **2005,** 40, 2833-2840.

293. Jin, L. J.; Ferrance, J.; Sanders, J. C.; Landers, J. P., A microchip-based proteolytic digestion system driven by electroosmotic pumping. *Lab Chip* **2003,** 3, 11-18.

294. Lee, J.; Soper, S. A.; Murray, K. K., Development of an efficient on-chip digestion system for protein analysis using MALDI-TOF MS. *Analyst* **2009,** 134, 2426-2433.

295. Palm, A. K.; Novotny, M. V., Analytical characterization of a facile porous polymer monolithic trypsin microreactor enabling peptide mass mapping using mass spectrometry. *Rapid Commun. Mass spectrom.* **2004,** 18, 1374-1382.

296. Gao, J.; Xu, J.; Locascio, L. E.; Lee, C. S., Integrated Microfluidic System Enabling Protein Digestion, Peptide Separation, and Protein Identification. *Anal. Chem.* **2001,** 73, 2648-2655.

297. Sakai-Kato, K.; Kato, M.; Toyo'oka, T., On-Line Trypsin-Encapsulated Enzyme Reactor by the Sol−Gel Method Integrated into Capillary Electrophoresis. *Anal. Chem.* **2002,** 74, 2943-2949.

298. Josic, D.; Buchacher, A.; Jungbauer, A., Monoliths as stationary phases for separation of proteins and polynucleotides and enzymatic conversion. *J. Chromatogr. B* **2001,** 752, 191-205.

299. Park, D. S.-W.; Hupert, M. L.; Witek, M. A.; You, B. H.; Datta, P.; Guy, J.; Lee, J.-B.; Soper, S. A.; Nikitopoulos, D. E.; Murphy, M. C., A titer plate-based polymer microfluidic platform for high throughput nucleic acid purification. *Biomed. Microdevices* **2008,** 10, 21-33.

300. Hashimoto, M.; Kaji, H.; Kemppinen, M. E.; Nishizawa, M., Localized immobilization of proteins onto microstructures within a preassembled microfluidic device. *Sens. Actuator B: Chemical* **2008,** 128, 545-551.

301. Lin, Y.-S.; Yang, C.-H.; Chen, Y.-C., Glass-chip-based sample preparation and on-chip tryptic digestion for matrix-assisted laser desorption/ionization mass spectrometric analysis using a sol-gel/2,5-dihydroxybenzoic acid hybrid matrix. *Rapid Commun. Mass spectrom.* **2004,** 18, 313-318.

302. Yao, Z.-P.; Afonso, C.; Fenselau, C., Rapid microoraganism identification with on-slide proteolytic digestion followed by matrix-assisted laser desorption/ionization tandem mass spectrometry and database searching. *Rapid Commun. Mass spectrom.* **2002,** 16, 1953-1956.

303. Zhang, H.; Caprioli, R. M., Capillary Electrophoresis Combined with Matrix-Assisted Laser Desorption/Ionization Mass Spectrometry; Continuous Sample Deposition on a Matrix-precoated Membrane Target. *J. Mass Spectrom.* **1996,** 31, 1039-1046.

304. Wall, D. B.; Berger, S. J.; Finch, J. W.; Cohen, S. A.; Richardson, K.; Chapman, R.; Drabble, D.; Brown, J.; Gostick, D., Continuous sample deposition from reversed-phase liquid chromatography to tracks on a matrix-assisted laser desorption/ionization precoated target for the analysis of protein digests. *Electrophoresis* **2002,** 23, 3193-3204.

305. Chen, H.-s.; Rejtar, T.; Andreev, V.; Moskovets, E.; Karger, B. L., High-Speed, High-Resolution Monolithic Capillary LC-MALDI MS Using an Off-Line Continuous Deposition Interface for Proteomic Analysis. *Anal. Chem.* **2005,** 77, 2323-2331.

306. Yokoigawa, K.; Inoue, K.; Okubo, Y.; Kawai, H., Primers for Amplifying an Alanine Racemase Gene Fragment to Detect E. coli Strains in Foods. *J. Food Sci.* **2006,** 64, 571-575.

307. Segura-Alvarez, M.; Richter, H.; Conraths, F. J.; Geue, L., Evaluation of Enzyme-Linked Immunosorbent Assays and a PCR Test for Detection of Shiga Toxins for Shiga Toxin-Producing Escherichia coli in Cattle Herds. *J. Clin. Microbiol.* **2003,** 41, 5760-5763.

308. Cavallini, A.; Notarnicola, M.; Berloco, P.; Lippolis, A.; Di Leo, A., Use of macroporous polypropylene filter to allow identification of bacteria by PCR in human fecal samples. *J Microbiol. Methods* **2000,** 39, (3), 265-270.

309. Basile, F.; Ferrer, I.; Furlong, E. T.; Voorhees, K. J., Simultaneous Multiple Substrate Tag Detection with ESI-Ion Trap MS for In Vivo Bacterial Enzyme Activity Profiling. *Anal. Chem.* **2002,** 74, 4290–4293.

310. Vaidyanathan, S.; Rowland, J. J.; Kell, D. B.; Goodacre, R., Discrimination of Aerobic Endospore-forming Bacteria via Electrospray-Ionization Mass Spectrometry of Whole Cell Suspensions. *Anal. Chem.* **2001,** 73, 4134-4144.

311. Smith, P. B. W.; Snyder, A. P.; Harden, C. S., Characterization of Bacterial Phospholipids by Electrospray Ionization Tandem Mass Spectrometry. *Anal. Chem.* **1995,** 67, 1824-1830.

312. Lay, J. O., MALDI-TOF mass spectrometry and bacterial taxonomy. *Trends Anal. Chem.* **2000,** 19, 507-516.

313. Fenselau, C.; Demirev, P. A., Characterization of intact microorganisms by MALDI mass spectrometry. *Mass Spectrom. Rev.* **2001,** 20, 157-171.

314. Krishnamurthy, T.; Ross, P. L., Rapid Identification of Bacteria by Direct Matrix-assisted Laser Desorption/Ionization Mass Spectrometric Analysis of Whole Cells. *Rapid Commun. Mass spectrom.* **1996,** 10, 1992-1996.

315. Arnold, R. J.; Reilly, J. P., Fingerprint matching of E. coli strains with matrix-assisted laser desorption/ionization time-of-flight mass spectrometry of whole cells using a modified correlation approach. *Rapid Commun. Mass spectrom.* **1998,** 12, 630-636.

316. Claydon, M. A.; Davey, S. N.; Edwards-Jones, V.; Gordon1, D. B., The rapid identification of intact microorganisms using mass spectrometry. *Nat. Biotechnol.* **1996,** 14, 1584-1586.

317. Meetani, M. A.; Voorhees, K. J., MALDI Mass Spectrometry Analysis of High Molecular Weight Proteins from Whole Bacterial Cells: Pretreatment of Samples with Surfactants. *J. Am. Soc. Mass Spectrom.* **2005,** 16, 1422-1426.

318. Madonna, A. J.; Voorhees, K. J.; Taranenko, N. I.; Laiko, V. V.; Doroshenko, V. M., Detection of Cyclic Lipopeptide Biomarkers from Bacillus Species Using Atmospheric Pressure Matrix-Assisted Laser Desorption/Ionization Mass Spectrometry. *Anal. Chem.* **2003,** 75, 1628-1637.

319. Ochoa, M. L.; Harrington, P. B., Immunomagnetic Isolation of Enterohemorrhagic Escherichia coli O157:H7 from Ground Beef and Identification by Matrix-Assisted Laser Desorption/Ionization Time-of-Flight Mass Spectrometry and Database Searches. *Anal. Chem.* **2005,** 77, 5258-5267.

320. Wang, Z.; Russon, L.; Li, L.; Roser, D. C.; Long, S. R., Investigation of spectral reproducibility in direct analysis of bacterial proteins by matrix-assisted laser desorption/ionization time-of-flight mass spectrometry. *Rapid Commun. Mass spectrom.* **1998,** 12, 456-464.

321. Valentine, N.; Wunschel, S.; Wunschel, D.; Petersen, C.; Wahl, K., Effect of culture conditions on microorganism identification by matrix-assisted laser desorption ionization mass spectrometry. *Appl. Environ. Microbiol.* **2005,** 71, 58-64.

322. Wunschel, D. S.; Hill, E. A.; McLean, J. S.; Jarman, K.; Gorby, Y. A.; Valentine, N.; Wahl, K., Effects of varied pH, growth rate and temperature using controlled fermentation and batch culture on matrix assisted laser desorption/ionization whole cell protein fingerprints. *J. Micobiol. Methods* **2005,** 62, 259-271.

323. Demirev, P. A.; Ho, Y.-P.; Ryzhov, V.; Fenselau, C., Microorganism Identification by Mass Spectrometry and Protein Database Searches. *Anal. Chem.* **1999,** 71, 2732-2738.

324. Salmon, K.; Hung, S.-p.; Mekjian, K.; Baldi, P.; Hatfield, G. W.; Gunsalus, R. P., Global gene expression profiling in Escherichia coli K12. The effects of oxygen availability and FNR. *J. Biol. Chem.* **2003,** 278, 29837-29855.

325. Han, M.-J.; Lee, S. Y., The Escherichia coli proteome: past, present, and future prospects. *Microbiol. Mol. Biol. Rev.* **2006,** 70, 362-439.

326. Haeberle, S.; Zengerle, R., Microfluidic platforms for lab-on-a-chip applications. *Lab Chip* **2007,** 7, 1094-1110.

327. Adams, A. A.; Okagbare, P. I.; Feng, J.; Hupert, M. L.; Patterson, D.; Göttert, J.; McCarley, R. L.; Nikitopoulos, D.; Murphy, M. C.; Soper, S. A., Highly Efficient Circulating Tumor Cell Isolation from Whole Blood and Label-Free Enumeration Using Polymer-Based Microfluidics with an Integrated Conductivity Sensor. *J. Am. Chem. Soc.* **2008,** 130, 8633–8641.

328. Kim, L.; Toh, Y.; Voldman, J.; Yu, H., A practical guide to microfluidic perfusion culture of adherent mammalian cells. *Lab Chip* **2007,** 7, 681-694.

329. Zhu, X.; Chu, L. Y.; Chueh, B.-h.; Shen, M.; Hazarika, B.; Phadke, N.; Takayama, S., Arrays of horizontally-oriented mini-reservoirs generate steadymicrofluidic flows for continuous perfusion cell culture andgradient generation. *Analyst* **2004,** 129, 1026-1031.

330. Hung, P. J.; Lee, P. J.; Sabounchi, P.; Lin, R.; Lee, L. P., Continuous Perfusion Microfluidic Cell Culture Array for High-Throughput Cell-Based Assays. *Biotechnol. Bioeng.* **2004,** 89, 1-8.

331. Leclerc, E.; Sakai, Y.; Fujii, T., Cell Culture in 3-Dimensional Microfluidic Structure of PDMS (polydimethylsiloxane). *Biomed. Microdevices* **2003,** 5, 109-114.

332. Gu, W.; Zhu, X.; Futai, N.; Cho, B. S.; Takayama, S., Computerized microfluidic cell culture using elastomeric channels and Braille displays. *Proc. Natl. Acad. Sci. USA* **2004,** 101, 15861-15866.

333. Chung, B. G.; Flanagan, L. A.; Rhee, S. W.; Schwartz, P. H.; Lee, A. P.; Monuki, E. S.; Jeon, N. L., Human neural stem cell growth and differentiation in a gradient-generating microfluidic device. *Lab Chip* **2005,** 5, 401-406.

334. Bettinger, C. J.; Weinberg, E. J.; Kulig, K. M.; Vacanti, J. P.; Wang, Y.; Borenstein, J. T.; Langer, R., Three-Dimensional Microfluidic Tissue-Engineering Scaffolds Using a Flexible Biodegradable Polymer. *Adv. Mater.* **2006,** 18, 165-169.

335. Owen, S. J.; Meier, F. S.; Brombacher, S.; Volmer, D. A., Increasing sensitivity and decreasing spot size using an inexpensive, removable hydrophobic coating for matrix-assisted laser desorption/ionisation plates. *Rapid Commun. Mass spectrom.* **2003,** 17, 2439-2449.

336. Wei, H.; Dean, S. L.; Parkin, M. C.; Nolkrantz, K.; O'Callaghan, J. P.; Kennedy, R. T., Microscale sample deposition onto hydrophobic target plates for trace level detection of neuropeptides in brain tissue by MALDI-MS. *J. Mass Spectrom.* **2005,** 40, 1388-1346.

APPENDIX A. LAB VIEW PROGRAMS

Moving-Stage Control Program

This program is used to control moving stages in the continuous sample deposition for MALDI

MS detection (Chapter 5). It can control actuator motor, moving speed, deposition range, and the

number of cycles. Figure A-1 shows the main page of moving control program.
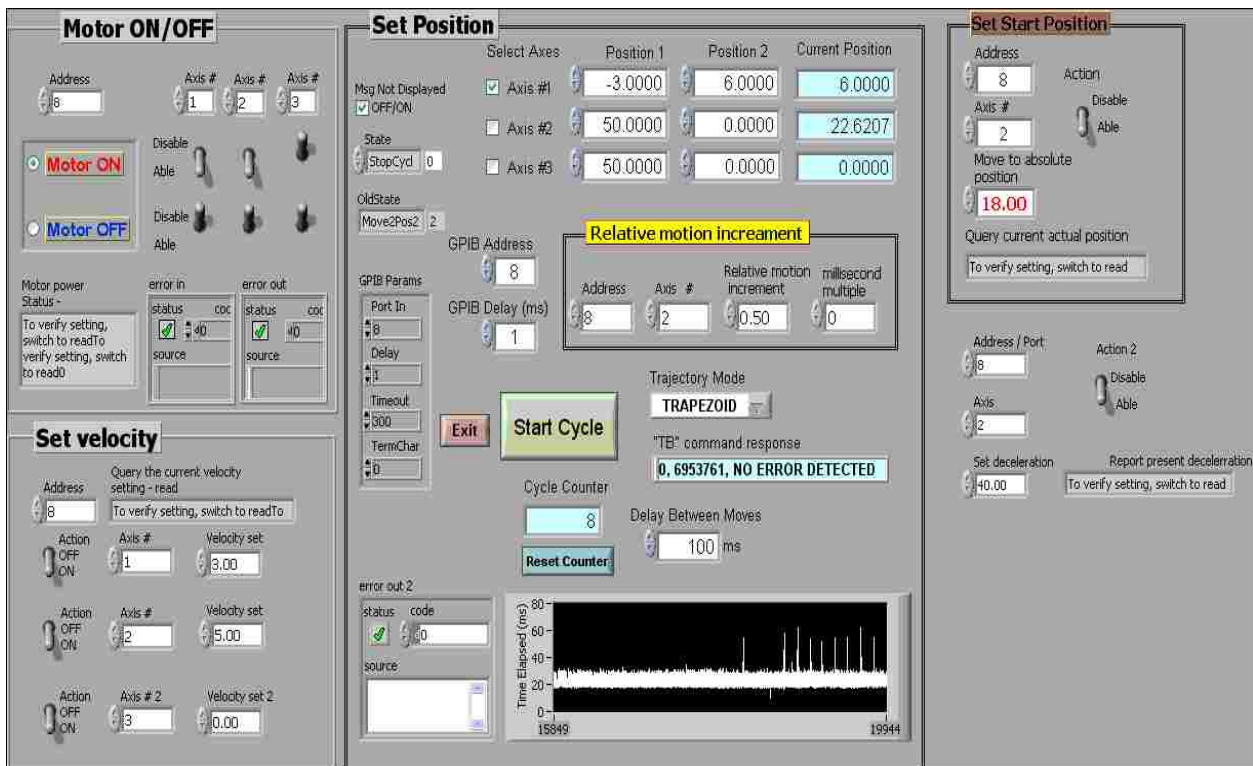
Figure A- 1. A photo of moving-stage control program.

VI name: XYZ Stage Microfluidics.vi

VI Description:

This program is used for starting the program to operate the xyz moving stages for sample

deposition. To start the controller program this VI should be loaded.

List of SubVIs:

VI Name: ESP 300.vi

VI Name: Motor On Off.vi

VI Name: On Off XYZ Moving.vi

VI Name: Set Velocity.vi

VI Name: Stop Motion.vi

VI Name: Motion Increment.vi

VI Name: Move to Absolute Position.vi

VI Name: Read Error Message.vi

VI Name: Read Actual Position.vi

ESP 300.vi

VI Description:

This VI reads controller configurations from hard disk and sends it to the ESP-300 controller.

List of SubVIs:

VI Name: ESP Read.vi

VI Name: ESP Send.vi

Motor On Off.vi

VI Description:

This VI is used to turn actuators on and off. When the motor is on, all actuators are ready to

move each stage.

On Off XYZ Moving.vi

VI Description:

This VI is used to select individual actuators for sample deposition.

Set Velocity.vi

VI Description:

This VI is used to set a moving speed of stages. The velocity of each stage can be controlled

individually

Stop Motion.vi

VI Description:

This VI is used to manually stop moving stages during operation.

Motion Increment.vi

VI Description:

This VI is used for selection of an interval length between traces and the number of traces.

List subVIs:

VI Name: Motor Off.vi

VI Name: Motor On.vi

VI Name: Moving.vi

VI Name: Multiflication.vi

Move to Absolute Position.vi

VI Description:

This VI is used for moving to a specified location to choose a starting point for sample deposition.

Read Actual Position.vi

VI Description:

This VI is used for finding the location of the stages.

Read Error Message.vi

VI Description:

This VI is used for record errors during the program operation.

ELSEVIER LICENSE
TERMS AND CONDITIONS

Jan 25, 2010

This is a License Agreement between Jeonghoon Lee ("You") and Elsevier ("Elsevier") provided by Copyright Clearance Center ("CCC"). The license consists of your order details, the terms and conditions provided by Elsevier, and the payment terms and conditions.

All payments must be made in full to CCC. For payment instructions, please see information listed at the bottom of this form.

Supplier	Elsevier Limited The Boulevard,Langford Lane Kidlington,Oxford,OX5 1GB,UK
Registered Company Number	1982084
Customer name	Jeonghoon Lee
Customer address	232 Choppin Department of Chemistry
	Baton Rouge, LA 70803
License Number	2353680520228
License date	Jan 21, 2010
Licensed content publisher	Elsevier
Licensed content publication	Journal of the American Society for Mass Spectrometry
Licensed content title	Development of an Automated Digestion and Droplet Deposition Microfluidic Chip for MALDI-TOF MS
Licensed content author	Jeonghoon Lee, Harrison K. Musyimi, Steven A. Soper, Kermit K. Murray
Licensed content date	July 2008
Volume number	19
Issue number	7
Pages	9
Type of Use	Thesis / Dissertation
Portion	Full article
Format	Both print and electronic
You are an author of the Elsevier article	Yes
Are you translating?	No

action to protect its copyright in the materials.

9. Warranties: Publisher makes no representations or warranties with respect to the licensed material.

10. Indemnity: You hereby indemnify and agree to hold harmless publisher and CCC, and their respective officers, directors, employees and agents, from and against any and all claims arising out of your use of the licensed material other than as specifically authorized pursuant to this license.

11. No Transfer of License: This license is personal to you and may not be sublicensed, assigned, or transferred by you to any other person without publisher's written permission.

12. No Amendment Except in Writing: This license may not be amended except in a writing signed by both parties (or, in the case of publisher, by CCC on publisher's behalf).

13. Objection to Contrary Terms: Publisher hereby objects to any terms contained in any purchase order, acknowledgment, check endorsement or other writing prepared by you, which terms are inconsistent with these terms and conditions or CCC's Billing and Payment terms and conditions. These terms and conditions, together with CCC's Billing and Payment terms and conditions (which are incorporated herein), comprise the entire agreement between you and publisher (and CCC) concerning this licensing transaction. In the event of any conflict between your obligations established by these terms and conditions and those established by CCC's Billing and Payment terms and conditions, these terms and conditions shall control.

14. Revocation: Elsevier or Copyright Clearance Center may deny the permissions described in this License at their sole discretion, for any reason or no reason, with a full refund payable to you. Notice of such denial will be made using the contact information provided by you. Failure to receive such notice will not alter or invalidate the denial. In no event will Elsevier or Copyright Clearance Center be responsible or liable for any costs, expenses or damage incurred by you as a result of a denial of your permission request, other than a refund of the amount(s) paid by you to Elsevier and/or Copyright Clearance Center for denied permissions.

LIMITED LICENSE

The following terms and conditions apply only to specific license types:

15. **Translation**: This permission is granted for non-exclusive world **English** rights only unless your license was granted for translation rights. If you licensed translation rights you may only translate this content into the languages you requested. A professional translator must perform all translations and reproduce the content word for word preserving the integrity of the article. If this license is to re-use 1 or 2 figures then permission is granted for non-exclusive world rights in all languages.

16. **Website**: The following terms and conditions apply to electronic reserve and author websites:
Electronic reserve: If licensed material is to be posted to website, the web site is to be password-protected and made available only to bona fide students registered on a relevant course if:
This license was made in connection with a course,
This permission is granted for 1 year only. You may obtain a license for future website posting,
All content posted to the web site must maintain the copyright information line on the bottom of each image,
A hyper-text must be included to the Homepage of the journal from which you are licensing at http://www.sciencedirect.com/science/journal/xxxxx or the Elsevier homepage for books at http://www.elsevier.com ,
and
Central Storage: This license does not include permission for a scanned version of the material to be stored in a central repository such as that provided by Heron/XanEdu.

17. **Author website** for journals with the following additional clauses:

All content posted to the web site must maintain the copyright information line on the bottom of each image, and
he permission granted is limited to the personal version of your paper. You are not allowed to download and post the published electronic version of your article (whether PDF or HTML, proof or final version), nor may you scan the printed edition to create an electronic version,
A hyper-text must be included to the Homepage of the journal from which you are licensing at

159

Terms and Conditions

INTRODUCTION

1. The publisher for this copyrighted material is Elsevier. By clicking "accept" in connection with completing this licensing transaction, you agree that the following terms and conditions apply to this transaction (along with the Billing and Payment terms and conditions established by Copyright Clearance Center, Inc. ("CCC"), at the time that you opened your Rightslink account and that are available at any time at http://myaccount.copyright.com).

GENERAL TERMS

2. Elsevier hereby grants you permission to reproduce the aforementioned material subject to the terms and conditions indicated.

3. Acknowledgement: If any part of the material to be used (for example, figures) has appeared in our publication with credit or acknowledgement to another source, permission must also be sought from that source. If such permission is not obtained then that material may not be included in your publication/copies. Suitable acknowledgement to the source must be made, either as a footnote or in a reference list at the end of your publication, as follows:

"Reprinted from Publication title, Vol /edition number, Author(s), Title of article / title of chapter, Pages No., Copyright (Year), with permission from Elsevier [OR APPLICABLE SOCIETY COPYRIGHT OWNER]." Also Lancet special credit - "Reprinted from The Lancet, Vol. number, Author(s), Title of article, Pages No., Copyright (Year), with permission from Elsevier."

4. Reproduction of this material is confined to the purpose and/or media for which permission is hereby given.

5. Altering/Modifying Material: Not Permitted. However figures and illustrations may be altered/adapted minimally to serve your work. Any other abbreviations, additions, deletions and/or any other alterations shall be made only with prior written authorization of Elsevier Ltd. (Please contact Elsevier at permissions@elsevier.com)

6. If the permission fee for the requested use of our material is waived in this instance, please be advised that your future requests for Elsevier materials may attract a fee.

7. Reservation of Rights: Publisher reserves all rights not specifically granted in the combination of (i) the license details provided by you and accepted in the course of this licensing transaction, (ii) these terms and conditions and (iii) CCC's Billing and Payment terms and conditions.

8. License Contingent Upon Payment: While you may exercise the rights licensed immediately upon issuance of the license at the end of the licensing process for the transaction, provided that you have disclosed complete and accurate details of your proposed use, no license is finally effective unless and until full payment is received from you (either by publisher or by CCC) as provided in CCC's Billing and Payment terms and conditions. If full payment is not received on a timely basis, then any license preliminarily granted shall be deemed automatically revoked and shall be void as if never granted. Further, in the event that you breach any of these terms and conditions or any of CCC's Billing and Payment terms and conditions, the license is automatically revoked and shall be void as if never granted. Use of materials as described in a revoked license, as well as any use of the materials beyond the scope of an unrevoked license, may constitute copyright infringement and publisher reserves the right to take any and all

162

action to protect its copyright in the materials.

9. Warranties: Publisher makes no representations or warranties with respect to the licensed material.

10. Indemnity: You hereby indemnify and agree to hold harmless publisher and CCC, and their respective officers, directors, employees and agents, from and against any and all claims arising out of your use of the licensed material other than as specifically authorized pursuant to this license.

11. No Transfer of License: This license is personal to you and may not be sublicensed, assigned, or transferred by you to any other person without publisher's written permission.

12. No Amendment Except in Writing: This license may not be amended except in a writing signed by both parties (or, in the case of publisher, by CCC on publisher's behalf).

13. Objection to Contrary Terms: Publisher hereby objects to any terms contained in any purchase order, acknowledgment, check endorsement or other writing prepared by you, which terms are inconsistent with these terms and conditions or CCC's Billing and Payment terms and conditions. These terms and conditions, together with CCC's Billing and Payment terms and conditions (which are incorporated herein), comprise the entire agreement between you and publisher (and CCC) concerning this licensing transaction. In the event of any conflict between your obligations established by these terms and conditions and those established by CCC's Billing and Payment terms and conditions, these terms and conditions shall control.

14. Revocation: Elsevier or Copyright Clearance Center may deny the permissions described in this License at their sole discretion, for any reason or no reason, with a full refund payable to you. Notice of such denial will be made using the contact information provided by you. Failure to receive such notice will not alter or invalidate the denial. In no event will Elsevier or Copyright Clearance Center be responsible or liable for any costs, expenses or damage incurred by you as a result of a denial of your permission request, other than a refund of the amount(s) paid by you to Elsevier and/or Copyright Clearance Center for denied permissions.

LIMITED LICENSE

The following terms and conditions apply only to specific license types:

15. **Translation**: This permission is granted for non-exclusive world **English** rights only unless your license was granted for translation rights. If you licensed translation rights you may only translate this content into the languages you requested. A professional translator must perform all translations and reproduce the content word for word preserving the integrity of the article. If this license is to re-use 1 or 2 figures then permission is granted for non-exclusive world rights in all languages.

16. **Website**: The following terms and conditions apply to electronic reserve and author websites:
Electronic reserve: If licensed material is to be posted to website, the web site is to be password-protected and made available only to bona fide students registered on a relevant course if:
This license was made in connection with a course,
This permission is granted for 1 year only. You may obtain a license for future website posting,
All content posted to the web site must maintain the copyright information line on the bottom of each image,
A hyper-text must be included to the Homepage of the journal from which you are licensing at http://www.sciencedirect.com/science/journal/xxxxx or the Elsevier homepage for books at http://www.elsevier.com ,
and
Central Storage: This license does not include permission for a scanned version of the material to be stored in a central repository such as that provided by Heron/XanEdu.

17. **Author website** for journals with the following additional clauses:

All content posted to the web site must maintain the copyright information line on the bottom of each image, and
he permission granted is limited to the personal version of your paper. You are not allowed to download and post the published electronic version of your article (whether PDF or HTML, proof or final version), nor may you scan the printed edition to create an electronic version,
A hyper-text must be included to the Homepage of the journal from which you are licensing at

163

This is a License Agreement between Jeonghoon Lee ("You") and John Wiley and Sons ("John Wiley and Sons") provided by Copyright Clearance Center ("CCC"). The license consists of your order details, the terms and conditions provided by John Wiley and Sons, and the payment terms and conditions.

All payments must be made in full to CCC. For payment instructions, please see information listed at the bottom of this form.

License Number	2353690501937
License date	Jan 21, 2010
Licensed content publisher	John Wiley and Sons
Licensed content publication	Journal of Mass Spectrometry
Licensed content title	Microfluidic chips for mass spectrometry-based proteomics
Licensed content author	Lee Jeonghoon, Soper Steven A., Murray Kermit K.
Licensed content date	Apr 16, 2009
Start page	579
End page	593
Type of Use	Dissertation/Thesis
Requestor type	Author of this Wiley article
Format	Print and electronic
Portion	Full article
Will you be translating?	No
Order reference number	
Total	0.00 USD

Terms and Conditions

TERMS AND CONDITIONS

party's right to enforce each and every term and condition of this Agreement. No breach under this agreement shall be deemed waived or excused by either party unless such waiver or consent is in writing signed by the party granting such waiver or consent. The waiver by or consent of a party to a breach of any provision of this Agreement shall not operate or be construed as a waiver of or consent to any other or subsequent breach by such other party.

11. This Agreement may not be assigned (including by operation of law or otherwise) by you without WILEY's prior written consent.

12. These terms and conditions together with CCC's Billing and Payment terms and conditions (which are incorporated herein) form the entire agreement between you and WILEY concerning this licensing transaction and (in the absence of fraud) supersedes all prior agreements and representations of the parties, oral or written. This Agreement may not be amended except in a writing signed by both parties. This Agreement shall be binding upon and inure to the benefit of the parties' successors, legal representatives, and authorized assigns.

13. In the event of any conflict between your obligations established by these terms and conditions and those established by CCC's Billing and Payment terms and conditions, these terms and conditions shall prevail.

14. WILEY expressly reserves all rights not specifically granted in the combination of (i) the license details provided by you and accepted in the course of this licensing transaction, (ii) these terms and conditions and (iii) CCC's Billing and Payment terms and conditions.

15. This Agreement shall be governed by and construed in accordance with the laws of England and you agree to submit to the exclusive jurisdiction of the English courts.

BY CLICKING ON THE "I ACCEPT" BUTTON, YOU ACKNOWLEDGE THAT YOU HAVE READ AND FULLY UNDERSTAND EACH OF THE SECTIONS OF AND PROVISIONS SET FORTH IN THIS AGREEMENT AND THAT YOU ARE IN AGREEMENT WITH AND ARE WILLING TO ACCEPT ALL OF YOUR OBLIGATIONS AS SET FORTH IN THIS AGREEMENT.

V1.2

Gratis licenses (referencing $0 in the Total field) are free. Please retain this printable license for your reference. No payment is required.

If you would like to pay for this license now, please remit this license along with your payment made payable to "COPYRIGHT CLEARANCE CENTER" otherwise you will be invoiced within 30 days of the license date. Payment should be in the form of a check or money order referencing your account number and this license number 2353690501937.
If you would prefer to pay for this license by credit card, please go to http://www.copyright.com/creditcard to download our credit card payment authorization form.

Make Payment To:
Copyright Clearance Center
Dept 001
P.O. Box 843006
Boston, MA 02284-3006

If you find copyrighted material related to this license will not be used and wish to cancel, please contact us referencing this license number 2353690501937 and noting the reason for cancellation.

Questions? customercare@copyright.com or +1-877-622-5543 (toll free in the US) or +1-978-646-2777.

RE: Permission Request Form: Jeonghoon Lee

1 message

CONTRACTS-COPYRIGHT (shared) <Contracts-Copyright@rsc.org>   **Mon, Jan 25, 2010 at 3:04 AM**

To: "jlee62@tigers.lsu.edu" <jlee62@tigers.lsu.edu>

Dear Dr Lee

The Royal Society of Chemistry (RSC) hereby grants permission for the use of your paper(s) specified below in the printed and microfilm version of your thesis. You may also make available the PDF version of your paper(s) that the RSC sent to the corresponding author(s) of your paper(s) upon publication of the paper(s) in the following ways: in your thesis via any website that your university may have for the deposition of theses, via your university's Intranet or via your own personal website. We are however unable to grant you permission to include the PDF version of the paper(s) on its own in your institutional repository. The Royal Society of Chemistry is a signatory to the STM Guidelines on Permissions (available on request).

Please note that if the material specified below or any part of it appears with credit or acknowledgement to a third party then you must also secure permission from that third party before reproducing that material.

Please ensure that the thesis states the following:

Reproduced by permission of The Royal Society of Chemistry

and include a link to the article on the Royal Society of Chemistry's website.

Please ensure that your co-authors are aware that you are including the paper in your thesis.

Regards

Gill Cockhead

Contracts & Copyright Executive

Gill Cockhead (Mrs), Contracts & Copyright Executive

168

Royal Society of Chemistry, Thomas Graham House

Science Park, Milton Road, Cambridge CB4 0WF, UK

Tel +44 (0) 1223 432134, Fax +44 (0) 1223 423623

http://www.rsc.org

-----Original Message-----
From: jlee62@tigers.lsu.edu [mailto:jlee62@tigers.lsu.edu]
Sent: 21 January 2010 17:21
To: CONTRACTS-COPYRIGHT (shared)
Subject: Permission Request Form: Jeonghoon Lee

Name   : Jeonghoon Lee

Address :

232 Choppin Hall, Department of Chemistry, Louisiana State University,
Baton Rouge, LA 70802

Tel   : 225-578-4346

Fax   : 225-578-3458

Email   : jlee62@tigers.lsu.edu

I am preparing the following work for publication:

Article/Chapter Title : MICROFLUIDIC DEVICES INTERFACED TO MATRIX-
ASSISTED LASER DESORPTION/IONIZATION MASS SPECTROMETRY FOR PROTEOMICS

Journal/Book Title   : Dissertation

Editor/Author(s)   : Jeonghoon Lee

```
Publisher                 : Louisiana State University
```

I would very much appreciate your permission to use the following
material:

```
Journal/Book Title        : Analyst

Editor/Author(s)          : Jeonghoon Lee, Steven A. Soper, Kermit K. Murray

Volume Number             : 134

Year of Publication       : 2009

Description of Material    : Paper

Page(s)                   : 2426 - 2433
```

```
Any Additional Comments        :
```

VITA

Jeonghoon Lee was born in Yangsan, Republic of Korea. He graduated with a Bachelor of Science degree from the department of chemistry, Kyungpook National University, Republic of Korea, in 1994. Following his graduation he extended his study in analytical chemistry with his advisor Dr. Zun-Ung Bae and received a Master of Science degree in 1996. During his graduate study, his research project was electrochemical characterization of asymmetric nickel(II)-macrocyclic complexes and their applications for analytical sensors. After receiving his master degree, he was employed as a research scientist with Samyang Central R&D Institute where he was involved in Genexol-PM project, anti-cancer agent using paclitaxel. As an analytical chemist, he conducted solid-state analysis of pacilitaxel and method validation and quantification of it in biological fluids. The Genexol-PM Injection, which greatly reduces the side effects of earlier anti-cancer medications, is being clinically tested in the United States. In addition, as an analytical responsible person in Korea Institute of Toxicology, the government-owned contract research organization (CRO) in Korea, he had been exposed to and participated in most aspects of managing GLP, including preparing SOP, and writing validation protocols and reports. After almost ten years of employment experiences, he had decided to extend his study at the doctoral program for chemistry at Louisiana State University in 2005 with his advisor Dr. Kermit K. Murray and co-advisor Dr. Steven A. Soper. During his doctoral program, the main focus of his research is the development of microfluidic devices interfaced to mass spectrometry for proteomics. He was involved in various research projects to design and develop various solid-phase bioreactors, microfluidic culture devices, and interfaces for MALDI MS detection. He is currently a member of the American Chemical Society (ACS) and the American Society for Mass Spectrometry (ASMS). He has presented his research at many national conferences and

he has four publications and two manuscripts in preparation as a first author. He is currently a candidate for the degree of Doctor of Philosophy in chemistry, which will be awarded at the May 2010 commencement.